The expert in WATER ENVIRONMENTS

Hydrodynamic modelling for flood reduction and climate resilient infrastructure development pathways in Jakarta

Hydrodynamic Flood Modelling Summary Report

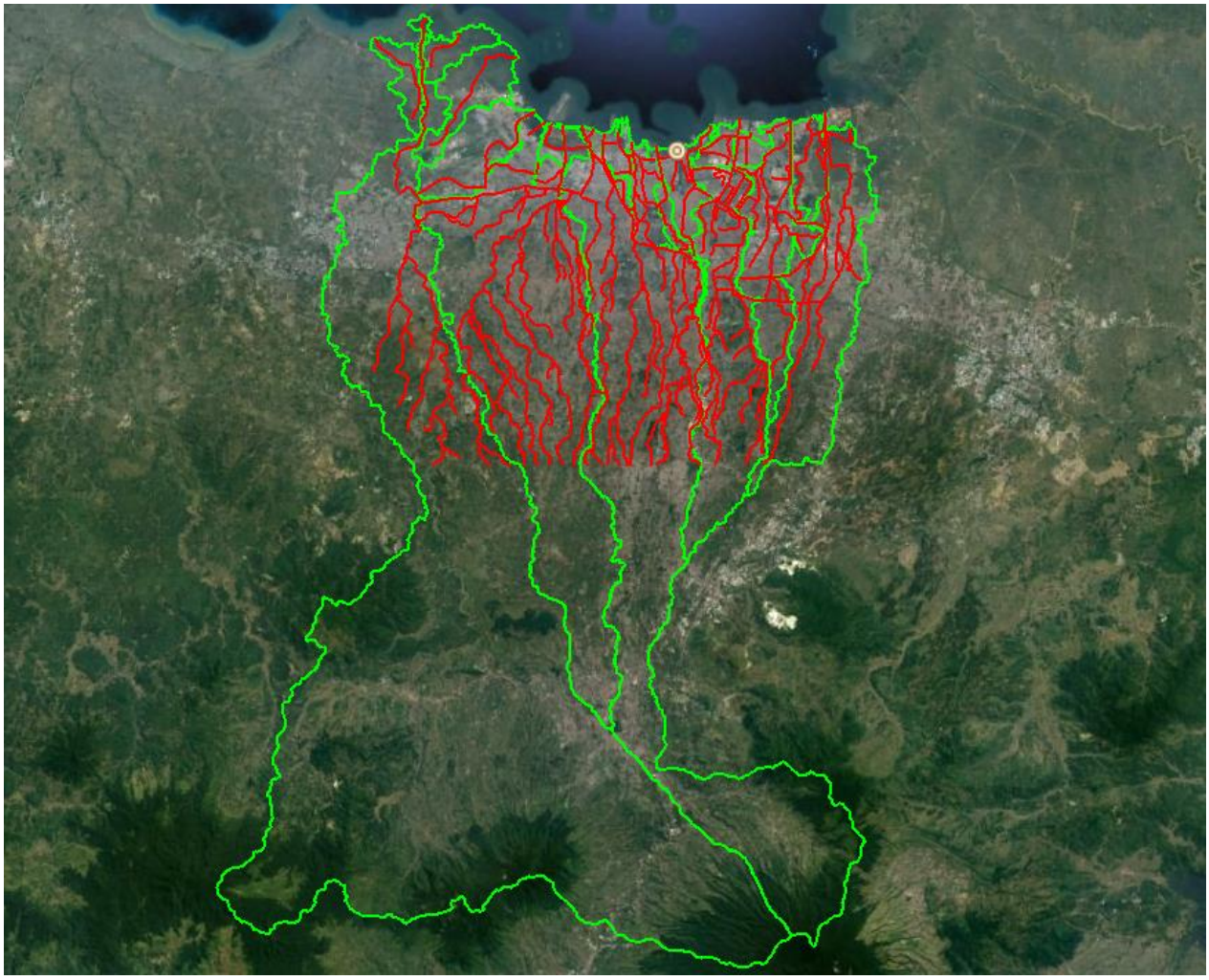

Hydrodynamic Modelling Report

May 2017

The expert in WATER ENVIRONMENTS

CTCN CLIMATE TECHNOLOGY CENTRE & NETWORK DHI DRD

This report has been prepared under the DHI Business Management System certified by DNV to comply with ISO 9001 (Quality Management), ISO 14001 (Environmental Management), OHSAS 18001 (Health and Safety Management)

The expert in WATER ENVIRONMENTS

Hydrodynamic modelling for flood reduction and climate resilient infrastructure development pathways in Jakarta

Hydrodynamic Flood Modelling Report

(Final Report)

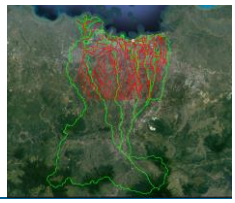

Prepared for	CTCN - UNEP
Represented by	Ms. Sandra Bry

Project manager	Dr. Budy Wiryawan

Project number	65800016
Approval date	15-05-2017
Revision	1
Classification	Open/Restricted/Confidential

PT. DHI Water & Environment • Oleos 2 Building, 5th Floor • Jl. Kebagusan 1 No.6 • Jakarta Selatan
Indonesia • 12520 •
Telephone: +62 21 2954 3959 • Telefax: +62 21 2954 3960 • info@dhigroup.com•

This page is intentionally left blank

CONTENTS

FIGURES

TABLES

APPENDICES

This page is intentionally left blank

Executive Summary

Jakarta is increasingly threatened by flooding from a combination of land subsidence, rising sea levels particularly with relation to the spring tide cycle and higher river levels resulting from potentially increasing rainfall intensity and land use changes within the catchment areas. To face such challenges on a sustainable way with a capacity building as a key objective, the Climate Technology Centre & Network (further called CTCN) is providing the technical assistance to Jakarta, (i) to better assess flood risks and hazards, and (ii) to design climate-resilient pathways to reduce the magnitude and scale of the impacts from this flooding. This assessment and strategy definition will help shape the design of climate resilient infrastructure projects including, but not limited to, the Giant Sea Wall (GSW), so called NCICD (National Capital Integrated Coastal Development). The outcomes are (a) a hydrodynamic flood model that can be used to evaluate a number of hard and soft engineering interventions to reduce the risk of flooding (b) a socio-cultural survey to examine inhabitants' perceptions of flooding, levels of acceptable risks and preferred adaptation options, (c) a series of technology transfer workshops to increase local capacity in high resolution hydrodynamic modelling and use of the model, (d) resultant policy and planning recommendations to reduce flood hazards, risk and vulnerability, and (e) a roadmap to sustain and expand the project using additional funding streams.

To meet the expected outcomes mentioned above, the project is divided into four main activities: Activity 1 – Flood Risk Assessment (Activity 1A – Model development; Activity 1B – Sociocultural Risk Assessment; Activity 1C – Technology Transfer); Activity 2 – Formulate Policy Recommendations; Activity 3 – Developing further funding streams; and Activity 4 – Knowledge sharing and South-South Cooperation. This report will be presenting Activity 1A – Model development as a major part of Activity 1 – Flood Risk Assessment. The objectives of this activity is to develop a high resolution hydrodynamic model for a pilot project area in Jakarta, shown in Figure 1, that is capable of producing flood levels under various climate and/or engineering scenarios. The following tasks are carried out sequentially to meet the objectives of Activity 1A: (1) Data gathering and pre-processing, (2) 1D modelling, (3) 2D modelling, (4) Coupling 1D and 2D modelling, (5) Production of Flood Maps, and (6) Analysis of flooding at the study area. The area has been chosen as one of the most flood-prone regions in Jakarta and is dominated by medium size commercial properties with additional medium-sized residential units, mainly to the north and south of the area.

Figure 1 (Left) The study area in northern part of DKI Jakarta shown in red polygon. (Right) Zoomed satellite image of the study area at the green circle. (Image source: Google Earth Pro)

Even though the pilot-scale project will only consider part of the total city drainage network and catchment of Jakarta, it is essential that the flood model should include

those parts of the wider network that are hydraulically connected to it, e.g. the east-west flood canals. Therefore, a coarser model set up, with resolution of ~30m, is generated as a boundary condition to the study area flood model (high resolution of ~3m).

The flood model will be simulated using 1D-2D coupled model. The flow in river and channel will be modelled using the 1D model MIKE HYDRO River software, and the inundation area will be captured in the 2D modelling program MIKE 21 Flow Model FM. The hydrodynamic interaction between the river and the flood areas will be handled by the 1D and 2D coupling software MIKE FLOOD.

The Digital Elevation Model (DEM) is used to generate the cross-section, river network and catchment definition. The current DEM used in this project is based on the Light Detection and Ranging (LiDAR) data of that was generated in the year 2012 (~1.33m resolution), which is provided by the Water Management Agency (DTA) shown in Figure 2. The final DEM is a composite of LiDAR DEM and other DEM data, pre-processed to cover the entire major catchments flowing through Jakarta.

The land subsidence map for Jakarta used in generating past and future topographical conditions is obtained from Budiyono *et al.* (2016). From that data, a yearly subsidence rate was calculated and used to generate projected topographies for the years 2007, 2013, and 2025.

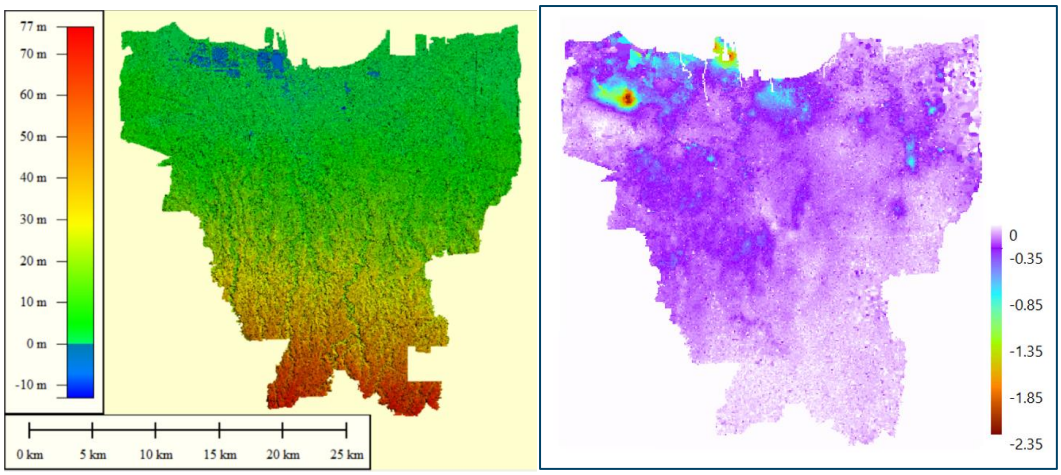

Figure 2 (Left) LiDAR DEM data of DKI Jakarta for year 2012. (Right) Land subsidence depths from 2012 to 2025 in meters to be used in generating past and future topographies. Source: Budiyono *et al.* (2016).

The rainfall data used in this project are the actual rainfall data and designed storm data. Actual rainfall data provided by Meteorological, Climatological, and Geophysical Agency (BMKG) is used in simulations for 2007, 2012 and 2013 rainfall events. The designed storm data, derived from design storm generation as described in van der Sleen and Lopez (2013), has been used for climate change scenarios. Climate change factors are determined from literature, which calculated values obtained from Global Climate Model (GCMs) and Representative Concentration Pathways (RCPs) scaled down to Jakarta region. Upon discussion with Jakarta Research Council (further called JRC), DHI agreed to simulate worst-case climate change flooding scenarios to aid in policy-making decisions. The upper 75-percentile values were chosen as climate change factors for this study, as summarised in Table 1.

Table 1 Climate change factors from five GCMs and four RCPs. Modified from Budiyono *et al.* (2016).

	5 GCM Median	5 GCM Std	upper 68%	upper 95%	upper 75%
2030 RCP2.6	0.79	0.33	1.12	1.45	1.18
2030 RCP4.5	0.76	0.47	1.23	1.70	1.31
2030 RCP6.0	0.79	0.51	1.30	1.81	1.39
2030 RCP8.5	0.85	0.49	1.34	1.83	1.43
2030 RCP Average	0.80	0.45	1.25	1.70	1.33
	5 GCM Median	**5 GCM Std**	**upper 68%**	**upper 95%**	**upper 75%**
2050 RCP2.6	0.79	0.32	1.11	1.43	1.17
2050 RCP4.5	0.82	0.48	1.30	1.78	1.39
2050 RCP6.0	0.79	0.56	1.35	1.91	1.45
2050 RCP8.5	0.96	0.58	1.54	2.12	1.64
2050 RCP Average	0.84	0.49	1.33	1.81	1.41

Tidal data was used as a boundary data in MIKE HYDRO River and MIKE 21 Flow Model FM. The tidal data for 2007, 2012, and 2013 scenario was obtained from tidal prediction models from DHI, while tidal data for 2030 and 2050 was obtained by applying the sea level rise to the Mean Highest High Water (MHHW) level. Model values are extracted from the point in Jakarta Bay nearest to the study area. From Hydrography and Oceanography Agency of Indonesia Navy (DISHIDROS) tidal constituents, some statistical values for peak tide levels can be calculated such as the MHHW. Sea level rise values for 2030 and 2050 was calculated based on sea level rise estimation done by BAPPENAS (2010), summarized in Table 2.

Table 2 Projection of the average increase of sea level in Indonesian water (Source: Bappenas, 2010)

Period	Sea Level Rise Projection since 2000			Level of confidence
	Tide Gauge	Altimeter ADT	Model	
2030	24.0 cm ± 16.0 cm	16.5 cm ± 1.5 cm	22.5 ± 1.5 cm	Moderate
2050	40.0 cm ± 20.0 cm	27.5 cm ± 2.5 cm	37.5 ± 2.5 cm	Moderate
2080	64.0 cm ± 32.0 cm	44.0 cm ± 4.0 cm	60.0 ± 4.0 cm	High
2100	80.0 cm ± 40.0 cm	60.0 cm ± 5.0 cm	80.0 ± 5.0 cm	High

During the discussion with DHI and JRC team, the scenario matrix in Table 3 is designed taking into account the available data and the modelling needs to meet the project's

objectives and deliverables. Models for 2007, 2012, and 2013 will be built to simulate the notable recent flood events over the past decade. For climate change scenarios, 2030 and 2050 time slices has been selected.

Table 3 Scenario matrix

Scenario	Flood Event (Rainfall Input)	Tide (Peak Level)	Subsidence based from 2012 year – Lidar DEM
1	01-02 Feb 2007 (31 Jan-05 Feb)	Actual tide (+0.500 m)	No Subsidence
2	01-02 Feb 2007 (31 Jan-05 Feb)	Actual tide (+0.500 m)	With negative subsidence (up to 2007)
3	16 Jan 2013 (15-19 Jan)	Actual tide (+0.276 m)	No Subsidence
4	16 Jan 2013 (15-19 Jan)	Actual tide (+0.276 m)	With positive subsidence (up to 2013)
5	21 Dec 2012 (20-24 Dec)	Actual tide (+0.286 m)	No Subsidence
6	2050 (50-year RP + 41% CC Factor)	MHHW + 0.375 SLR (+0.610 m)	No Subsidence
7	2050 (50-year RP + 41% CC Factor)	MHHW + 0.375 SLR (+0.610 m)	With positive subsidence (up to 2025)
8	2030 (50-year RP + 33% CC Factor)	MHHW + 0.225 SLR (+0.460 m)	No Subsidence
9	2030 (50-year RP + 33% CC Factor)	MHHW + 0.225 SLR (+0.460 m)	With positive subsidence (up to 2025)

RP – Return Period
CC Factor – Climate Change Factor
MHHW – Mean Highest High Water
SLR – Sea Level Rise

Prior to scenario model runs, flood models have to be calibrated and then validated based on observed data. However, there are currently no data available that can be used for calibration of the Jakarta flood model, which requires comprehensive data of observed rainfall, water level and discharge during flood events. Since the calibration process is not possible for this flood model, we have validated the model performance using available information and previous research study in Budiyono *et al.* (2016). Comparisons of both 2007 and 2013 model results shows that MIKE model results have a good comparison with flood maps in the referenced paper.

In order to assess the flood risk in the study area, flood maps were generated for various flood scenarios as listed in the Scenario Matrix (Table 3) Flood maps were produced by

extracting maximum flood depth from modelling results within the 4-5 days simulation period. Figure 3 shows a flood map for Scenario 9 as an example.

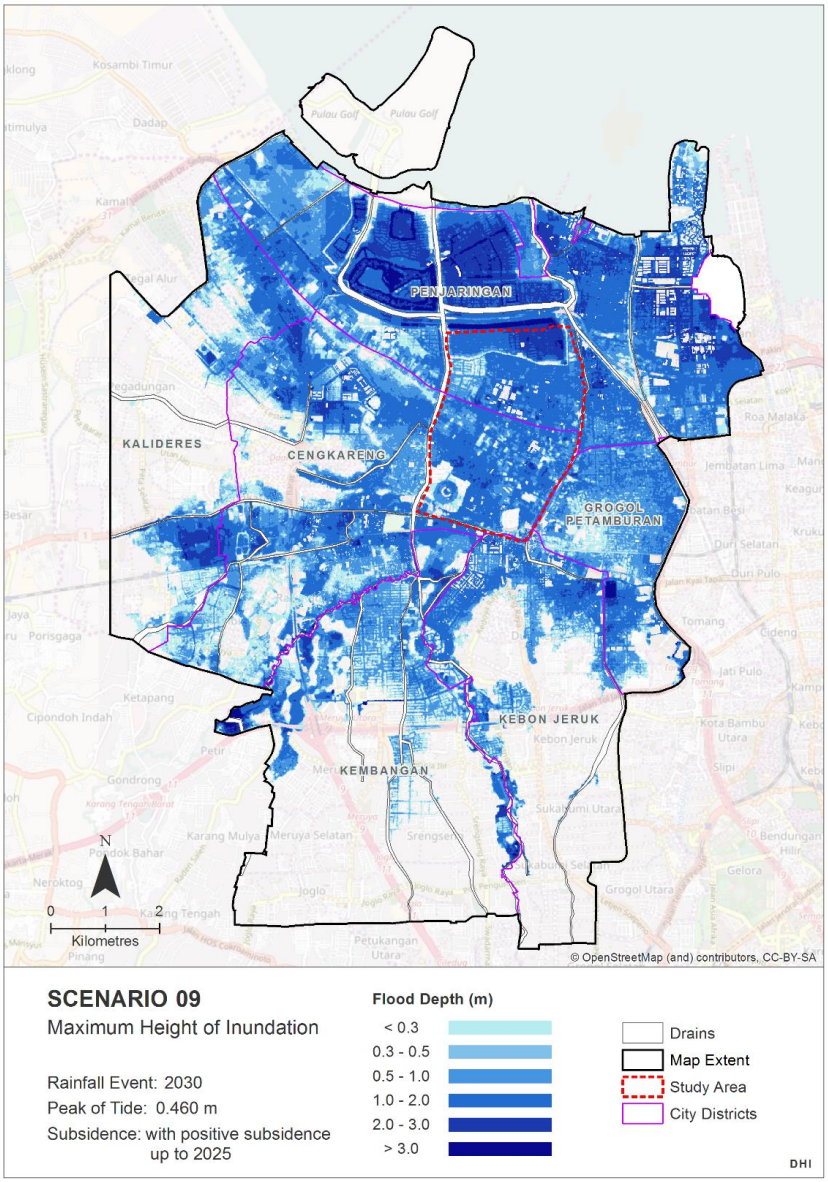

Figure 3 Flood map for Scenario 9.

To investigate the land subsidence effect toward flooding in the study area, flood maps from scenarios without land subsidence, i.e. using the base DEM, are compared with scenarios where land subsidence is applied. The comparison is done by plotting the inundation depth differences, for example between Scenarios 9 and 8 for 2030 shown in Figure 4a. One can see that the flood was worsened almost entirely in the study area (in Pantai Indah Kapuk polder, Kapuk Muara polder, and Kapuk Poglar polder).

In order to evaluate the effects of climate change towards flooding in the study area, various maps of flood depth differences were generated. Figure 4b shows the flood depths difference between 2030 and 2007 (Scenarios 8 and 1). The rainfall event in 2007 is calculated to have a frequency of 50-year return period (Budiyono *et al.*, 2016), which

is the same frequency as in 2030 with calculated climate change factor of +1.33. Therefore, increased the rainfall intensities due to climate change alone is enough to increase the inundation depths at the study area. Among the three polders that are located in the study area, Pantai Indah Kapuk polder has the highest sensitivity from the effects of climate change.

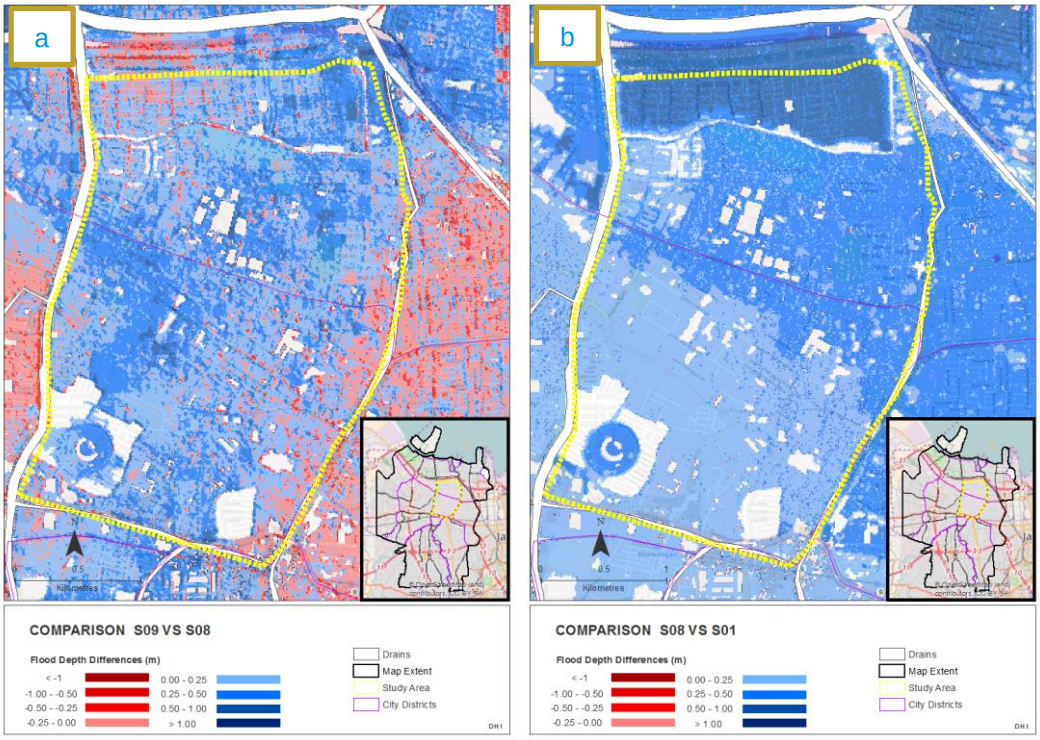

Figure 4 (a) Flood depth differences in the study area between with-subsidence scenario and without-subsidence scenarios for year 2030. (b) Flood depth differences in the study area between 2007 and climate change scenarios 2030.

To identify the critical areas where flood mitigation should be prioritised, DHI uses the dynamic flood maps that can show the progression of flooding within the 4-5 day simulation period. It is observed that flood start to occur: in the north part of Pantai Indah Kapuk polder (Penjaringan district), Pluit polder, west part of Penjaringan district, Teluk Gong polder (Grogol Petamburan district), and around Angke river. A plot of the 1D results show that flooding occurs when the water level overtops the cope levels of the river bank, particularly at shallow parts of Mookervart river and Angke river. One of the sets of dynamic flood maps is shown in Figure 5 for Scenario 9.

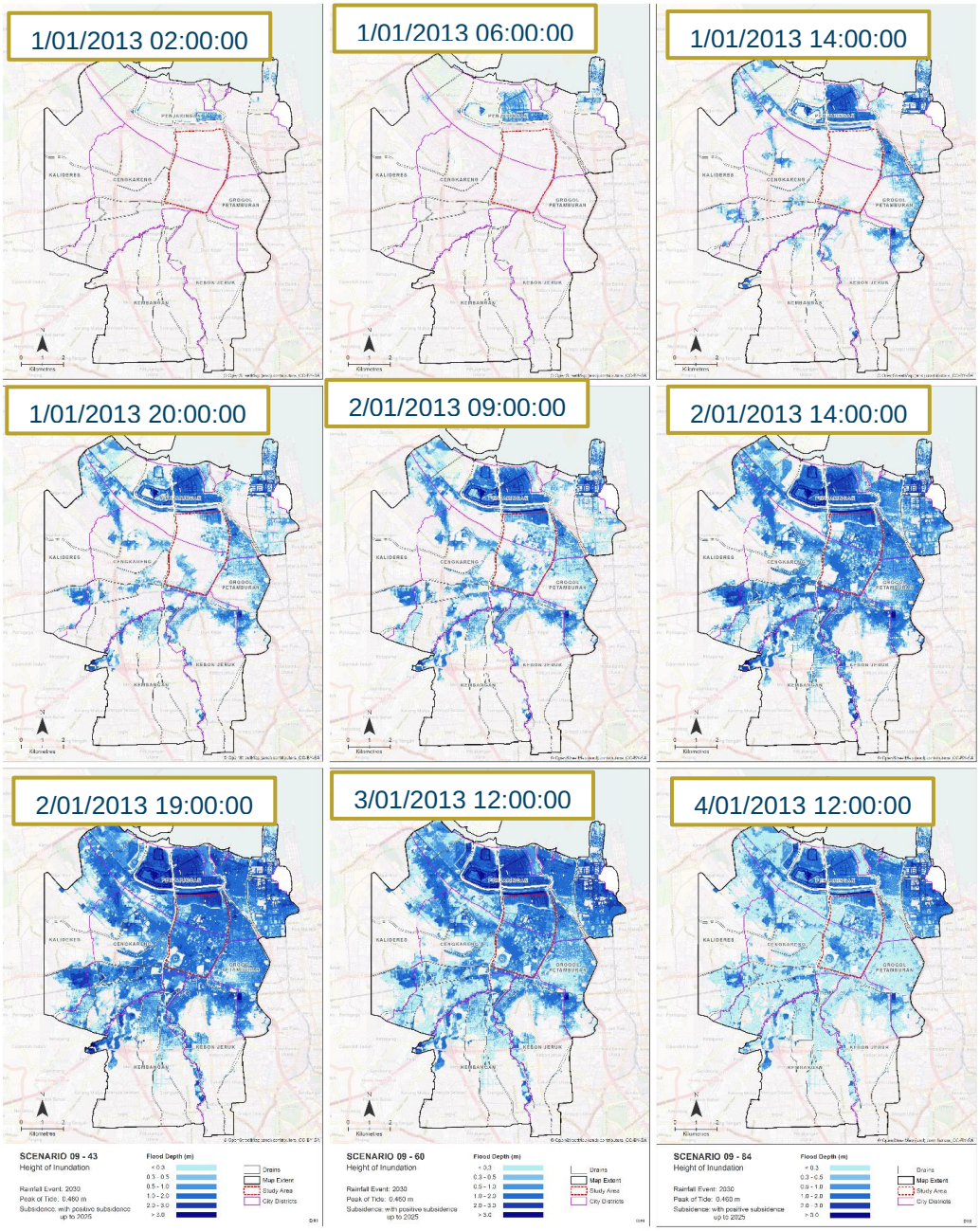

Figure 5 Dynamic flood maps from Scenario 9 model result. For 2030, the simulation period is not indicative of actual flood event, since rainfall/tide are derived from calculations

Test simulations have been done to further analyse the effects of tide in coastal flooding. DHI simulated two scenarios of 2030 tidal input without rainfall, i.e. no subsidence and with positive subsidence until 2025. Results in Figure 6 show that tide causes flooding in the projected subsidence in 2025, but not in 'no subsidence' scenario (i.e. 2012 ground levels). The flood caused by the tide has not reached the study area since the spreading of the flood only occurred in some part of Penjaringan district, especially in Pluit polder. It shows that tide will cause flooding but only when land subsidence is applied. Therefore, the flooding is mostly sensitive to the increase of rainfall/rainfall intensity.

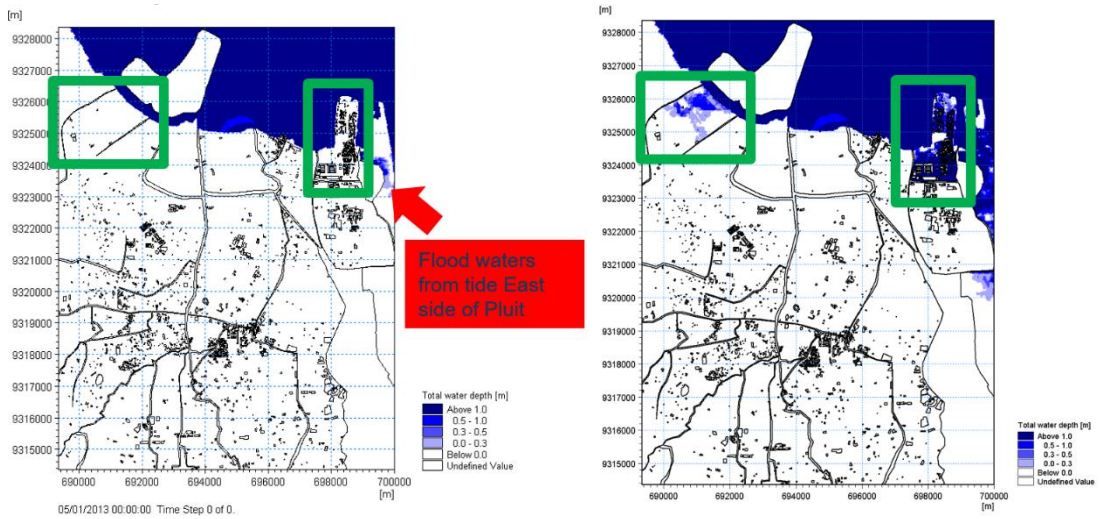

Figure 6 Model results with only 2030 tidal input. (Left) Without subsidence – 2012 DEM, and (right) with subsidence – until 2025.

The Blue Green Jakarta is the winning proposal in the Green Metropolis Jakarta 2050 competition. The retention pond included in Blue Green Jakarta is planned to be located in Kapuk Polder system (study area), because this area is continuously flooded, notably in 2007 and 2013. The area is also affected by land subsidence. This retention pond is a proposed measure in reducing the flood by diverting the flood into the pond. The retention pond is designed to help prevent the 50-year return period flood. Therefore, to estimate the capacity of retention pond, DHI's flood model results from Scenario 2 (2007 flood event with subsidence) were used. Furthermore, model results from Scenario 9 (2030 with subsidence) were also used for the pond capacity estimation as a mitigation of future flooding from climate change and subsidence in 2030, summarised in Table 4. This capacity estimation for 2030 (~11M m^3) is well within the estimation of Pond Capacity (10 – 15M m^3) described in the Blue Green Jakarta proposal.

Table 4 Estimation of the retention pond capacity

Year	Mean Flood Depth (m)	Pond Volume (m^3)	Depth in 200 ha Pond (m)
2007	0.84	7,463,854.30	3.73
2030	1.24	11,028,313.31	5.51

From the above results and analysis, the following conclusions can be made easily: the current flood model setup generates reasonable flood maps consistent with increasing rainfall, tide and subsidence. Current flood maps are validated with other models and surveys on 2007 (~50-year return period) and 2013 (~25-year return period) flood events. It is observed that flood is caused more by increased rainfall rather than tide and projected sea level rise. It is also observed that land subsidence significantly worsens the flooding, similar to the findings of previous studies. Further analysis of tidal influence show that coastal flooding from tides is observed only in future land subsidence scenarios (2025 projected ground levels). If a worst-case climate change scenario is taken into account, i.e. increased rainfall, the study area is almost fully inundated compared to 2007 flood event (one of worst flood occurred). The hydrodynamic model also provides the "weak points" where flood starts to overflow. This will help to mitigate the flood with different options for the relevant authorities in Jakarta.

1 Introduction

Jakarta is increasingly threatened by flooding from a combination of land subsidence, rising sea levels particularly with relation to the spring tide cycle and higher river levels resulting from potentially increasing rainfall intensity and land use changes within the catchment areas. Strategies currently defined to address these threats include but not limited to creation of a Giant Sea Wall (GSW) to reduce the risk of flooding and coastal inundation.

The objectives of the Climate Technology Centre & Network (further called CTCN) technical assistance are (i) to better assess flood risks and hazards, and (ii) to design climate-resilient pathways to reduce the magnitude and scale of the impacts from this flooding. This assessment and strategy definition will help shape the design of climate resilient infrastructure projects including, but not limited to, the GSW. The outcomes are (a) a hydrodynamic flood model that can be used to evaluate a number of hard and soft engineering interventions to reduce the risk of flooding (b) a socio-cultural survey to examine inhabitants' perceptions of flooding, levels of acceptable risks and preferred adaptation options, (c) a series of technology transfer workshops to increase local capacity in high resolution hydrodynamic modelling and use of the model, (d) resultant policy and planning recommendations to reduce flood hazards, risk and vulnerability, and (e) a roadmap to sustain and expand the project using additional funding streams.

To meet the expected outcomes mentioned above, the project is divided into the following activities:

- Activity 1 – Flood Risk Assessment
  - Activity 1A – Model development
  - Activity 1B – Sociocultural Risk Assessment
  - Activity 1C – Technology Transfer
- Activity 2 – Formulate Policy Recommendations
- Activity 3 – Developing further funding streams
- Activity 4 – Knowledge sharing and South-South Cooperation

This report will be presenting Activity 1A – Model development as a major part of Activity 1 – Flood Risk Assessment. The high-resolution hydrodynamic modelling of Jakarta has been done for a pilot project area in Northern Jakarta, and the result will be used as a basis for socio-economic risk assessment and as decision support system. This activity included data gathering from related institute, pre-processing of the data, modelling one dimensional model (further called as 1D model) using MIKE HYDRO River, modelling two dimensional model (further called as 2D model) using MIKE 21 Flow Model FM, and also couple 1D model and 2D model to get the flood area.

1.1 Objectives and Tasks

The objectives of Activity 1A – Model development is to develop a high resolution hydrodynamic model for a pilot project area in Jakarta that is capable of producing flood levels under various climate and/or engineering scenarios.

The following tasks are carried out sequentially to meet the objectives of Activity 1A: (1) Data gathering and pre-processing, (2) 1D modelling, (3) 2D modelling, (4) Coupling 1D and 2D modelling, (5) Production of Flood Maps, and (6) Analysis of flooding at the study area. Figure 1.1 summarises the workflow to accomplish these tasks.

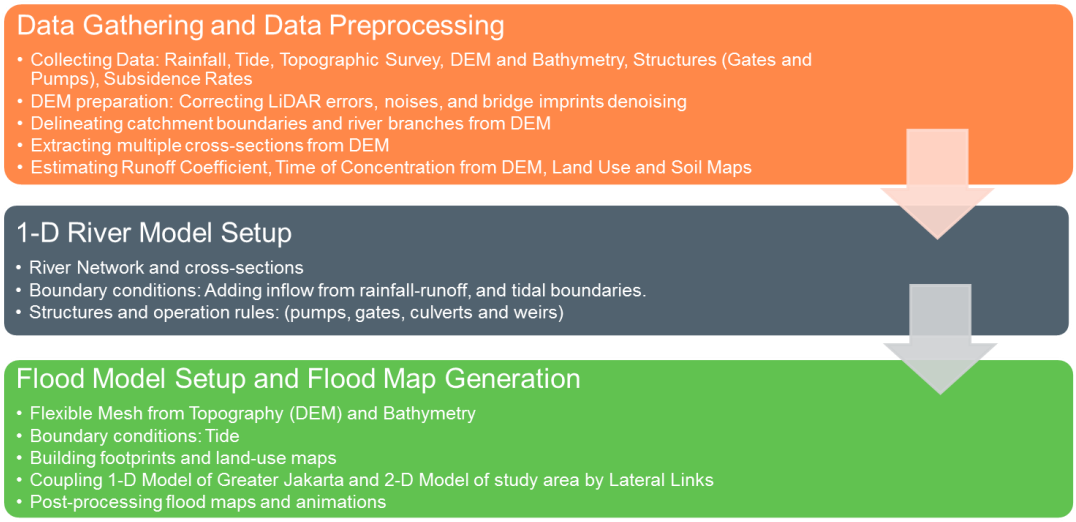

Figure 1.1 Workflow for Activity 1A - Model development.

1.2 Study Area

A flood model will be designed for a pilot project area in northern part of *Daerah Khusus Ibukota Jakarta* ("Special Capital City District of Jakarta"), henceforth called DKI Jakarta (Figure 1.2). The study area is located at an intersection of two cities: West Jakarta (Cengkareng district) and North Jakarta (Penjaringan district). The area has been chosen as one of the most flood-prone regions in Jakarta and is dominated by medium size commercial properties with additional medium-sized residential units, mainly to the north and south of the area.

Figure 1.2 (Left) The study area in northern part of DKI Jakarta shown in red polygon. (Right) Zoomed satellite image of the study area at the green circle. (Image source: Google Earth Pro)

According to the water planning agency of DKI Jakarta province, the study area is part of the west river system, which includes the following rivers and drainages: Pesanggrahan, Grogol, Sekertaris, Sepak/Uwangan, Cengkareng, Kamal and West Banjir Kanal (WBC). It is also an intersection of three polder system: Pantai Indah Kapuk polder (PIK polder), East Cengkareng polder, and Kapuk Poglar polder as shown in Figure 1.3. The area is dominated with warehouses and slum areas, with modern housing units in Pantai Indah Kapuk Polder. Snapshots of the environmental conditions at the study area are shown in Figure 1.4.

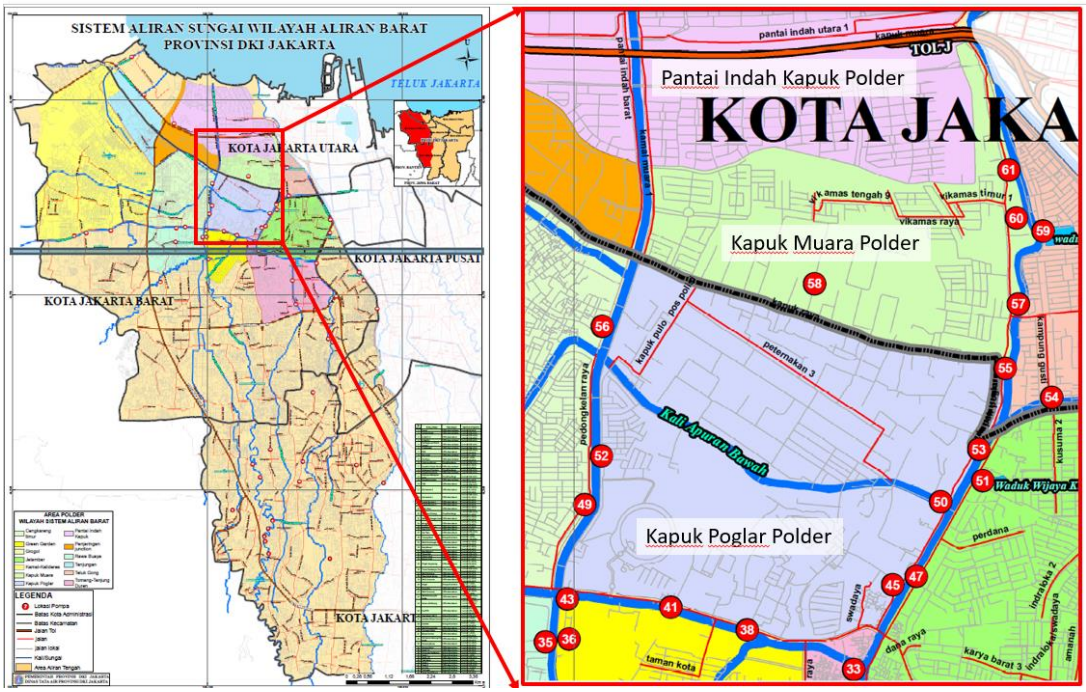

Figure 1.3 Three existing polders in the study area (red dash).

Figure 1.4 Ground photos at study area. Clockwise from top left: slum areas in Jalan Peternakan Raya; makeshift protections from flood; Angke river at the east side of the study area; warehouses.

Even though the pilot-scale project will only consider part of the total city drainage network and catchment of DKI Jakarta, it is essential that the flood model should include those parts of the wider network that are hydraulically connected to it, e.g. the east-west

flood canals. Therefore, a coarser model set up, with resolution of ~30m, is generated covering Greater Jakarta (urban areas surrounding DKI Jakarta) as a boundary condition to the study area flood model, as described in further detail in Chapter 3.

The report is hence divided into the following: Chapter 1 contains the introduction, objectives and study area of this project. Chapter 2 provides description of our methodologies; Model setup, calibration and validation are described in Chapters 3 and 4. Flood Maps are presented in Chapter 5 and discussions on Chapter 6. The report is concluded in Chapter 6 along with our recommendations for future studies. Appendix A (Comparison of SOBEK and MIKE Model) is also attached in this report.

2 Methodology

An overview of the modelling methodology employed for this project is provided below, including descriptions of the numerical modelling software and approach used, and the model input prepared for this study.

2.1 Flood Modelling by MIKE Software

The flood model will be simulated using 1D-2D coupled model. The flow in river and channel will be modelled using the 1D model MIKE HYDRO River software, and the inundation area will be captured in the 2D modelling program MIKE 21 Flow Model FM. The hydrodynamic interaction between the river and the flood areas will be handled by the 1D and 2D coupling software MIKE FLOOD.

2.1.1 MIKE HYDRO River (1D model and Rainfall-Runoff model)

DHI model will include all significant drainage to cater for all catchment areas under this study. The DHI 1D model, MIKE HYDRO River, is capable of simulating channel flow in common drainage structure such as culverts, weirs, gate operations, etc. The MIKE HYDRO River model schematises the significant river network as 1D channels, as well as simulating the rainfall-runoff process as detailed input to this network. The rainfall-runoff processes are simulated by the Rainfall-Runoff model (further called RR model). Therefore, the 1D model consists of two primary components:

- Hydrological model: simulating rainfall-derived runoff into the river network
- Hydraulic model: simulating water levels and discharges throughout the river network

Catchment runoff is proposed to be estimated using the Unit Hydrograph Model (UHM). The Unit Hydrograph approach applied by MIKE Hydro River is a single storm event model with parameters directly related to the physical characteristics of the catchments. As such, the model is particularly adapted to simulate the hydrological conditions of an existing catchment without gauging data or to simulate future land-use scenarios. The model divides the storm rainfall in excess rainfall (runoff) and water loss (infiltration), described as follows:

- Runoff: The SCS dimensionless hydrograph is derived from a large number of natural unit hydrographs from catchments of varying size and location
- Infiltration: Infiltration is calculated as a proportional loss from the rainfall input, employing the Runoff Coefficient and Lag Time that characterizes the catchment in terms of soil type and land use

With its intuitive, user-friendly interface, MIKE HYDRO River provides advanced facilities for the input of necessary data, as well as the review and presentation of results. A screen shot of in the MIKE HYDRO River interface is provided in Figure 2.1, showing the modelled river network and catchment map, sample cross-section at Cengkareng, and sample boundary conditions of highest Tide and 100-year rainfall-runoff.

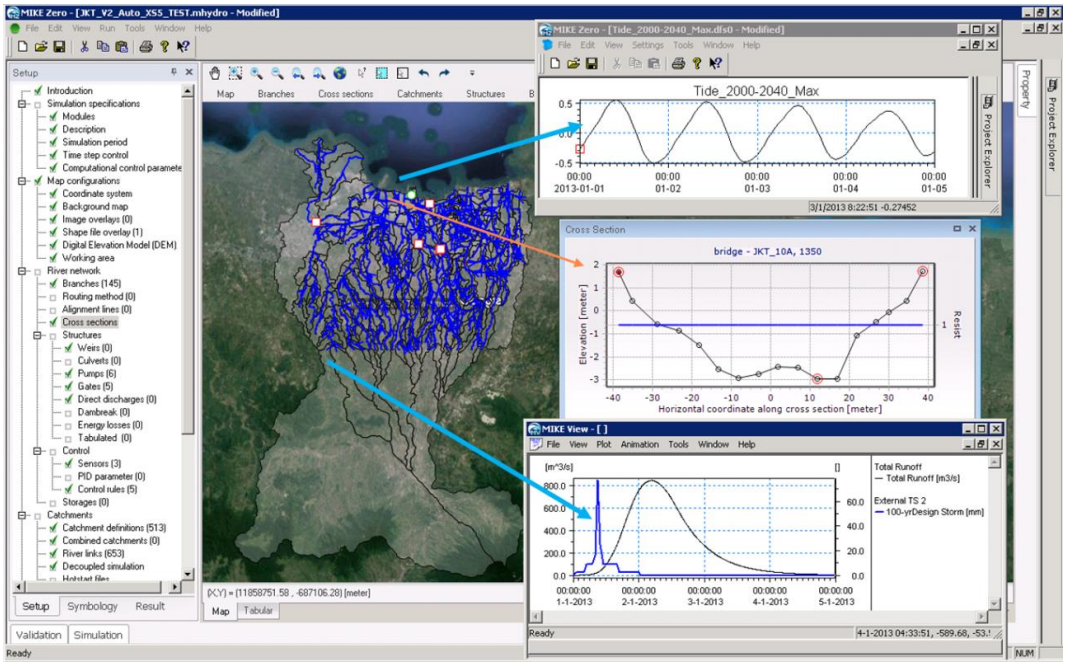

Figure 2.1 MIKE HYDRO interface

2.1.2 MIKE 21 Flow Model FM (2D Model)

DHI's 2D model, MIKE 21 Flow Model FM, is used to identify the level of inundation arising from coastal and inland inundation and any residual overland flow identified from the 1D model. The 2D model is capable of modelling the flow of water on land and through common urban features by using flexible mesh (FM) as its computational grid.

MIKE 21 Flow Model is a modelling system for 2D free-surface flows. MIKE 21 Flow Model is applicable to the simulation of hydraulic and environmental phenomena in lakes, estuaries, bays, coastal areas and seas. It may be applied wherever stratification can be neglected. The hydrodynamic (HD) module is the basic module in the MIKE 21 Flow Model. It provides the hydrodynamic basis for the computations performed in the Environmental Hydraulics modules.

The application areas are generally problems where flow and transport phenomena are important with emphasis on coastal and marine applications, where the flexibility inherited in the unstructured meshes can be utilized.

The use of flexible mesh in MIKE 21 Flow Model FM offers flexibility in resolving the geometry. When necessary, the triangular and quadrangular elements can be combined to allow resolution of channelized flows with quadrangular elements, such as the incised main channel seen clearly running east of the eye of the spur. High resolution in the main area of interest will be schematized with the DEM provided. Coarser horizontal scales can be utilised for areas outside the immediate area of interest.

The modelling system is based on the numerical solution of the two-dimensional shallow water equations - the depth-integrated incompressible Reynolds averaged Navier-Stokes equations. Thus, the model consists of continuity, momentum, temperature, salinity and density equations. In the horizontal domain both cartesian and spherical coordinates can be used.

The spatial discretization of the primitive equations is performed using a cell-centered finite volume method. The spatial domain is discretized by subdivision of the continuum

into non-overlapping element/cells. In the horizontal plane an unstructured grid is used comprising of triangles or quadrilateral element. An approximate Riemann solver is used for computation of the convective fluxes, which makes it possible to handle discontinuous solutions. An explicit scheme is used for the time integration.

2.1.3 MIKE FLOOD (1D-2D coupled model)

MIKE FLOOD is the most complete toolbox for flood modelling available. It includes a wide selection of 1D and 2D flood simulation engines, which enables modelling virtually any flood problem - whether it involves rivers, floodplains, floods in streets, drainage networks, coastal areas, dam, levee and dike breaches or any combination of these. The basic MIKE FLOOD model schematization to be used for this study is presented in Figure 2.2

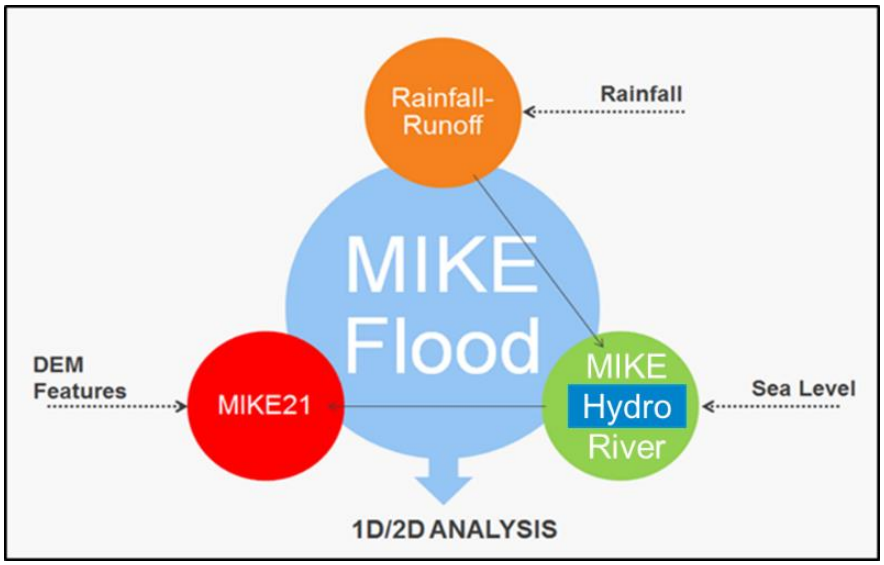

Figure 2.2 MIKE FLOOD approach (DHI, 2016a)

Figure 2.3 presents a visual impression of a coupled MIKE HYDRO River and MIKE 21 Flow Model FM model using MIKE Flood. The modelled river network, extending from the top of the image down, is schematized as 1D branches using MIKE HYDRO River, while MIKE 21 Flow Model FM is used to model the coastal area in the lower half of the image, indicated by the 2D grid. These two models are coupled at the coastline at two locations, as shown by the green boxes in Figure 2.3.

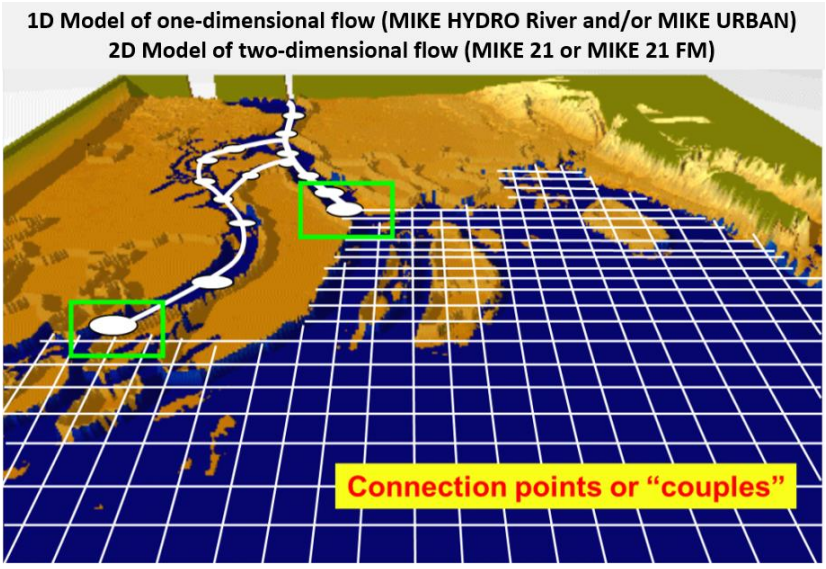

Figure 2.3 Coupling of MIKE HYDRO River and MIKE 21 Flow Model FM through MIKE FLOOD (DHI, 2016a)

For this modelling study, the coupling of the MIKE HYDRO River and MIKE 21 Flow Model FM model is made through lateral linkage options provided in MIKE FLOOD. Schematisation of lateral links is illustrated in Figure 2.4.

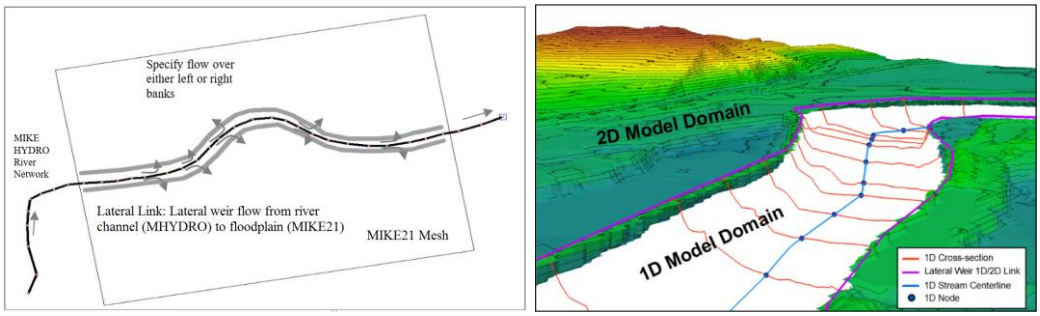

Figure 2.4 Lateral linkage option in MIKE FLOOD (DHI, 2016b).

The main inputs needed for the coupled 1D-2D coupled model are bathymetry, rainfall, tide, and structures. Data gathering and pre-processing for these model inputs are described in the next sections.

2.2 Topography and Bathymetry

Topography and bathymetry data were generated from different sources. Topography data in the model is taken primarily from a fine-resolution Digital Elevation Model (DEM), while bathymetry data was generated from previous DHI models. These two datasets have been combined to be used as the main input for the 2D flood model. The DEM data is also extensively used to generate several model components in the 1D model, i.e. catchments, river network and cross-sections. This section also includes the application of land subsidence rates in the study area by modifying the base topography. Beside for mesh generation, DEM data also has been used for catchment and river delineation, as well as cross-section generation. In this project, impact of land subsidence also has been assessed by running the model with modified topography that already added with subsidence map.

2.2.1 Digital Elevation Model (DEM)

The DEM data play the most important rule for this project. DEM data will be used to generate the cross-section, river network and catchment definition. The current DEM used in this project is based on the Light Detection and Ranging (LiDAR) data of that was generated in the year 2012, which is provided by the Water Management Agency (DTA). The LiDAR DEM data given to DHI has been pre-processed so that extracting "bare earth" from "surface models", in which typical raw LiDAR DEM data includes tree covers and building heights, was not necessary. The spatial resolution of the LiDAR DEM data is ~1.33 m. and covers the area of Jakarta as shown in Figure 2.5.

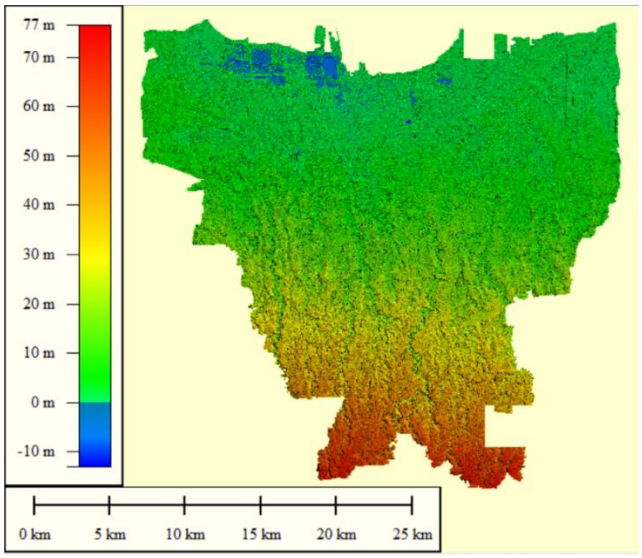

Figure 2.5 LiDAR DEM data of DKI Jakarta for year 2012.

The coverage of the LiDAR DEM data must be extended to include the whole Pessangrahan and Ciliwung catchments, the two main catchments draining in our area of interest, as well as the Cisadane river system at west of Jakarta. This was done by filling the data gap with DEM based on ALOS 30-m. Advanced Land Observing Satellite (ALOS) is a Japanese satellite, which its captured images are used to derive the raw Digital Surface Model (DSM). The ALOS DSM is a public-access data with ~30-m horizontal resolution at the equator (http://www.eorc.jaxa.jp/ALOS/en/aw3d30/). Further processing of this dataset includes patching null values using the more commonly used Shuttle Radar Topography Mission (SRTM) 30-m DSM (http://www2.jpl.nasa.gov/srtm/). The mosaic DSM is converted to DTM (Digital Terrain Model) using DTM Filter (radius 1, slope percent 100) based on Vosselman (2000). Bare earth is extracted using Multi-level B-Spline interpolation. Further resampling is applied in the ALOS+SRTM mosaic 30-m DEM to match that of LiDAR dataset using bilinear interpolation.

Aside from extending its coverage, the LiDAR DEM also has artefacts that needs to be corrected, such as striping errors, stretched pixels, and missing patches. Localized corrections, as in the case for striping errors, are done by focal mean, while errors in wider areas are patched with the aforementioned ALOS+SRTM mosaic DEM. Figure 2.6 illustrates these corrections applied in some areas of the DEM.

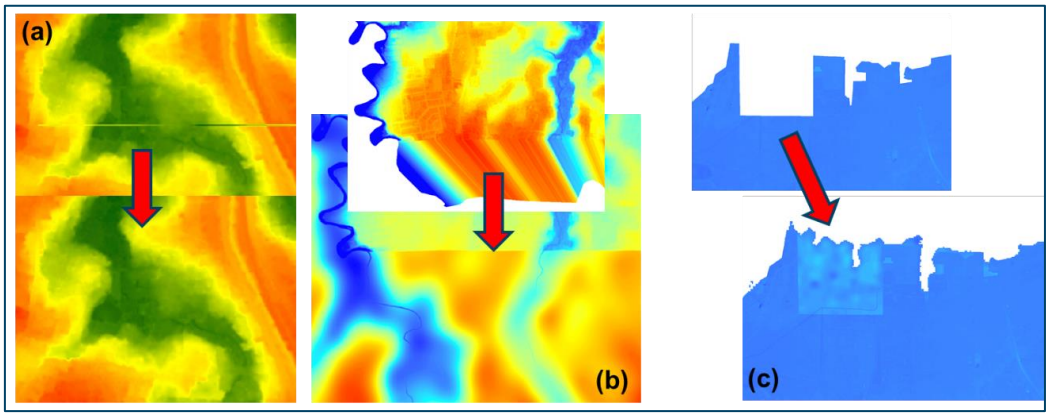

Figure 2.6 Errors and correction applied in LiDAR DEM: (a) striping errors corrected by focal mean, (b) stretched pixels and (c) missing patches filled with ALOS+SRTM mosaic DEM.

Another necessary pre-processing of the DEM data include denoising, i.e. reducing noise and spikes from the fine resolution images captured by LiDAR. This was achieved by combination of multiple pre-processing techniques, first of which was by resampling the DEM from 1.33-m to 3-m resolution. The resampling technique reduces noises and spikes in the DEM, especially along the river branches where LiDAR was able to capture debris and temporary sedimentation. In Figure 2.7, it is seen that the 3-m DEM was able to preserve road imprints and changes in terrain when compared to the original 1.33-m data.

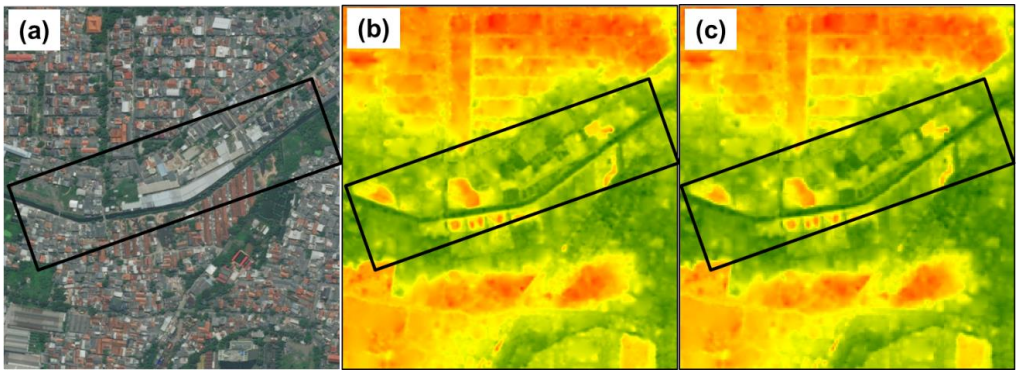

Figure 2.7 Comparison of original and resampled DEM: (a) Google Earth Pro imagery of an urban area of Jakarta with a river drain, (b) original LiDAR 1.33-m DEM, (c) resampled LiDAR 3-m DEM

Impediments inside the rivers, e.g. bridges, debris and sedimentation, were removed to ensure correct drainage delineation. This was done by hydro-enforcement, a process applied in fine-resolution DEMs to ensure that lakes and reservoirs are level and streams flow downstream (Maune, 2010). To hydro-enforce rivers inside the DEM, LiDAR elevated values such as elevation of bridges are removed and replaced by interpolation between nearest upstream and nearest downstream water level values. Thus, the centerline of the rivers and their flow paths should be provided. For this project, existing drawings and maps of drainage network in Jakarta are used, as discussed more in Section 3.1.2. This process is applied extensively in central part of Jakarta where multiple bridges and presence debris and sedimentation were captured, an example of which is illustrated in Figure 2.8.

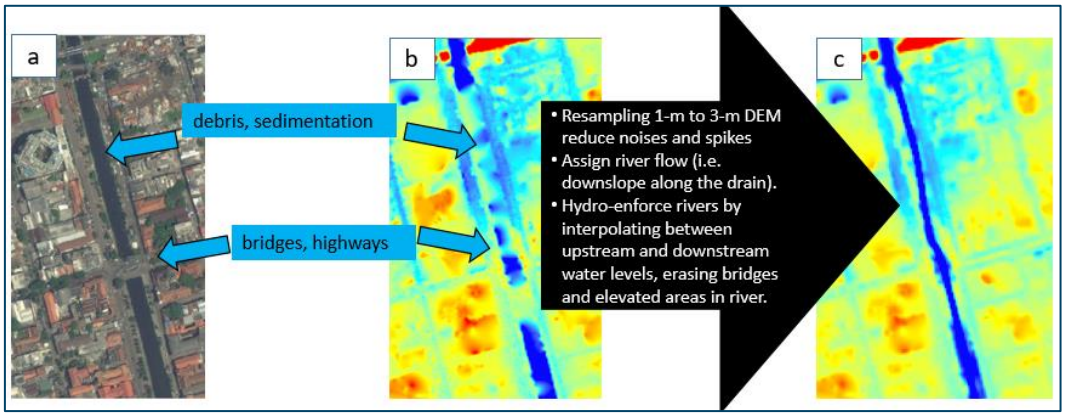

Figure 2.8 The overview of LiDAR data pre-processing: (a) Google Earth Pro image, (b) the original DEM, (c) final DEM after hydro-enforcement.

Further adjustment to the DEM is applied because of the complex drainage network and polder systems inside central Jakarta. In low-lying areas in between river canals, manual adjustments are made along the riverbanks so water systems can be distinguished from land elevations. Looping canal network such as in polders are simplified during the pre-processing stage, and are reinstituted back in 1D model setup (Chapter 3) to reflect the multi-directional river flow in the polder system.

The final DEM, as show in Figure 2.9, is a composite of DEM at 3-m and 30-m resolution. The red box shows the coverage of the 3-m LiDAR DEM (extended with ALOS+SRTM mosaic DEM), and is the current extent of the 1D river modelling. The rest of the area use ALOS+SRTM mosaic DEM with 30-m resolution to cover the entire major catchments flowing through Jakarta.

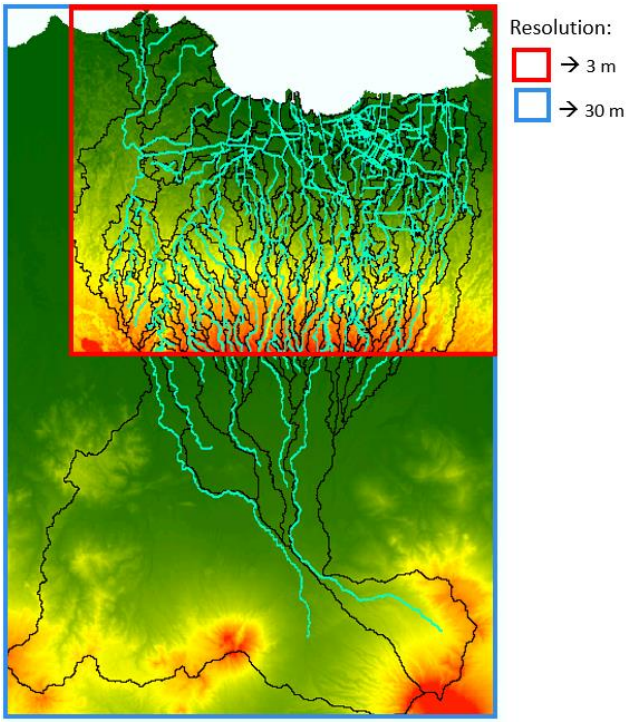

Figure 2.9 Final DEM data used in the Jakarta flood model. The river network and catchments are also shown for reference.

Using this DEM, we were able to delineate the river network and catchment boundaries. The DEM is also used to generate cross-sections of the rivers. Both processes are further discussed in the Sections 3.1.2 and 3.1.3. The DEM is also used as the bathymetry input in 2D modelling in Section 3.2.

2.2.2 Land Subsidence Map

The land subsidence map for DKI Jakarta used in generating past and future topographical conditions is obtained from Budiyono *et al.* (2016). Values in Figure 2.10 represent subsidence depths from 2013 to 2025 in meters. From that data, a yearly subsidence rate was calculated and used to generate topographies for the years 2007, 2013, and 2025. It should be noted that in the referenced paper, it is stated that land subsidence reaches a plateau in 2025.

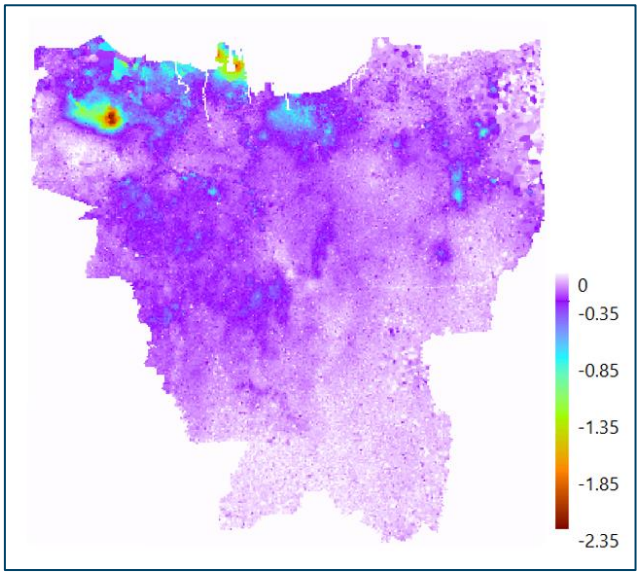

Figure 2.10 Land subsidence depths from 2012 to 2025 in meters to be used in generating past and future topographies. Source: Budiyono *et al.* (2016)

Figure 2.11 shows the generated topographies in the study area. The final DEM, as stated above, represents topography in 2012. The calculated land subsidence rates are then applied to the DEM values to extrapolate topographies for different years. For year 2007, negative subsidence rates are applied, i.e. the land elevation levels increase from 2012 values. For years 2013 and 2025, subsidence depths calculated in one year and in 13 years are applied respectively. As is with the 2012 DEM, the extrapolated topographies are used to generate cross-sections of the rivers and as bathymetry input in 2D modelling for their respective scenarios.

The pre-processed land subsidence applied to the final DEM and to be used for generating cross-section and mesh. In the final, there are 4 final mesh, i.e. the baseline mesh (using schematization of 2012), three mesh for scenarios subsidence (2007, 2013, and 2025). The final topography used for all scenarios can be seen in Figure 2.11, where the effect of subsidence to the mesh (topography) can be seen in the north part of concerned area.

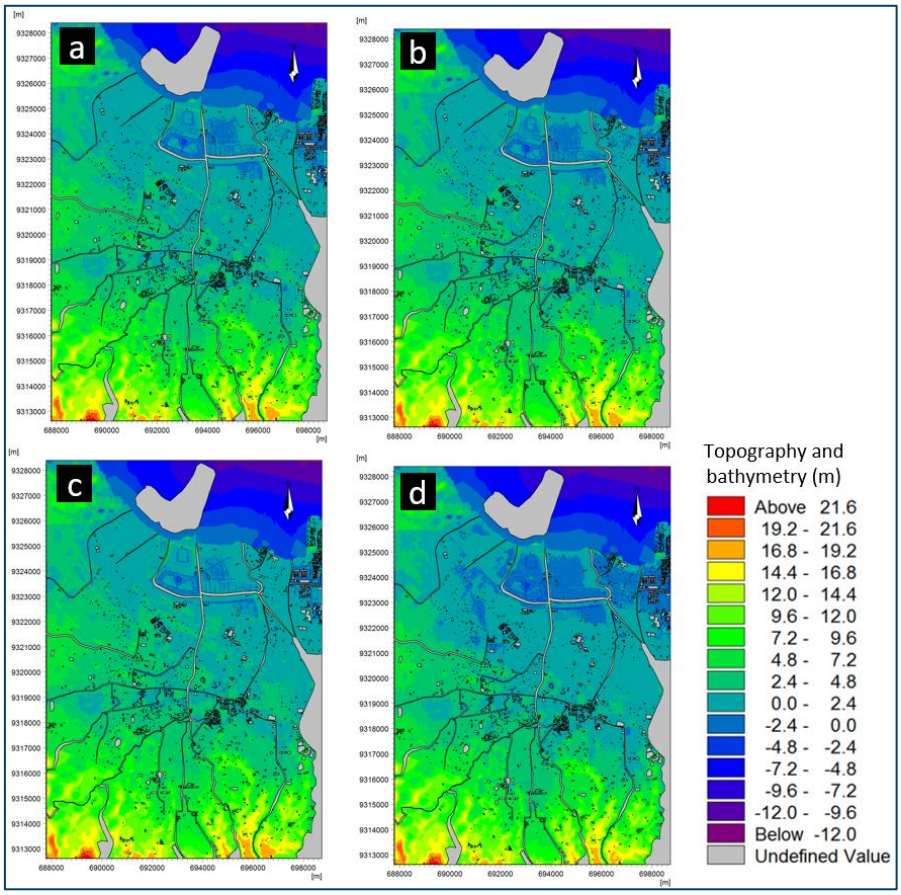

Figure 2.11 Topographies for (a) 2012 derived directly from DEM, (b) 2013 where one year subsidence is applied from 2012, (c) 2007 where negative subsidence is applied from 2012, and (d) 2025 – 13 years of subsidence from 2012.

2.3 Rainfall

The rainfall data used in this project are the actual rainfall data and designed storm data. Actual rainfall data is used in simulations for 2007, 2012 and 2013 rainfall events. The designed storm data has been used for climate change scenario. The actual rainfall data is provided by Meteorological, Climatological, and Geophysical Agency (BMKG), while the designed storm data was derived from design storm generation as described in van der Sleen and Lopez (2013).

Based on the discussions with Jakarta Research Council (further called JRC) team, three particular rainfall events that caused notably huge flooding in Jakarta have been selected for model simulations, i.e. flood in 2007, 2012, and 2013. Also from the discussion, 2030 and 2050 have been chosen for climate change scenarios. The total number of rainfall stations that have been used in this project is 67 stations but only a few stations have data for all the five years. Hence, there are 41 stations for 2013; 51 stations for 2012; 29 stations for 2007 and 12 stations for 2030 and 2050 used for modelling scenarios. The location of the rainfall stations are shown in Figure 2.12.

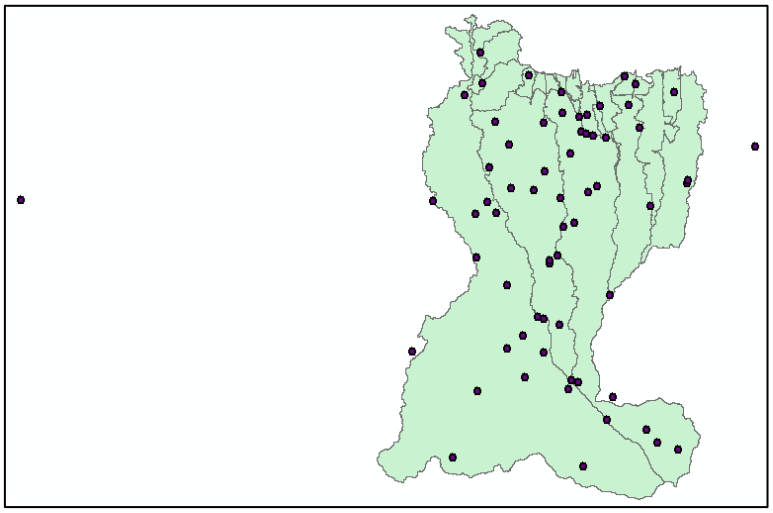

Figure 2.12 Available rainfall stations in DKI Jakarta.

2.3.1 Actual rainfall

As described above, the rainfall for actual scenario was provided by BMKG. Two types of rainfall instrumentation was used to gather rainfall data: one is from technical implementation unit stations of BMKG (further called as UPT stations) and BMKG *Pos Hujan* ("rainfall stations"). The rainfall data from those two station types have slightly different recording periods and different data sampling time as seen in Table 2.1. The data from UPT stations are recorded four times daily while the data from rainfall station is recorded daily.

From the discussion with JRC, 4-5 days of model simulation period should be done for each rainfall event that includes the days of the flooding event, 1 day prior to the flooding event for initialization, and 2 days succeeding the flooding event to capture flood recession conditions. All recorded data for the full 4-5 days of simulation period were then obtained upon request made to BMKG. A summary of the rainfall data are summarized in Table 2.1.

Table 2.1 Summary of rainfall data recordings provided by BMKG.

Year	Simulation Period	Rainfall data from UPT station	Rainfall data from BMKG *Pos Hujan*
2007	31 January 00:00 UTC - 5 February 00:00 UTC	29 January 00:00 UTC – 4 February 00:00 UTC	28 January 00.00 UTC – 5 February 00:00 UTC
2012	20 December 00:00 UTC - 24 December 00:00 UTC	18 December 00:00 UTC – 24 December 00:00 UTC	17/18 December 00.00 UTC - 25 December 00.00 UTC
2013	15 January 00:00 UTC - 19 January 00:00 UTC	13 January 00:00 UTC – 19 January 00:00 UTC	11 January 00.00 UTC – 20 January 00.00 UTC

2.3.2 Design Storm and Climate Change Factors

The design storm used in this project is derived from design rainfall of 50-year return period. climate change factors are determined from literature, which calculated values obtained from Global Climate Model (GCMs) and Representative Concentration Pathways (RCPs) scaled down to Jakarta region. The rainfall data from 12 stations to be used for design storm generation were obtained from van der Sleen and Lopez (2013), provided in Table 2.2.

As agreed during the discussion with JRC, a 50-year return period of rainfall will be used to simulate rainfall events for 2030 and 2050 scenarios. This return period was chosen to coincide with the 2007 rainfall event, which was calculated as a 50-year rainfall event (Budiyono *et al.*, 2016). For initialization, the first day of the simulation period (also one day prior to the 50-year return period of rainfall) will have 1-year return period of rainfall.

Table 2.2 Derived daily rainfall in mm for 1-year and 50-year return period values from van der Sleen and Lopez (2013).

Station	Return period	
	1-year	50-year
Cengkareng	76	202
Kemayoran	92	196
Ragunan	86	164
Jatipadang	84	177
Ciputat	78	174
Depok	92	189
Bojonggede	100	187
Bogor(DamEmpang)	110	209
Gunungmas	99	183
Gunung Geulis	112	192
Gunung Sindur	89	191
Cidokom	90	201

To calculate daily rainfall events for 2030 and 2050, the values in Table 2.2 were multiplied by their respective climate change factors. These factors are derived from 20 GCMs+RCP combination averages determined in Budiyono *et al.* (2016), presented in the first two columns in Table 2.3. It is worth noting that the calculated median for 2030 and 2050 are factors less than one, i.e. rainfall is reduced during the first decades of climate change scenarios. According the Budiyono *et al.* (2016), these median values reflect drought conditions projected in Jakarta region. Upon discussion with JRC however, we agreed to simulate worst-case climate change flooding scenarios to aid in policy-making decisions. Hence, for this study, we calculated upper percentiles from the median values to obtain projected flooding conditions in Jakarta for 2030 and 2050. The

upper 75-percentile values were chosen as climate change factors for this study, as summarised in Table 2.3.

Table 2.3 Climate change factors from five GCMs and four RCPs. Modified from Budiyono *et al.* (2016).

	5 GCM Median	5 GCM Std	upper 68%	upper 95%	upper 75%
2030 RCP2.6	0.79	0.33	1.12	1.45	1.18
2030 RCP4.5	0.76	0.47	1.23	1.70	1.31
2030 RCP6.0	0.79	0.51	1.30	1.81	1.39
2030 RCP8.5	0.85	0.49	1.34	1.83	1.43
2030 RCP Average	0.80	0.45	1.25	1.70	1.33
	5 GCM Median	**5 GCM Std**	**upper 68%**	**upper 95%**	**upper 75%**
2050 RCP2.6	0.79	0.32	1.11	1.43	1.17
2050 RCP4.5	0.82	0.48	1.30	1.78	1.39
2050 RCP6.0	0.79	0.56	1.35	1.91	1.45
2050 RCP8.5	0.96	0.58	1.54	2.12	1.64
2050 RCP Average	0.84	0.49	1.33	1.81	1.41

2.3.3 Hourly Rainfall and Mean Areal Precipitation

Since we are modelling event-based flooding, the daily rainfall data needs to be discretised into smaller, more meaningful time steps. A standard hyetograph in van der Sleen and Lopez (2013) is used to converted daily data to hourly data as illustrated in Figure 2.13. The indicative rainfall peak happens on the ninth hour within 24-hours. This is kept for rainfall in 2030 and 2050. For 2007, 2012 and 2013 rainfall, the converted hourly rainfall is adjusted in time such that its rainfall peak coincides with the peak of that actual rainfall events recorded in UPT stations.

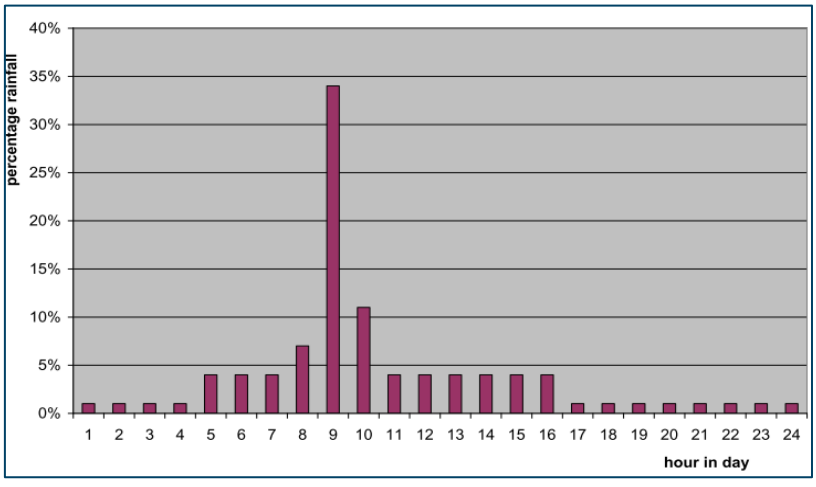

Figure 2.13 Assumed standard hyetograph. (Source: van der Sleen and Lopez, 2013).

The differences of rainfall input in one of the rainfall station can be seen in Figure 2.14. The station was located in Depok. From the figure, we can see that the design storm rainfall (2030 and 2050 scenario) has higher rainfall intensity compared with actual rainfall (2007, 2012, and 2030 scenario). The figure also show that compared with all actual ranfall scenario in that location, the highest rainfall occurred in 2007, while the lowest occurred in 2012.

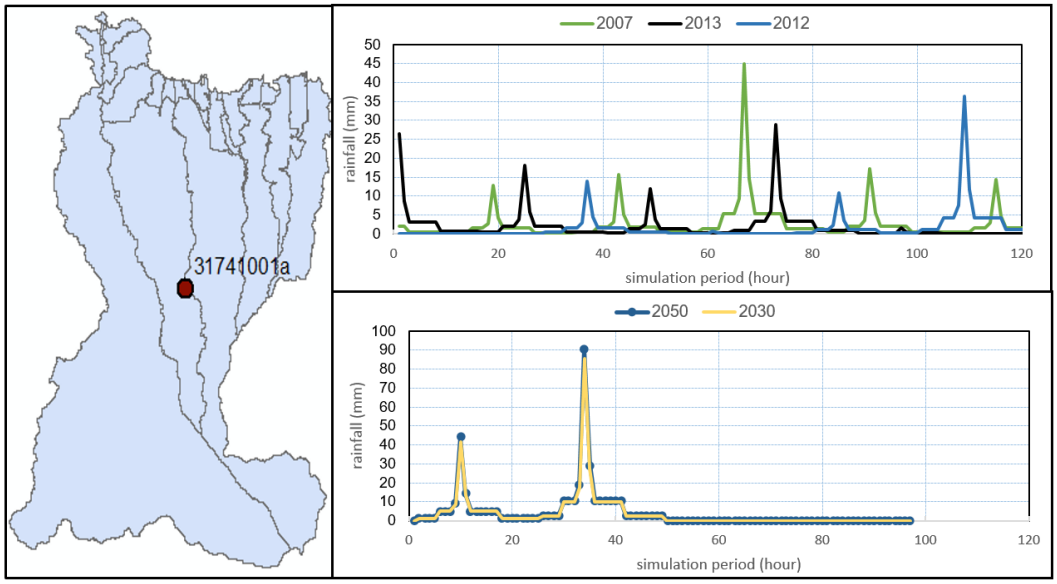

Figure 2.14 Comparison rainfall input in station number 31741001a (Depok); left: station location, right: the rainfall input

The project used all available rainfall data from rainfall stations that has been prepared by the procedures discussed in previous paragraphs. After consistency and quality checks, we were able to collate the following number of stations for each rainfall event: 41 stations for 2013; 51 stations for 2012; 29 stations for 2007 and 12 stations for 2030 and 2050 (climate change scenarios). In order to determine the weights of each rainfall station as representative rainfall within a single catchment area, the mean areal rainfall for each combination of stations is generated by Thiessen method, a commonly used methodology by A.H. Thiessen (2011). This method assumes that at any point in the catchment, the rainfall is the same as that at the nearest gauge so the depth recorded at a given gauge is applied out to a distance halfway to the next station in any direction. Some gauges are therefore considered more representative of the area in question than others. Areas corresponding to each gauge are determined through the construction of Thiessen polygon network, where the polygon boundaries are formed by the perpendicular bisectors of the lines joining adjacent gauges. Figure 2.15 shows the Thiessen polygons for 2013 rainfall event, which used 41 rainfall stations.

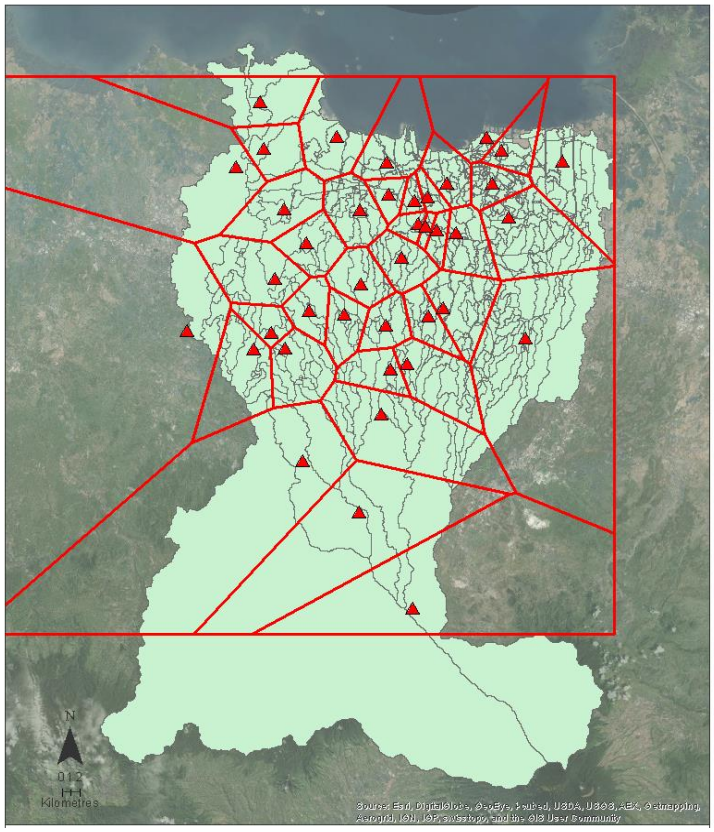

Figure 2.15 Spatial distribution of available rainfall station for 2013 rainfall event by Thiessen polygon method (in red), overlaid on catchment map for Jakarta (in green).

2.4 Tide

Tidal data was used as a boundary data in MIKE HYDRO River and MIKE 21 Flow Model FM. The tidal data for 2007, 2012, and 2013 scenario was obtained from tidal prediction models from DHI, while tidal data for 2030 and 2050 was obtained by applying the sea level rise to the Mean Highest High Water (MHHW). Model values are extracted from the point in Jakarta Bay nearest to the study area.

The tidal prediction models used tidal constituents from Hydrography and Oceanography Agency of Indonesia Navy (DISHIDROS). Zero value was assumed as a datum for this prediction. The data is already shifted in Greenwich Time. The predicted tidal data can be seen in the figures below.

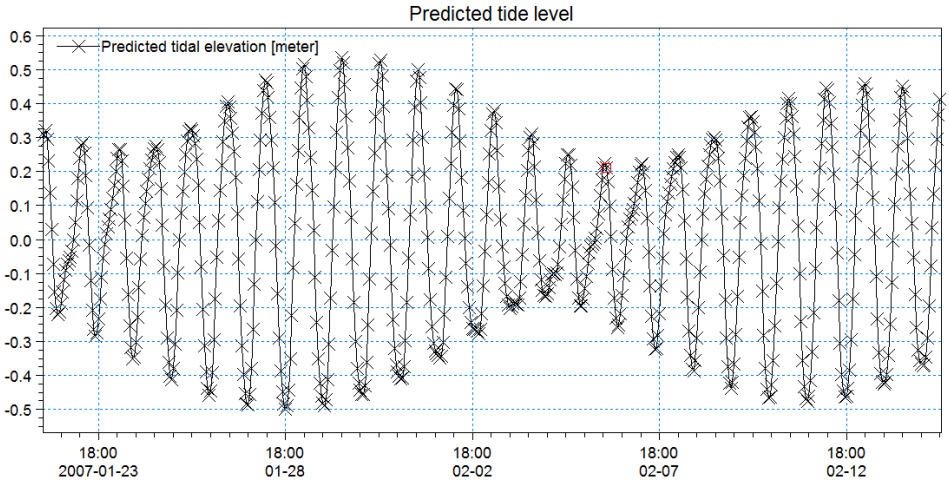

Figure 2.16 Predicted tidal elevation for 2007 scenario

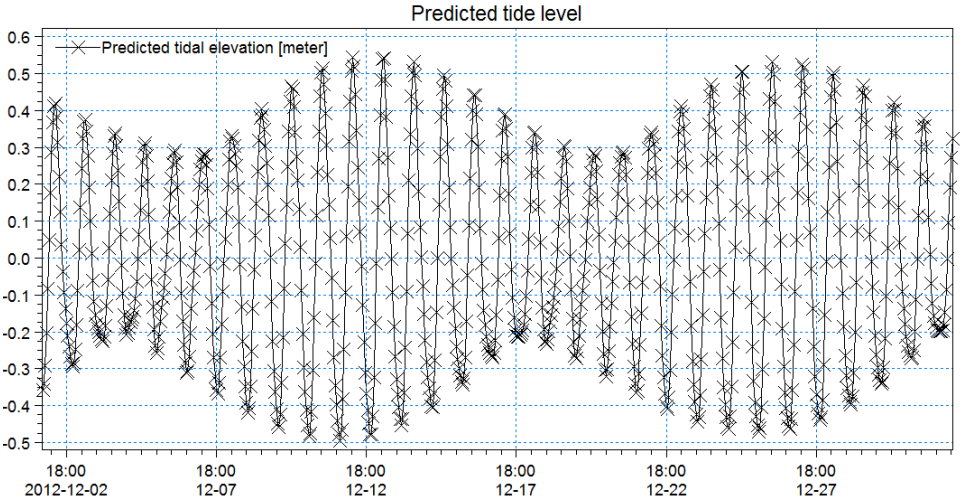

Figure 2.17 Predicted tidal elevation for 2012 scenario

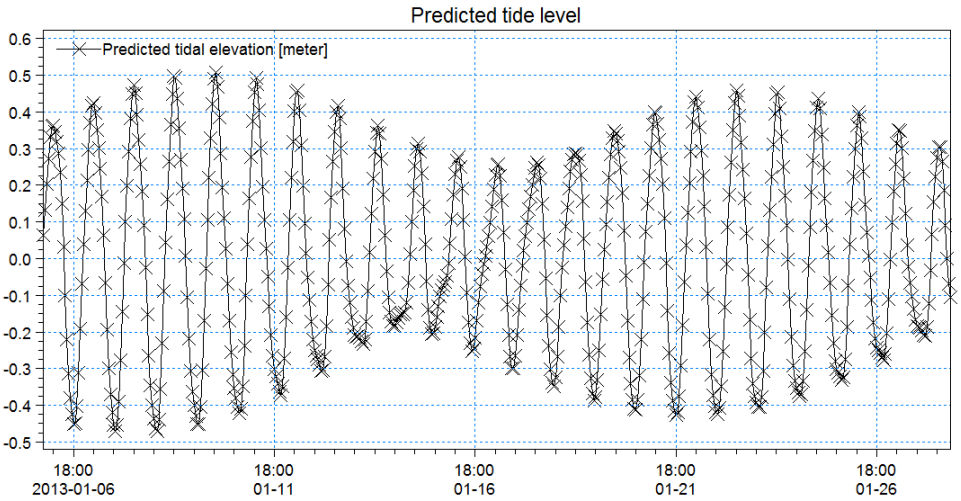

Figure 2.18 Predicted tidal elevation for 2013 scenario

Formzahl numbers are also calculated using DISHIDROS tidal constituents. The calculated formzahl numbers nearest to our study area is 4.67, which means the tidal in Jakarta is of diurnal type. From DISHIDROS tidal constituents, some statistical values for

peak tide levels can be calculated as shown in Table 2.4. Again, zero is assumed as the datum. For 2030 and 2050, MHHW was considered as the base peak tide level, since it represents a worse-case flooding scenario than other mean values.

Table 2.4 Water level statistic derived from DISHIDROS.

Statistic	Peak Tide Water Levels (m)
Highest Astronomical Tide (HAT)	0.620
Mean Highest High Water (MHHW)	0.235
Mean Lowest High Water (MLHW)	0.105
Mean Highest Low Water (MHLW)	-0.055
Mean Lowest Low Water (MLLW)	-0.235
Lowest Astronomical Tide (LAT)	-0.568

2.4.1 Sea Level Rise

The peak tidal water level for 2030 and 2050 is calculated by MHHW plus sea level rise values to represent the projected sea level rise for climate change scenarios. Sea level rise values for 2030 and 2050 was calculated based on sea level rise estimation done by BAPPENAS (2010). The reference paper projected sea level rise using altimeter, tide gauge, and model data. The result shows the same trend, with average rise rates ranging from 0.6 cm per annum to 0.8 cm per annum. The projection for the average increase of the sea level in the Indonesian waters is summarized in Table 2.5.

Table 2.5 Projection of the average increase of sea level in Indonesian water (Source: Bappenas, 2010)

Period	Sea Level Rise Projection since 2000			Level of confidence
	Tide Gauge	Altimeter ADT	Model	
2030	24.0 cm ± 16.0 cm	16.5 cm ± 1.5 cm	22.5 ± 1.5 cm	Moderate
2050	40.0 cm ± 20.0 cm	27.5 cm ± 2.5 cm	37.5 ± 2.5 cm	Moderate
2080	64.0 cm ± 32.0 cm	44.0 cm ± 4.0 cm	60.0 ± 4.0 cm	High
2100	80.0 cm ± 40.0 cm	60.0 cm ± 5.0 cm	80.0 ± 5.0 cm	High

The tide time series is extracted from the tide prediction model where the peak tide level is the calculated MHHW plus sea level rise. Then, to simulate a worst-case scenario of flooding, the peak tide level must coincide with the peak runoff inland. Hence, the tide time series is adjusted in time to match with the calculated peak total runoff from design storm events, as demonstrated in Figure 2.19.

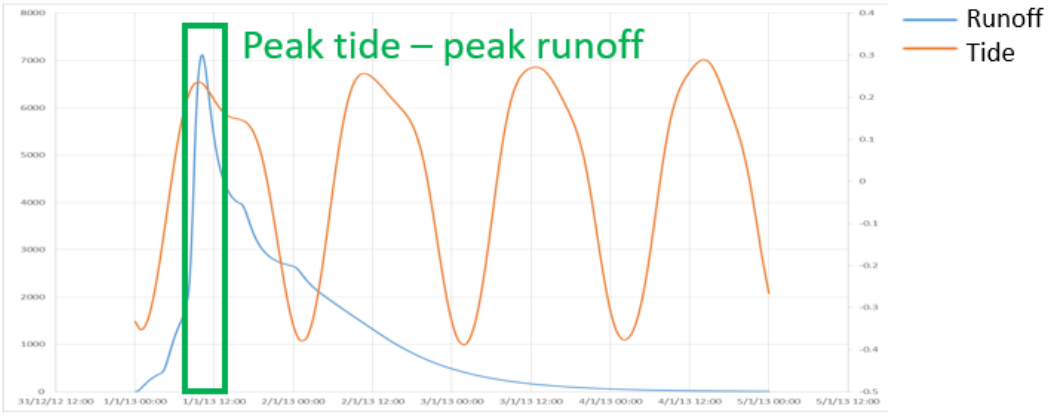

Figure 2.19 Adjustment of tide time series to simulate worst-case climate change scenario.

The differences of the tidal input for years 2007, 2012, 2013, 2030 and 2050 can be seen in Figure 2.20. The figure shows that the highest water level occurred in 2050. The highest tidal range occurred in 2007, because in this time the tide was in spring condition.

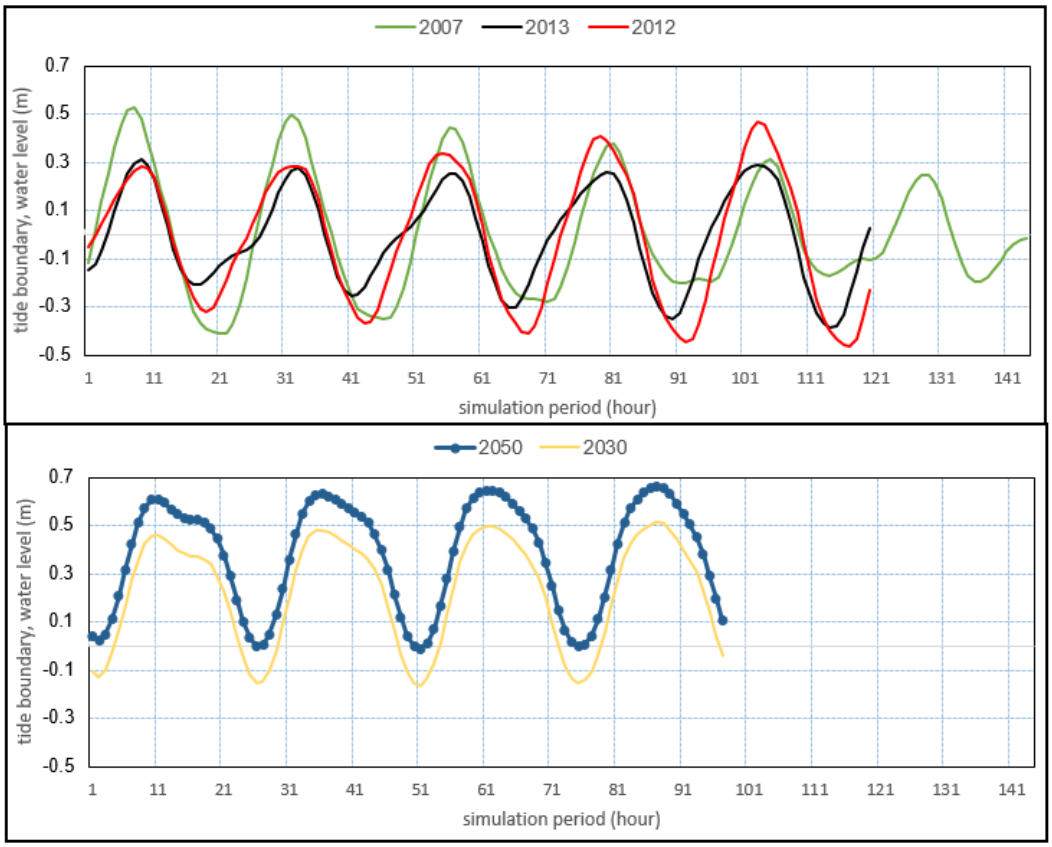

Figure 2.20 Tide time series used as downstream boundary in all scenarios.

2.5 Scenario Matrix

During the discussion with DHI and JRC team, the scenario matrix in Table 2.6 is designed taking into account the available data and the modelling needs to meet the project's objectives and deliverables. Models for 2007, 2012, and 2013 will be built to simulate the notable recent flood events over the past decade. For climate change scenarios, 2030 and 2050 time slices has been selected. Previously, the years 2003 and

2100 were considered to be included. However, it was decided by both DHI and JRC team that climate change studies in Jakarta for 2100 has high uncertainties, and therefore 2030 was chosen with better confidence. Due to lack of rainfall stations that provided data for the 2003 rainfall event, this scenario was decided not to be included in the scenario matrix. As noted in Section 2.2.2, topographies for 2030 and 2050 scenarios will both reflect land subsidence up to 2025.

The 1D river model will include all the Greater Jakarta river network, but the 2D flood maps have been generated only at the area of interest. It was agreed in the discussion during the workshop that the polder system would be further studied after the initial flood maps (i.e. the scenario matrix defined below). It is also agreed during discussion with JRC that the Great Sea Wall will be included when the polder system performance is analysed.

Table 2.6 Scenario matrix

Scenario	Flood Event (Rainfall Input)	Tide (Peak Level)	Subsidence based from 2012 year – LiDAR DEM
1	01-02 Feb 2007 (31 Jan-05 Feb)	Actual tide (+0.500 m)	No Subsidence
2	01-02 Feb 2007 (31 Jan-05 Feb)	Actual tide (+0.500 m)	With negative subsidence (up to 2007)
3	16 Jan 2013 (15-19 Jan)	Actual tide (+0.276 m)	No Subsidence
4	16 Jan 2013 (15-19 Jan)	Actual tide (+0.276 m)	With positive subsidence (up to 2013)
5	21 Dec 2012 (20-24 Dec)	Actual tide (+0.286 m)	No Subsidence
6	2050 (50-year RP + 41% CC Factor)	MHHW + 0.375 SLR (+0.610 m)	No Subsidence
7	2050 (50-year RP + 41% CC Factor)	MHHW + 0.375 SLR (+0.610 m)	With positive subsidence (up to 2025)
8	2030 (50-year RP + 33% CC Factor)	MHHW + 0.225 SLR (+0.460 m)	No Subsidence
9	2030 (50-year RP + 33% CC Factor)	MHHW + 0.225 SLR (+0.460 m)	With positive subsidence (up to 2025)

RP – Return Period
CC Factor – Climate Change Factor
MHHW – Mean Highest High Water
SLR – Sea Level Rise

3 Model Setup

There are three main processes in modelling the flood event namely the RR model, the 1D model and the 2D model. The RR modelling will transfer the rainfall data into the River runoff, and the flow of the runoff in the river from the RR model will be modelled using 1D Hydrodynamics model. The overland flood spreading from the river will be modelled in 2D Hydrodynamics model. The summary of the overall modelling process are described in a flowchart illustrated in Figure 3.1.

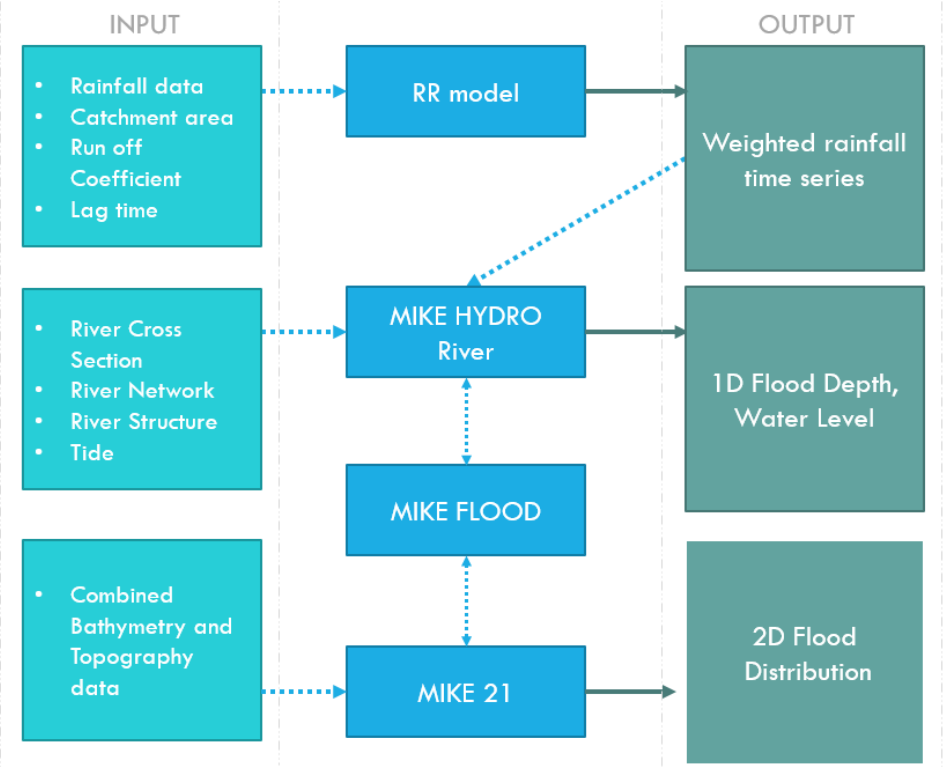

Figure 3.1 Modelling flowchart

The next sections describes the schematizations used in 1D model: catchment and rainfall-runoff, river network, cross-sections and control structures; and flexible mesh and roughness maps in the 2D model. Other modelling parameters include initial values are describe in brief.

3.1 Schematization of 1D River Model

The river model, simulated in 1D model domain, will follow the latest river schematisation i.e. 2013. It covers the rivers inside the Greater Jakarta catchments including Cisadane, Pesanggrahan, Ciliwung and canals in the east such as Sunter. This is necessary to capture the most accurate upstream boundary conditions from rainfall input. For control structures, however, information is limited to data from government agencies in DKI Jakarta and data from literature.

3.1.1 Catchment and Rainfall-Runoff (RR) Model

One of the boundary conditions necessary for 1D river model is the amount of water draining into the river branches from catchment runoff. Hence, prior to river model, the RR model is needed to be built to get the most accurate runoff discharge from rainfall

input. Before running the RR model, catchment boundaries and derivation of rainfall-runoff parameters are generated during catchment delineation.

The process of catchment delineation is illustrated in Figure 3.2. The elevations and depressions detected in elevation values provided by the DEM are used to estimate the flow directions and flow accumulations. From these two spatial values, the critical pour points are identified and from it, the catchment boundaries and rivers flowing into those pour points are delineated. Catchment delineation is done separately for each of the two datasets: (1) LiDAR merged with ALOS+SRTM mosaic DEM (3-m resolution) and (2) ALOS+SRTM mosaic DEM (30-m resolution). The 3-m DEM captures more accurate catchment boundaries, e.g. dikes, flood walls, which are necessary to define runoff in highly urbanised areas of DKI Jakarta (Figure 3.2a). The 30-m DEM extends to the whole catchment covering Greater Jakarta, and is able to capture additional areas and flow accumulation at the south side (Figure 3.2b). In Figure 3.2c, we merged the catchment and river generated from these two datasets. The drainage areas and flow accumulation values from 30-m DEM are added into the values in the model area. This is done along the boundary extent of the 1D model area (drawn in red box). From the catchment delineation process, the number of catchments that have been generated totals to 513 as shown in Figure 3.3.

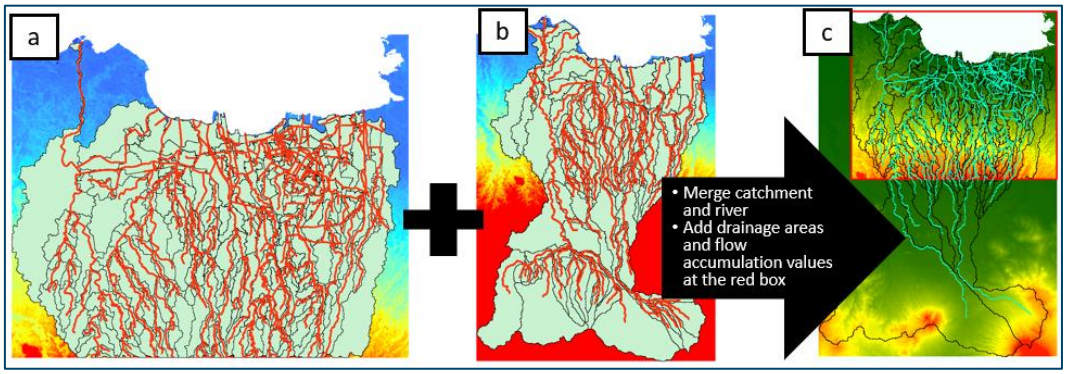

Figure 3.2 Catchment generation (a) from 3-m DEM, (b) from 30-m DEM, and (c) from the combination those two data.

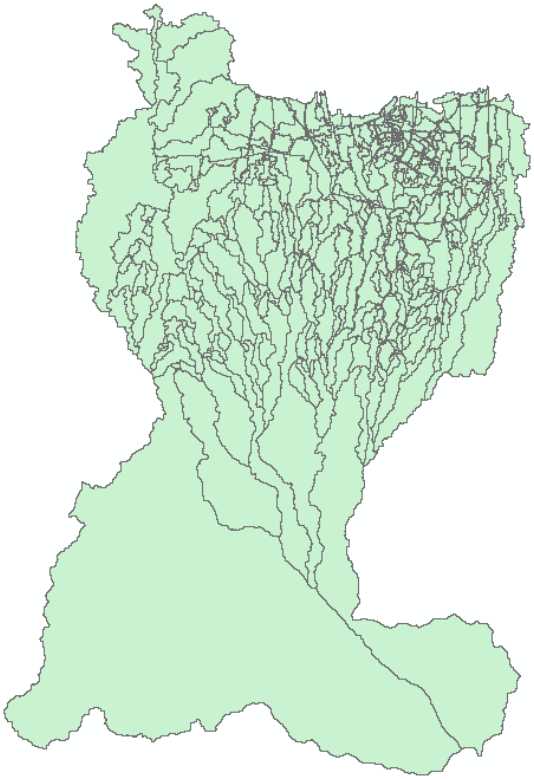

Figure 3.3 Catchment map for Jakarta flood model.

The catchment UHM parameters such as runoff coefficient (proportion of rain that becomes instant runoff), lag time (time difference between centre of unit rainfall event and runoff peak) and time of concentration (time for water to flow from most remote point in catchment to the outlet) are also derived using geo-processing of spatial data. We employed the use of the DEM for topography parameters such as slopes and elevations. For characterization of the catchments in terms of land cover and soil moisture, we used public-access global maps for Land Cover (ESA GlobCover v2010, 300-m) and Soil Map (Harmonized World Soil Database v1.2, 30 arc-second). An in-house DHI toolbox is used to generate the UHM parameters using indexing methods. Generally, the parameters are determined through different possible combinations of land cover and soil multiplied by a factor from elevation slope. A diagram of this workflow is illustrated in Figure 3.4.

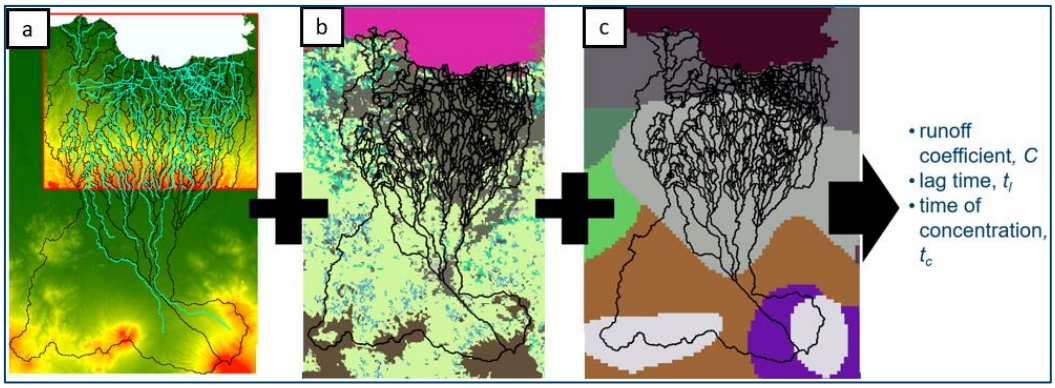

Figure 3.4 Data used in generating catchment UHM parameters: (a) DEM and the delineated catchment boundaries and river branches, (b) Land Use derived from Land Cover data (ESA GlobCover v2010, 300-m), and (c) Soil Map (Harmonized World Soil Database v1.2, 30 arc-second).

The runoff is then calculated in the RR model, using the catchments boundaries and each of their UHM parameters as model input. The runoff of each of the 513 catchments are then distributed along the river network as boundaries for 1D model, further described in Section 3.1.2.

3.1.2 River Network

Drawings of the river network encompassing, but not limited to DKI Jakarta is provided by the Agency of Ciliwung-Cisadane River Area (BBWS-CC). A river map is also published by BPBD, which is made available publicly through their website (https://petajakarta.org/). The river network data covers the two main rivers, Ciliwung and Cisadane, but also includes small creeks and drains flowing inside Jakarta. Hence, the river network data should be cleaned to include only major river systems prior to catchment and river delineation. This was done by referring to a previous river delineation by HydroSHEDS (2006). Hydrological data and maps based on shuttle elevation derivatives at multiple scales, or HydroSHEDS, is a project providing hydrographic information in regional and global scale derived from SRTM 90-m DEM and is released to the public online (http://hydrosheds.cr.usgs.gov/dataavail.php).

To ensure consistency between the river network and the topography datasets, the river network is converted to a shapefile format and use georeferencing to match the river shapefile to the river imprint observed in the DEM. Figure 3.5 illustrates an example of this process. This river network data is also used in pre-processing of the DEM as stated in Section 2.2.1.

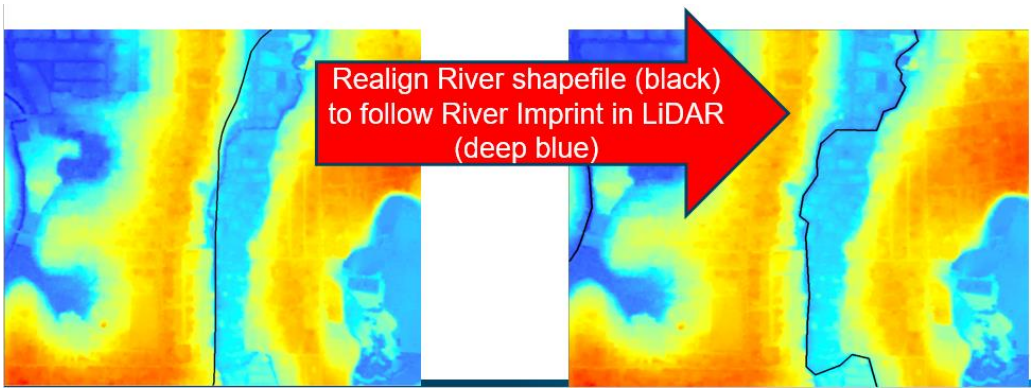

Figure 3.5 River network realignment to match with DEM data.

The final river network map in Figure 3.6 is generated from the catchment and river delineation using LiDAR DEM described in Section 3.1.1. There are about 147 branches that have been generated, including almost all important rivers that flow in DKI Jakarta province, as well as the rivers from surrounding area that are still integrated in the catchment area. Further verification of the generation river network was done to ensure that complex networks are captured in the model, such as drain canals connecting two rivers which are otherwise not captured during the DEM-based river and catchment delineation. River branches upstream of the model network but are inside Greater Jakarta catchment areas are excluded in the hydrodynamic river modelling, since cross-section cannot be extracted beyond the extent of the LiDAR DEM (further discussed in the Section 3.1.3). However, the rainfall-runoff for the whole catchment areas was used to refine the boundary conditions within the model river network.

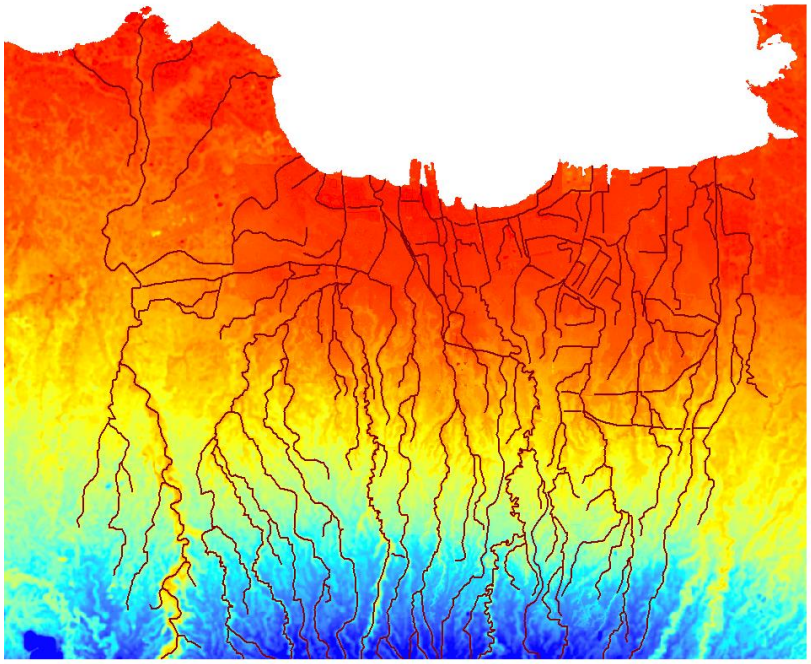

Figure 3.6 Generated river network for Jakarta flood model.

To assign the calculated runoff in Section 3.1.1 as upstream boundary conditions of the river network, coupling the 1D RR model to the river model is defined explicitly through Runoff-River Links in MIKE HYDRO River. Figure 3.7 illustrates an example in MIKE HYDRO River environment. A proportion of the catchment area is linked to specific chainage points (or range) of a river branch. The drainage area values are determined through flow accumulation values calculated during the catchment and river delineation process, whereas the locations are geo-referenced by superimposing catchment and river network maps. Additionally, we also need to link the runoff from the upstream of the 1D model extent to the most upstream point of the river branches, still using the runoff-river links. The boundary conditions at the downstream of all river branches is a water level boundary from tide level time series.

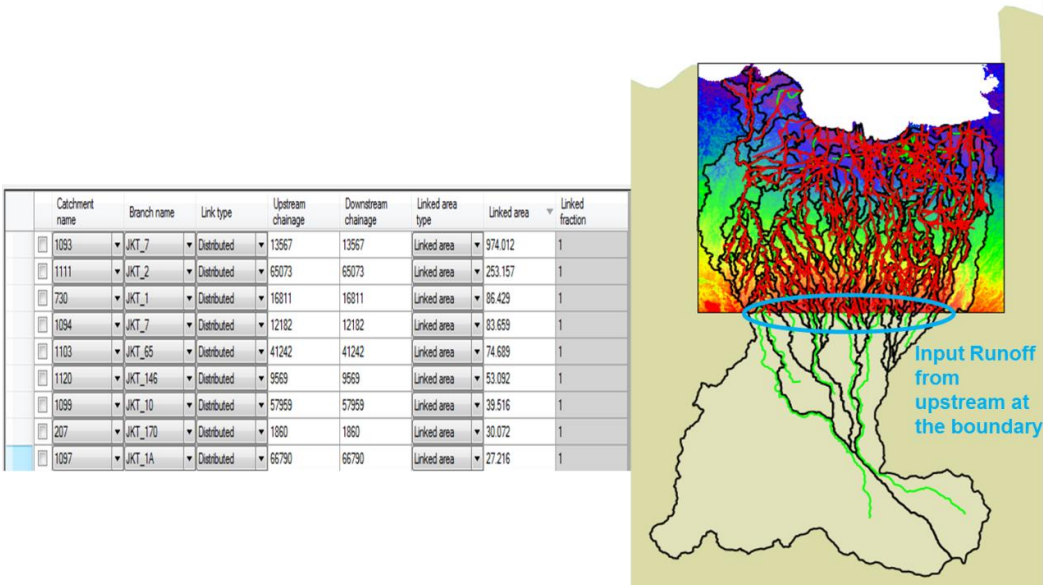

Figure 3.7 (Left) Coupling 1D RR and river models by defining runoff-river links in MIKE HYDRO River, (Right) superimposing catchment and river network maps for geo-referencing.

With catchment and river network defined in the 1D model, the river cross-sections is needed to complete the model input. The cross-sections will also be influenced by changes in topography such as during land subsidence scenarios.

3.1.3 Cross-sections

Cross-sections of the rivers, where there is information available, are obtained from survey measurements. As mentioned previously, cross-sections with no measurements available are extracted from the DEM data and artificially estimated based on the contributing upstream catchment area. The generated river network and cross-sections is calibrated from the survey data provided by the government agencies.

The cross-section data has been collected from BBWS-CC, which includes the rivers Angke, Buaran, Cakung, Cengkareng, Cikeas, Ciliwung, Ciliwung Lama, Cipinang, Cisadane, Jati Kramat, West Flood Canal (KBB), East Flood Canal (KBT), Krukut, Mookervart, Pesanggrahan, and Sunter. The cross-section data is not available in the whole network area. The available data is shown in pink and red line in Figure 3.8.

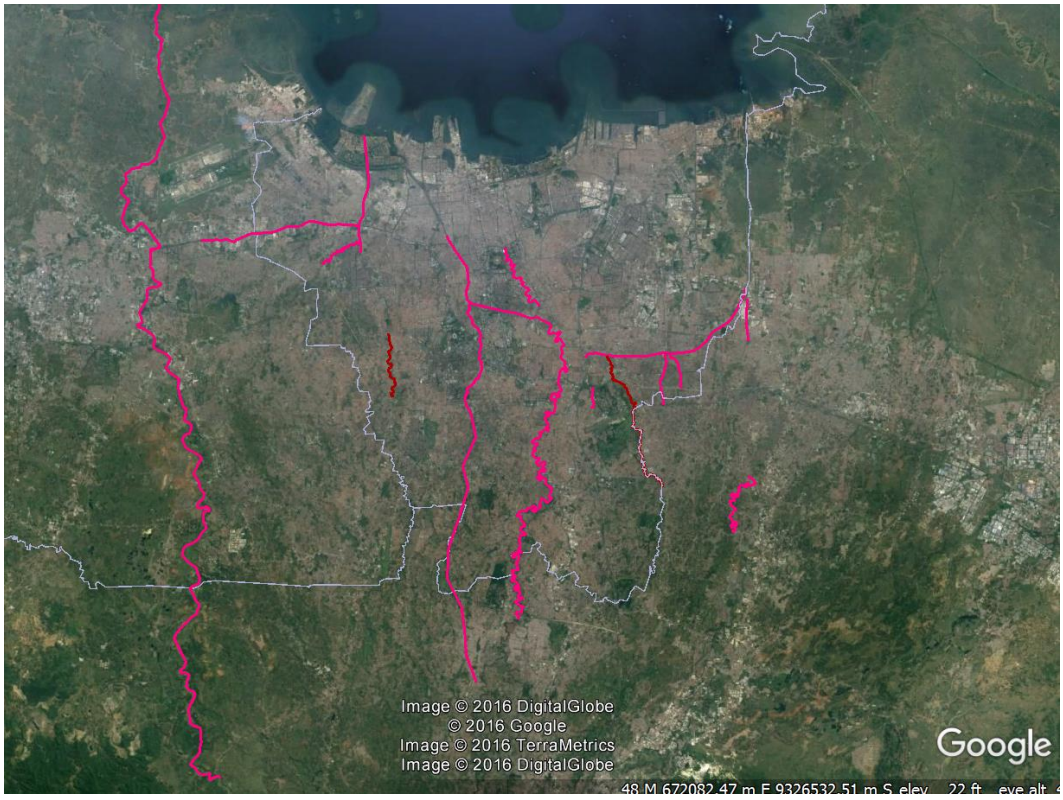

Figure 3.8 Available cross-section data shown in pink and red lines. Image source: Google Earth Pro.

To fill the data gaps of the survey measurements, the cross-sections for the rest of the river branches were generated based on LiDAR DEM values. First version of river cross-sections are extracted from the elevations provided in the DKI DEM, with 3-m data points at each width. Since LiDAR cannot penetrate water bodies to get actual river bed/invert levels, only the cope levels, bank/levees and floodplains are extracted from DEM, and the drain cross-section areas are calculated from Manning's equation. Generally, the discharge of a cross-section is scaled based on its catchment drainage area, and so the cross-section area is largely based on their locations at the catchment i.e. upstream = less catchment area = less river discharge = less cross-section area and vice-versa. This is achieved by assigning a reference discharge proportional to the entire catchment size,

Q_{ref} and then scaling the discharge at each cross-section point of the river branch according to its catchment drainage size. Calibration of Q_{ref} is explained in the next paragraphs. Slope can be calculated directly from DEM to complete the equation. An illustration of this concept is provided in Figure 3.9.

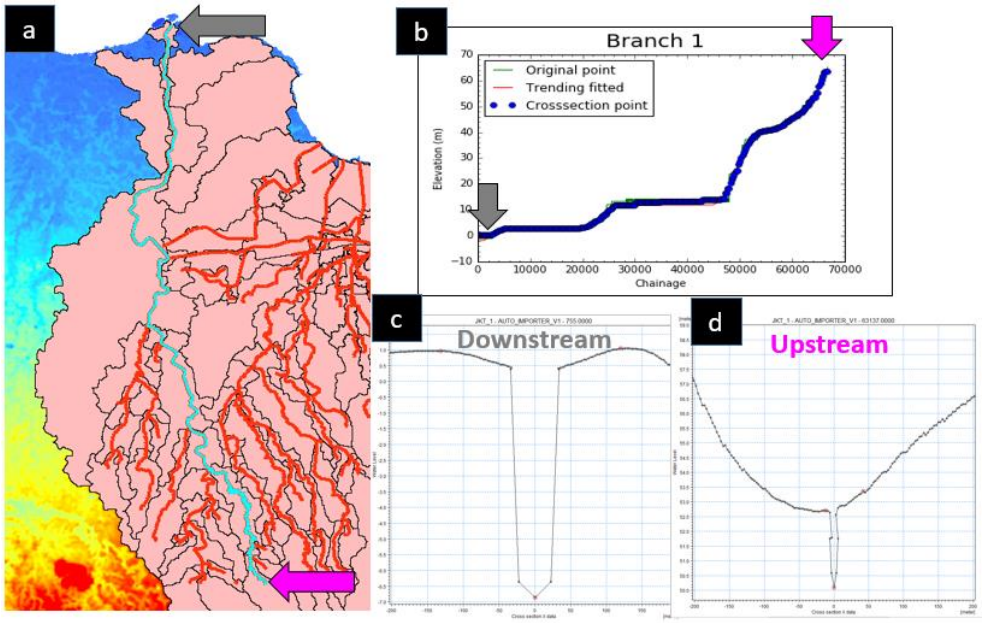

Figure 3.9 The example of cross-section discharge scaling process; (a) branch location in the map, vertical profile of the branch, (c) cross-section extracted in downstream and (d) in upstream.

Prior to the calibration of the overall cross-section generated by the LiDAR data, the cross-section data from field measurement is converted from the AutoCAD format to MIKE HYDRO River format. Only survey measurements at Angke, Cengkareng, Ciliwung, KBB and Krukut rivers were found useful for the MIKE HYDRO model. Using the survey cross-section measurements, the Q_{ref} values are estimated for every major catchments by comparing the areas of both generated and survey cross-sections. The Q_{ref} values are given in Figure 3.10 and Figure 3.11. This method can be improved if more data points will be provided in the future.

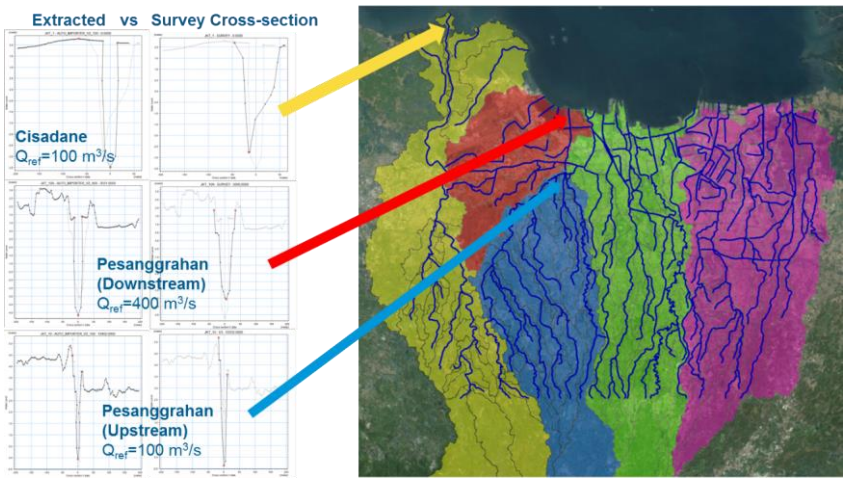

Figure 3.10 Estimation of reference discharge, Q_{ref}, for each major catchment areas: Cisadane and Pesaggrahan. Pesanggrahan is further divided into downstream and upstream for better match.

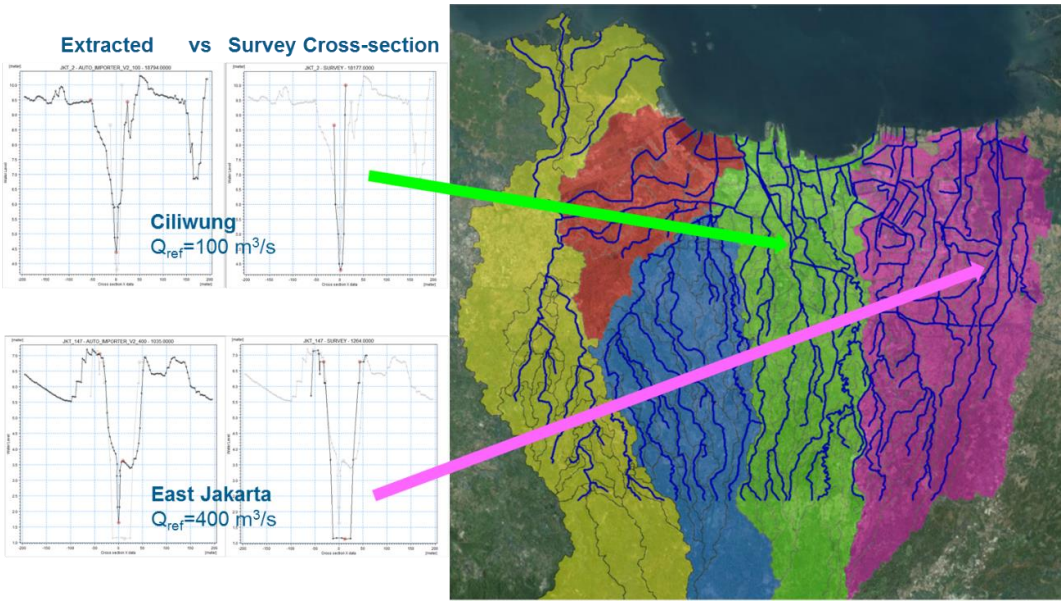

Figure 3.11 Estimation of reference discharge, Q_{ref}, for each major catchment areas: Ciliwung and East Jakarta.

Figure 3.12 shows the comparison between cross-sections extracted from LiDAR DEM and survey measurement data in Cengkareng river. Wherever possible, the cross-sections from survey measurements are used in the model. For consistency of datum, the actual cross-sections are adjusted so that their cope levels matches those that are extracted from the LiDAR DEM. Similarly, the cross-sections will be adjusted when land subsidence is applied.

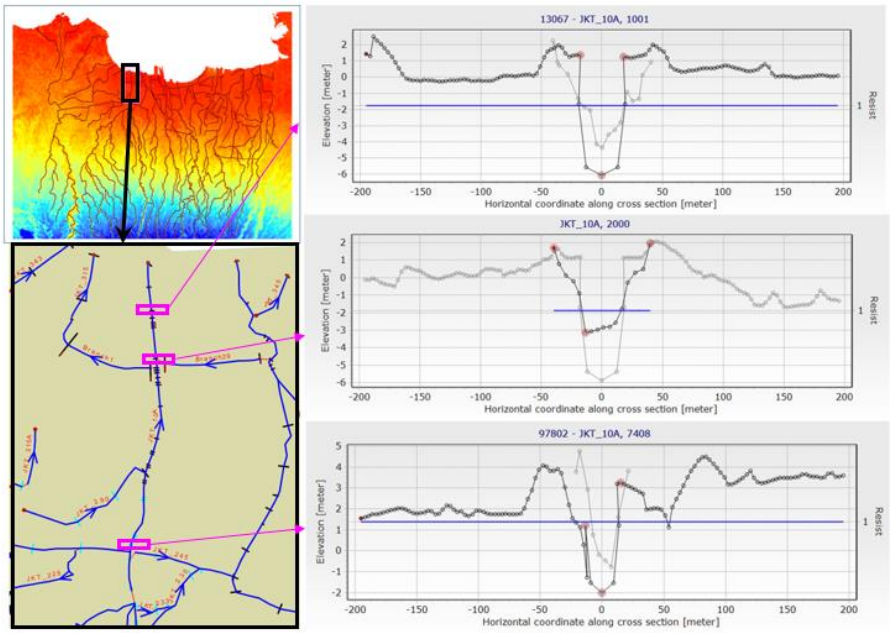

Figure 3.12 Example of cross-section comparison between data and auto generated cross-section from LiDAR data. The cross-section measurement is located at Cengkareng drain.

3.1.4 River Control Structures

River control structures that are considered influential for flood modelling are pumps, gates and weirs. The flooding phenomenon in a river system is usually sensitive to the sizes and operations of these structures, so extreme care is done when they are included in the 1D model. With this caveat, the structures included in the Jakarta model are only those whose dimensions and operations rules are well known.

The list of those structures at Jakarta have been already summarized by Water Management Agency (DTA) of DKI Jakarta and is made publicly available online (http://portaldatadta.com/ro/list/view). There are about 138 pump stations and 36 gates that available in DKI Jakarta area, but for this case, the model only included several structures that play important rule in the flood management of DKI Jakarta region. The structures included in the Jakarta model are summarised in Table 3.1 and Table 3.2, with their locations mapped in Figure 3.13.

Table 3.1 Details of pumps that are used in the Jakarta model

S/N	Name	Unit	Capacity	Operational Rule		Reference
				start level	stop level	
1	Cideng pump	6	6.7	0.8	0.6	van der Sleen and Lopez (2013)
			6.7	1.15	0.8	
			6.7	1.3	1.15	
			6.7	1.45	1.3	
			6.7	1.6	1.45	
			6.7	1.6	1.45	
2	Pluit pump	6	6	-1.4	-1.5	
			6	-1	-1.1	
			6	-0.9	-1	
			8	-1.7	-1.8	
			4	-1.5	-1.6	
			6	-1.1	-1.2	

Table 3.2 Details of gates that are used in the Jakarta model

S/N	Name	Gate type	Unit and size	Operational Rule	Reference
1	Manggarai gate to KBB	Sluice gate (underflow)	3 units width: 5.5m height: 0.8m	Always open	PIC of Manggarai gate (Mr. Adi)

S/N	Name	Gate type	Unit and size	Operational Rule	Reference
2	Manggarai gate to Ciliwung Lama	Sluice gate (underflow)	1 unit width: 5.1m height: 0.8m	The gate is always opened, minimal 100 cm If water level at Marina gate is under 150 cm, the gate will be opened 130 cm, and will be opened 100 cm again if the water level in Marina gate is above 150 cm If water level at Karet gate is in *siaga 3* condition, about 450-550 m, the gate will be opened 150 cm If water level at Karet gate is in *siaga 2* condition, about 550-600 m, the gate will be opened 175 cm If water level at Karet gate is in *siaga 1* condition, above 600 m, the gate will be opened 200 cm *the regulation point 3-5 will still be conducted although the water level in Marina gates is above 150 *if there is construction or maintenance in downstream area, there is probability to reduce the opening of the gate.	
3	Karet gate	Sluice gate (underflow)	5 units width: 4-5m	Always open	PIC of Karet gate
4	Marina gate	Sluice gate (underflow)	5 units width: 9m depth: 6m	In normal condition (if the tide level at the sea is lower than in the river), the gate is always opened. During high tide or any condition which water level in the seaside is higher than in the river, the gate will be closed to avoid seawater coming inland.	PIC of Marina gate
5	Bendung 10 gate	Sluice gate (overflow)	10 units width: 10m	Only used as weir.	https://www.youtube.com/watch?v=MpX0dp5kxu0 (accesed at 26 January 2017)

S/N	Name	Gate type	Unit and size	Operational Rule	Reference
					Field survey held by JRC
6	Grogol Lama gate to Pesang-grahan	Sluice gate (underflow)	Entire cross-section.	Always closed. The gate diverts the flow from Grogol Lama to Pesanggrahan.	Field survey held by JRC

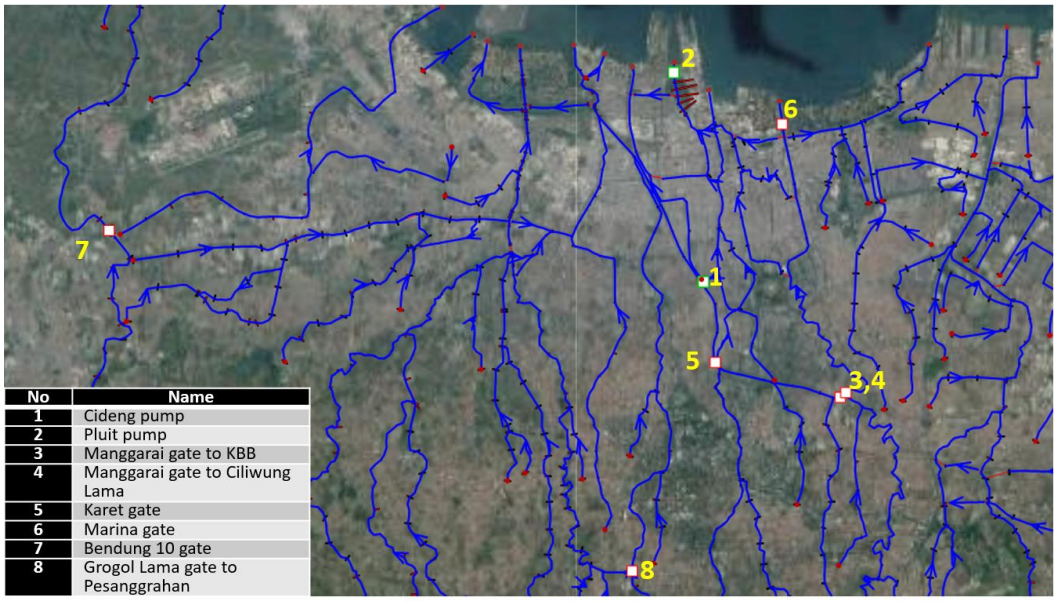

Figure 3.13 Location of the structures included in the Jakarta model.

3.2 Schematization of 2D Model

The main model input of the 2D model is the bathymetry, in which the model boundaries are defined in its domain. For MIKE 21 Flow Model FM, the bathymetry data is obtained from the model mesh, which includes the topography and also the island, the first reclamation land for the GSW concept of Jakarta. The next sections will described the mesh generation in detail.

3.2.1 Flexible Mesh

In this project, the domain of 2D model covers only the study area, i.e. around Cengkareng and Penjaringan district. To ensure proper simulation of the tidal effect, the model domain is extended to the open sea, thereby the mesh includes both topography from DEM and bathymetry values. The model mesh was able to capture the jetty near Pluit area. For the island structure of GSW, it is represented in the model mesh as an obstruction between inland and the open sea, assumed to have very high elevations. The whole domain area can be seen in the Figure 3.14a.

The model mesh is a flexible mesh consisting of irregular triangular elements. Flexible mesh have some advantages compared with fixed grid, e.g. the shape of flexible mesh can be adjusted with the boundary and the mesh resolution can be set differently

according the needs. In this project, all the scenarios used flexible mesh with gradual resolution, as illustrated in Figure 3.14b. The finest resolution is 10-m, located in all the land area in and surrounding the study area. The 10-m resolution of the model mesh is illustrated in Figure 3.14d.

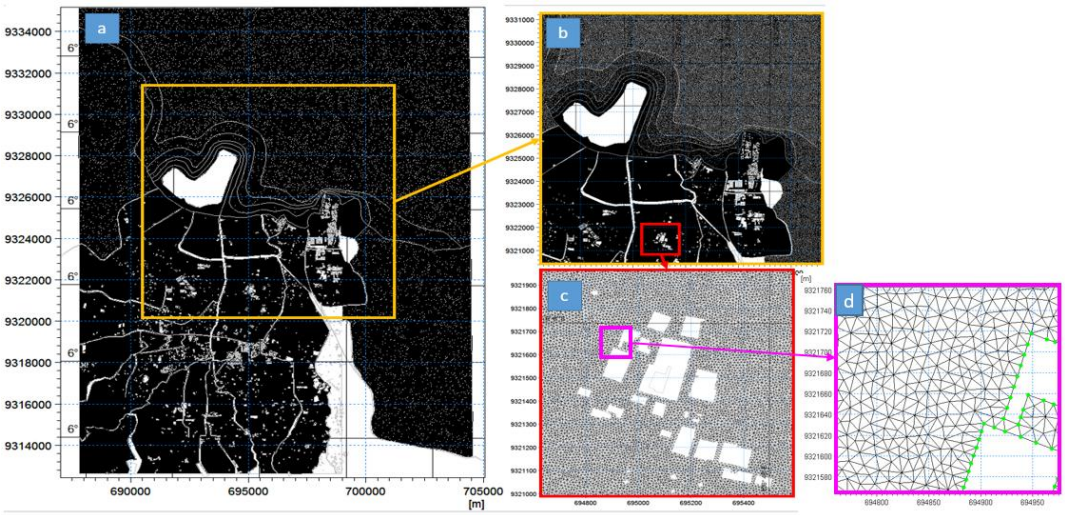

Figure 3.14 (a) Flexible mesh in the domain model. (b) The gradual resolution in flexible mesh, where (c and d) the finest resolution of 10-m is generated in the land area.

To simulate flooding in an urbanised area such as in Jakarta, there are some elements that need to be excluded from the model mesh to ensure correct flood area estimation. One of these elements is the drain polygon. Since the hydrodynamics inside the river is calculated in the 1D model, it is appropriate to exclude the river imprints in the mesh to avoid double conveyance of the river. As observed in Figure 3.14, the drain polygons, derived from the river network in 1D model, are excluded in the mesh domain.

In the mesh, buildings that are not overtopped from flooding was excluded in the mesh. This is done in the assumption that no flood waters are coming inside the building because they are well-built (made with concrete) and are too high for flood to overtop. It is worth noting that not all buildings are expected to be included, and this is important in Section 3.2.2. The building shapefile for Jakarta are obtained from a database of OpenStreetMap, which is converted into various formats and made publicly available online by Metro Extracts (https://mapzen.com/data/metro-extracts/).

3.2.2 Land Use and Roughness Map

The effect of the land use toward the spread of flood has been included in the model by assigning the varying roughness coefficients at the model area. In this model, the spatial roughness, (or floodplain roughness) is represented by the Manning's number (M), which is an inverse of the Manning's coefficient *n*. Three main categories of land use is determined for Jakarta model. First is the urban areas, which are assumed to be very rough due to the presence of well-built and closely-packed buildings. Not all buildings are detected and therefore only a few are filtered out in the mesh, as described in Section 3.2.1. There are also other buildings structures such as residential houses that do get flooded during extreme events, and should be included in the mesh. However, we only have terrain values where building heights cannot be determined. To reflect these conditions, we increase the floodplain roughness at building blocks, while decreasing the roughness at pavements and roadsides.

The second category of land-use for Jakarta model is pavement areas, such as roads, that are assumed to be very smooth because flood waters travel smoothly over less friction materials. The last category includes vegetation and other natural areas, which are assumed to have commonly used roughness value. The values for M are estimated based from floodplain *n* values in Chow (1959) as summarised in Table 3.3.

Table 3.3 Applied Manning number (M) as function of land use.

Land use	Manning's M	Manning's n (M^{-1})
Urban areas	7	0.14
Pavement	35	0.03
Vegetation, natural areas	22	0.06

Since the land-use map was not provided, we generated the roughness map based on public information and assumptions to identify areas according to the categories in Table 3.3. First, we identified the urban areas by drawing building blocks. This is achieved by first extracting roads shapefile for Jakarta, which is obtained from the same database (OpenStreetMap, Metro Extracts). Then, buildings blocks are identified as those areas contained inside road intersections. All other areas, such as those covered in vegetation, are placed in the third category. An illustration of this is shown in Figure 3.15 where we zoomed in to an area in the final roughness map used in the Jakarta model.

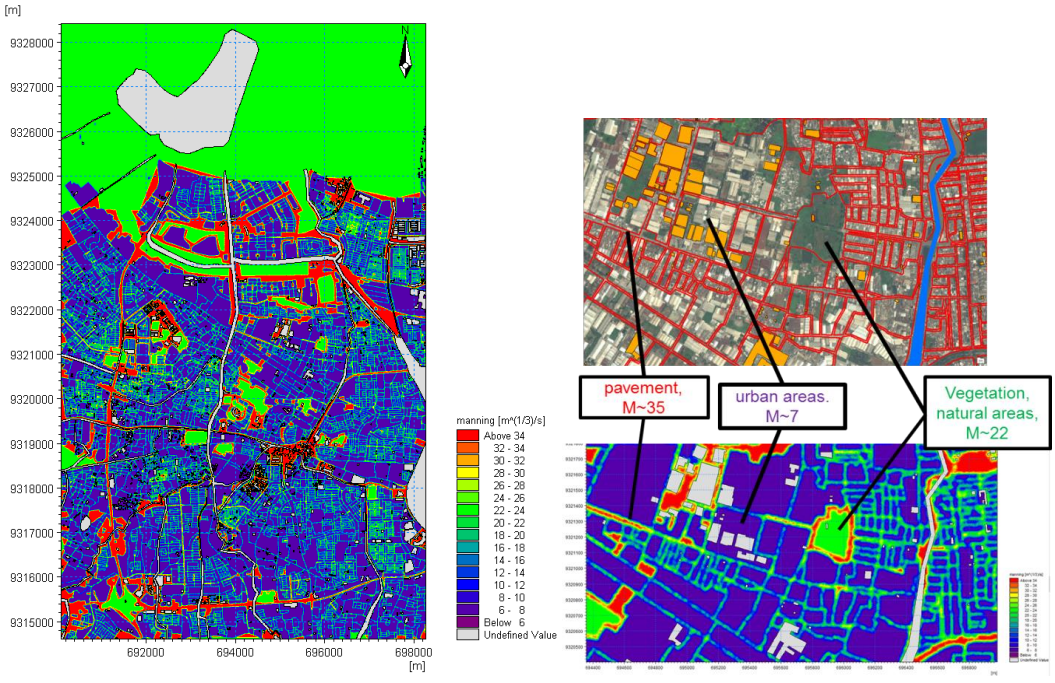

Figure 3.15 (Left) Roughness map used in the Jakarta model, values are in Manning's M. (Right) Zooming in to pavements and building blocks.

3.3 Model Setup for Scenario Runs

Initial values for all scenario was varying in domain. The initial value of surface elevation was set 0 m for all land, which means the river was dry in initial condition. Whereas for the sea area, initial tide value was set as initial value. To obtain this varying-in-domain

initial values, initial values map was made to applied in 2D model. Initial values was a water level data, which means the height of the water measured from chart datum 0. To reach this intention, the initial water level values for land area was set the same as topography values, and initial tide level was set as initial water level values for sea area.

Taking into account the boundary conditions and modelling input described in the previous sections, the model setup for each scenarios are presented in the tables below. Each table is provided for Rainfall-Runoff model (Table 3.4), 1D model (Table 3.5), and 2D model (Table 3.6).

In coupling 1D-2D models by MIKE FLOOD, 74 lateral links are defined. No exponential smoothing factor is defined, so default value of 1 are kept. Numerical parameters for lateral links, explained in Section 2.1.3, are kept default: Weir 1 (standard weir formula) for flow calculation type, levee height source is the highest between cross-sections and mesh value (HGH).

Table 3.4 Rainfall-Runoff (MIKE HYDRO River) model setup. *For 2030/2050, the simulation period is not indicative of actual flood event, since rainfall/tide are derived from calculations.

RR model, Year:		**2007**	**2012**	**2013**	**2030/2050**
Simulation period	Start	31/1/2007 00:00	20/12/2007 00:00	1/15/2013 00:00	1/1/2013 00:00*
	End	05/2/2007 00:00	24/12/2007 00:00	1/19/2013 00:00	1/5/2013 00:00*
Time step		5 minutes			
Catchments		513			
Rainfall runoff model		UHM (Unit Hydrograph Model) method			
Area adjustment factor		1			
Baseflow		0, initialization included in simulation period			
Hydrograph		SCS dimensionless			
Runoff coefficient		Varied per catchment.			
Lag time					
Total rainfall station		27	51	40	12
Rainfall timeseries		*Pos Hujan*, daily data converted to hourly data			50-year return period with climate change Factors Design storms
		UPT station, hourly data			

Table 3.5 1D model (Mike HYDRO River) model setup. *For 2030/2050, the simulation period is not indicative of actual flood event, since rainfall/tide are derived from calculations

Mike HYDRO River model, year:		**2007**	**2012**	**2013**	**2030/2050**
Simulation period	Start	31/1/2007 00:00	20/12/2007 00:00	1/15/2013 00:00	1/1/2013 00:00*
	End	5/2/2007 00:00	24/12/2007 00:00	1/19/2013 00:00	1/5/2013 00:00*
Time step	Rainfall runoff time step multiplier	1			
	Time step length	1 second			
Coordinate system		WGS_1984_UTM_zone_48S			
River network		147 branches			
Cross-sections		No subsidence - 2012 With (negative) subsidence - 2007	No subsidence - 2012	No subsidence - 2012 With subsidence - 2013	No subsidence - 2012 With subsidence - 2025
Structure		5 gates			
		11 pumps			
		Control (Sensor 3, control rules 5)			
Bed resistance		Constant Manning (M) = 30			
Boundary Conditions	Upstream	0 (from runoff)			0 (from runoff)
	Downstream	Tide from tidal prediction DISHIDROS tidal constituent			Tide + Sea Level Rise
Initial condition	Type	Water level (first tide water level)			
	Value	-0.11 m	-0.05 m	-0.15 m	-0.11 m / 0.04 m
Total river link (from catchment)		653			

Table 3.6 2D model (MIKE 21 Flow Model FM) model setup. *For 2030/2050, the simulation period is not indicative of actual flood event, since rainfall/tide are derived from calculations.

MIKE 21 FM, Year:		2007	2012	2013	2030/2050
Simu-lation period	Start	31/1/2007 00:00	20/12/2007 00:00	1/15/2013 00:00	1/1/2013 00:00*
	End	5/2/2007 00:00	24/12/2007 00:00	1/19/2013 00:00	1/5/2013 00:00*
Time step		1 second			
Solution technique		Shallow Water Equation Time integration: low order, fast algorithm Space discretization: low order, fast algorithm Minimum time step : 0.5 second Maximum time step: 1 second Critical CFL number : 0.8			
		Transport Equation Minimum time step : 0.5 second Maximum time : 1 second Critical CFL number: 0.8			
Depth		No Depth correction			
Flood and dry		Type: Advanced flood and dry (floodplain) Drying depth: 0.002 m Flooding depth : 0.02 m Wetting depth : 0.04 m			
Density		Barotropic			
Eddy viscosity		Eddy type : Constant Eddy formulation Format: Constant Constant value: 0.002 m^2/s			
Bed resistance		Resistance type: Manning number Format: Constant in time varying in domain			
Initial condi-tion	Type	Spatially varying surface elevation			
	Value	Dry at land area Sea: -0.11 m	Dry at land area Sea: -0.05 m	Dry at land area Sea: -0.15 m	Dry at land area Sea:-0.11 m/0.04 m
Boundary		In the seaside: tide from tidal prediction from DISHIDROS tidal constituent In the land side: Land (zero normal velocity)			

4 Model Calibration and Validation

Prior to scenario model runs, flood models has to be calibrated and then validated based on observed data. However, there are currently no data available that can be used for calibration of the Jakarta flood model, which requires comprehensive data of observed rainfall, water level and discharge during flood events. Since the calibration process is not possible for this flood model, we have validated the model performance using available information and previous research study in Budiyono *et al.* (2016). The model validation process for this flood model is based on previous simulations and visual observations during the 2007 and 2013 flood events.

The previous hydrology study in Budiyono *et al.* (2016) included both 2007 and 2013 flooding conditions. The hydrology model in Budiyono *et al*. (2016) uses SOBEK Hydrology suite which was developed during the flood hazard mapping project and the Flood Management Information System project (further called as SOBEK model). This model is developed by Deltares, National Bureau for Meteorology (BMKG), Research Centre for Water Resource (Pusair) and Jakarta Office of Public Works (DPU-DKI). The comparison of SOBEK input model and MIKE model are explained more in detail in Appendix A.

Another data that can be used to validating the model is the inundation map of National Disaster Management Office (BNPB) in Budiyono *et al*. (2016). The map shows the village administration units that were reported to be inundated in the 2007 and 2013 flood by the village administrator to BNPB. The modelling result of Budiyono *et al*. (2016) and BNPB map are shown in Figure 4.1 and Figure 4.2.

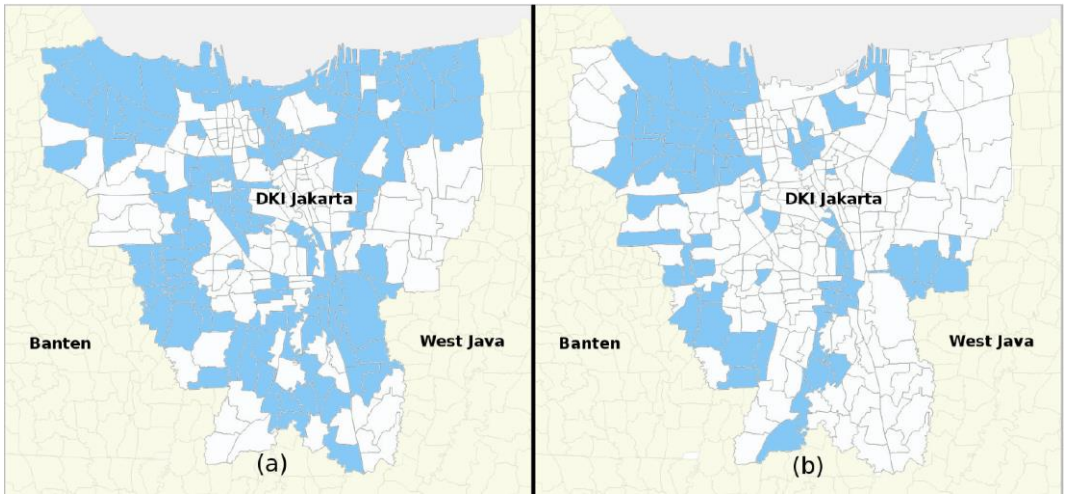

Figure 4.1 Village administration map which was reported to be inundated in (a) 2007 and (b) 2013 by the village administrator to National Disaster Management Office (BNPB). (Source: Budiyono *et al.*, 2016)

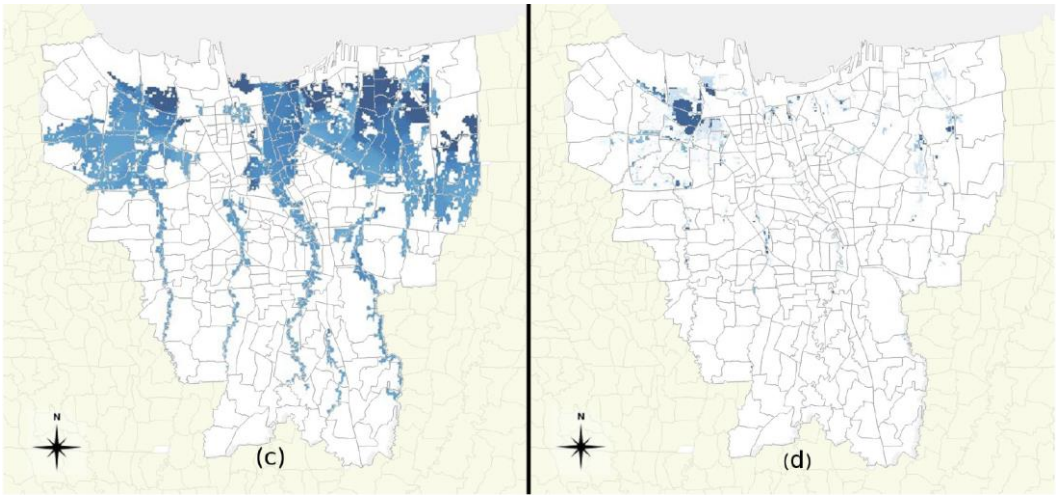

Figure 4.2 the inundation maps of Budiyono *et al*. (2016) from SOBEK model based on (c) 2007 schematization and a return period of 50 years, and (d) 2013 schematization and a return period of 25 years. (Source: Budiyono *et al.*, 2016)

4.1 Validation of 2007 flood event

The comparison of 2007 flood maps from different sources is shown in Figure 4.3. Green polygons represent the inundated areas from this project's Jakarta flood model (further called as MIKE model), but no flood in SOBEK model, a possibility that MIKE model over-predicted. Pink polygon represent areas with no inundation in MIKE model result, while there is inundation in SOBEK model, a possibility that MIKE model under-predicted. Orange polygon represent matching inundation areas detected in both MIKE model and SOBEK model. From this comparison, we can see that MIKE model results have a good comparison with SOBEK model, especially in the area of interest which also confirmed by the flood map of BNPB.

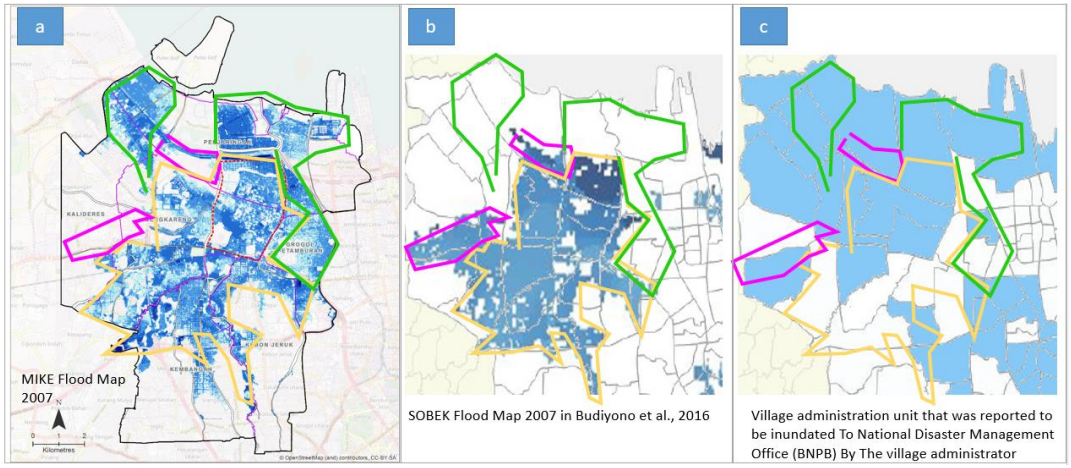

Figure 4.3 Validation of Jakarta model based on 2007 flood event. (a) Flood map results from this project (MIKE model), (b) Flood Map from SOBEK Model (Budiyono *et al*., 2016), (c) BNPB Map.

4.2 Validation of 2013 flood event

Similar exercise is done for the comparison of 2013 flood maps from different sources as shown in Figure 4.4. Green polygons represent areas where MIKE model over-predicted

the flood areas compared to SOBEK model. Pink polygons represent areas where MIKE model under-predicted compared to SOBEK model. Yellow polygons represent matching inundation areas detected in both MIKE model and SOBEK model. From this comparison, we can see that MIKE model results have a good comparison with SOBEK model, and better comparison with BNPB flood maps.

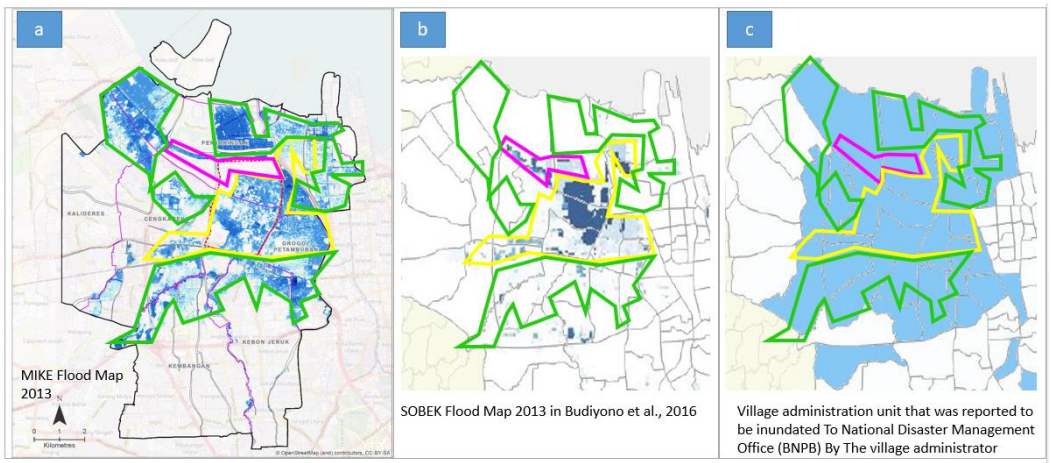

Figure 4.4 Validation of Jakarta model based on 2013 flood event. (a) Flood map results from this project (MIKE model), (b) Flood Map from SOBEK Model (Budiyono *et al*., 2016), (c) BNPB Map.

This page is intentionally left blank

5 Flood Maps

In order to assess the flood risk in the study area, flood maps were generated for various flood scenarios as listed in the Scenario Matrix in Chapter 2.5, designed to show flooding from different rainfall intensities, climate change factors and land subsidence conditions. Flood maps were produced by extracting maximum flood depth from modelling results within the 4-5 days simulation period.

From 2007 flood maps (Scenarios 1 and 2), it can be seen that the entire study area is almost covered by flood waters, with inundation depth range from 0 to 3m. Among the three polders located in the study area (Pantai Indah Kapuk Polder, Kapuk Muara Polder, and Kapuk Poglar Polder), the polder that has the highest inundation depth is located in Kapuk Poglar polder.

Compared to 2007 flood maps, 2013 flood maps (Scenarios 3 and 4) has lower inundation depths almost in all areas except in Pluit (east side of Penjaringan district) and in Grogol Petamburan district. This is expected, since the 2007 rainfall event is statistically bigger than the 2013 event: with frequencies of 50-year and 25-year return periods respectively (Budiyona *et al*., 2016). Like in 2007 flood maps, the highest inundation in 2013 flood maps is located in Kapuk Poglar polder.

On the other hand, the 2012 flood map (Scenario 5) show that the flood event in 2012 caused the lowest inundation compared to flood events in 2007 and 2013, because the rainfall during this period is also the lowest. The inundation mostly varies from 0-1 m and the most impacted area from this scenario are Grogol Petamburan district and north part of of Penjaringan district. In 2012, there is no flooding in the area of interest, except in some part of Kapuk Poglar polder with minimal inundation depth (less than 0.3 m).

Flood maps for 2030 (Scenarios 8 and 9) and 2050, (Scenarios 6 and 7) shows that climate change scenarios of higher rainfall and sea level rise have higher inundation depths and have wider flood areas. Analysis of the effects of land subsidence and climate change conditions are discussed further in Chapter 6.

Succeeding figures in this chapter presents the Flood Maps for each of the nine scenarios in the scenario matrix.

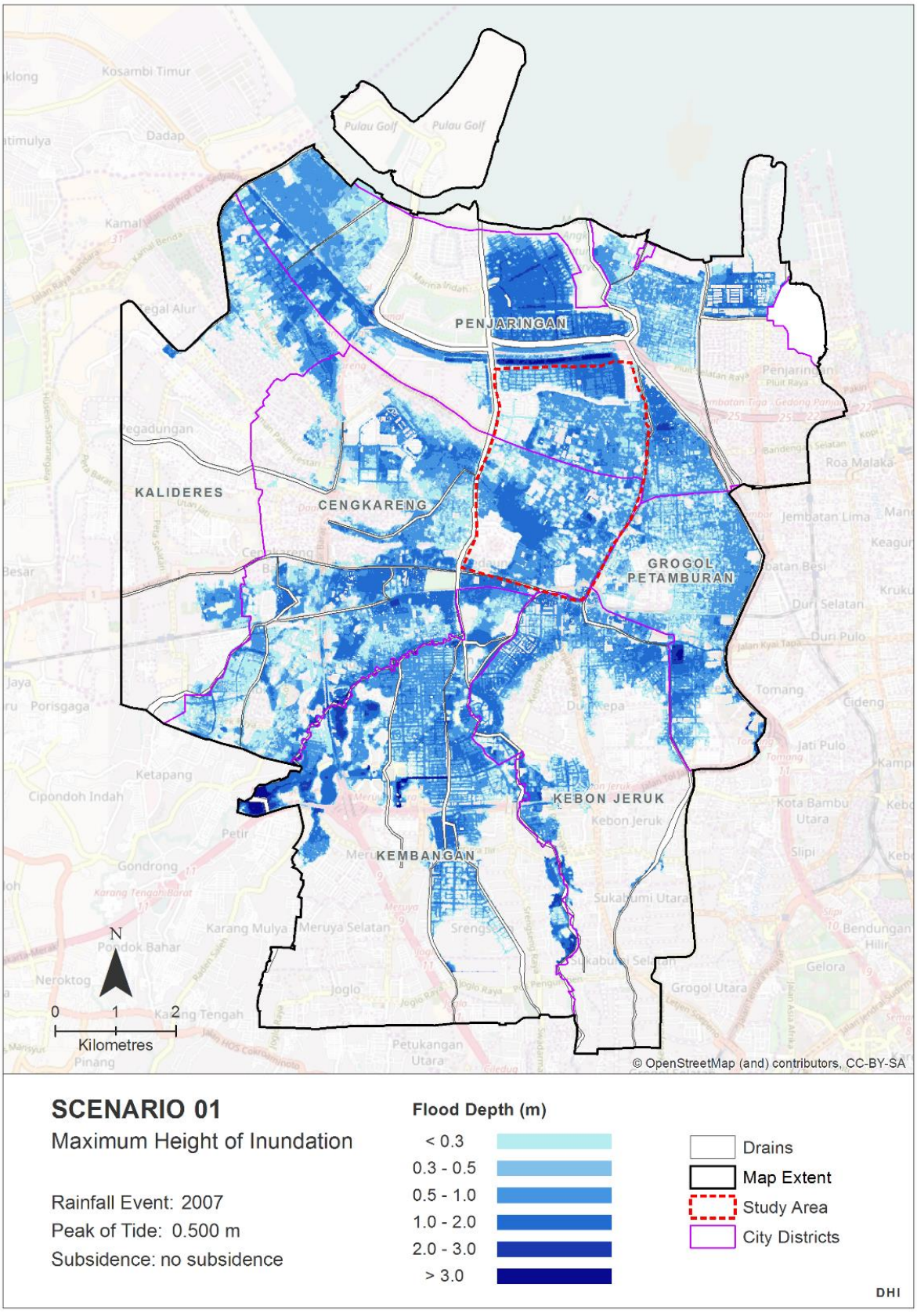
PENJARINGAN
KALIDERES
CENGKARENG
GROGOL PETAMBURAN
KEBON JERUK
KEMBANGAN
Pulau Golf
Kosambi Timur
Dadap
Kamal
Tegal Alur
Pegadungan
Roa Malaka
Jembatan Lima
Duri Selatan
Duri Pulo
Tomang
Cideng
Jati Pulo
Kota Bambu Utara
Slipi
Bendungan Hilir
Gelora
Grogol Utara
Kebon Jeruk
Ketapang
Cipondoh Indah
Petir
Gondrong
Karang Mulya
Meruya Selatan
Srengseng
Joglo
Petukangan Utara
Pinang
Neroktog
Pondok Bahar
Porisgaga
Jaya
N
0
1
2
Kilometres
© OpenStreetMap (and) contributors, CC-BY-SA
SCENARIO 01
Maximum Height of Inundation
Rainfall Event: 2007
Peak of Tide: 0.500 m
Subsidence: no subsidence
Flood Depth (m)
< 0.3
0.3 - 0.5
0.5 - 1.0
1.0 - 2.0
2.0 - 3.0
> 3.0
Drains
Map Extent
Study Area
City Districts
DHI

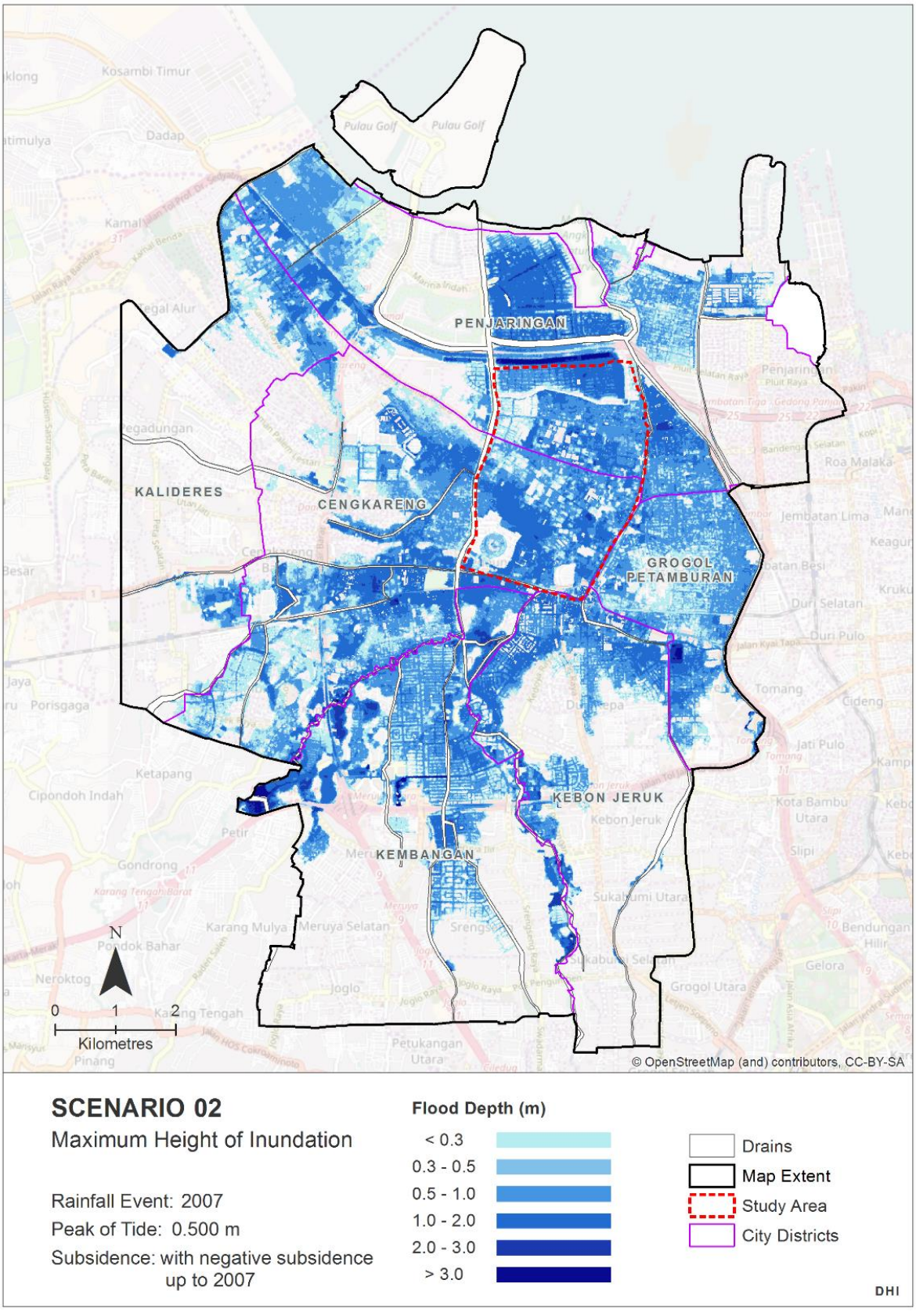
PENJARINGAN
KALIDERES
CENGKARENG
GROGOL PETAMBURAN
KEBON JERUK
KEMBANGAN
N
0 1 2
Kilometres
© OpenStreetMap (and) contributors, CC-BY-SA
SCENARIO 02
Maximum Height of Inundation
Rainfall Event: 2007
Peak of Tide: 0.500 m
Subsidence: with negative subsidence up to 2007
Flood Depth (m)
< 0.3
0.3 - 0.5
0.5 - 1.0
1.0 - 2.0
2.0 - 3.0
> 3.0
Drains
Map Extent
Study Area
City Districts
DHI

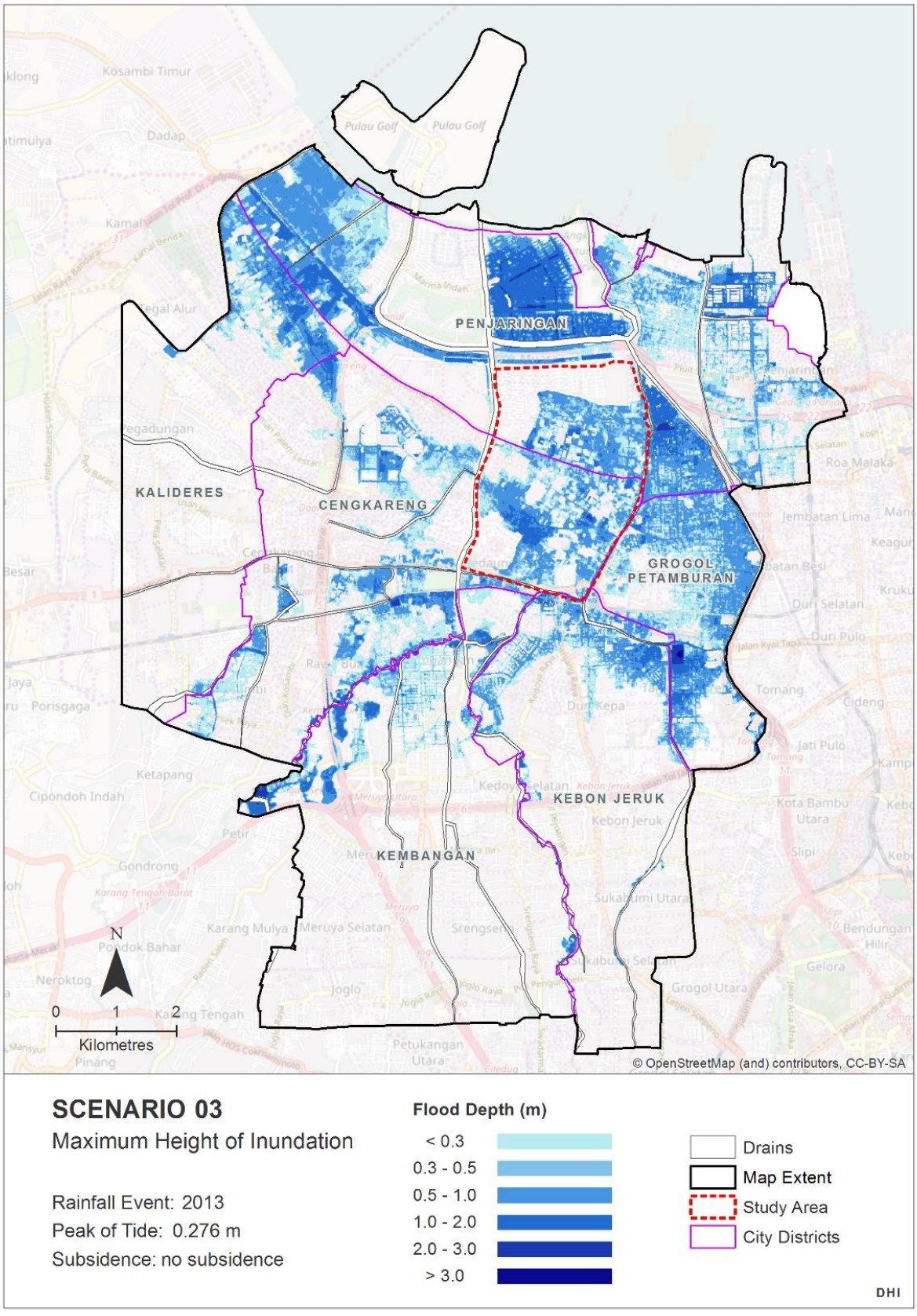
PENJARINGAN
KALIDERES
CENGKARENG
GROGOL PETAMBURAN
KEBON JERUK
KEMBANGAN
N
0 1 2
Kilometres
© OpenStreetMap (and) contributors, CC-BY-SA
SCENARIO 03
Maximum Height of Inundation
Rainfall Event: 2013
Peak of Tide: 0.276 m
Subsidence: no subsidence
Flood Depth (m)
< 0.3
0.3 - 0.5
0.5 - 1.0
1.0 - 2.0
2.0 - 3.0
> 3.0
Drains
Map Extent
Study Area
City Districts
DHI

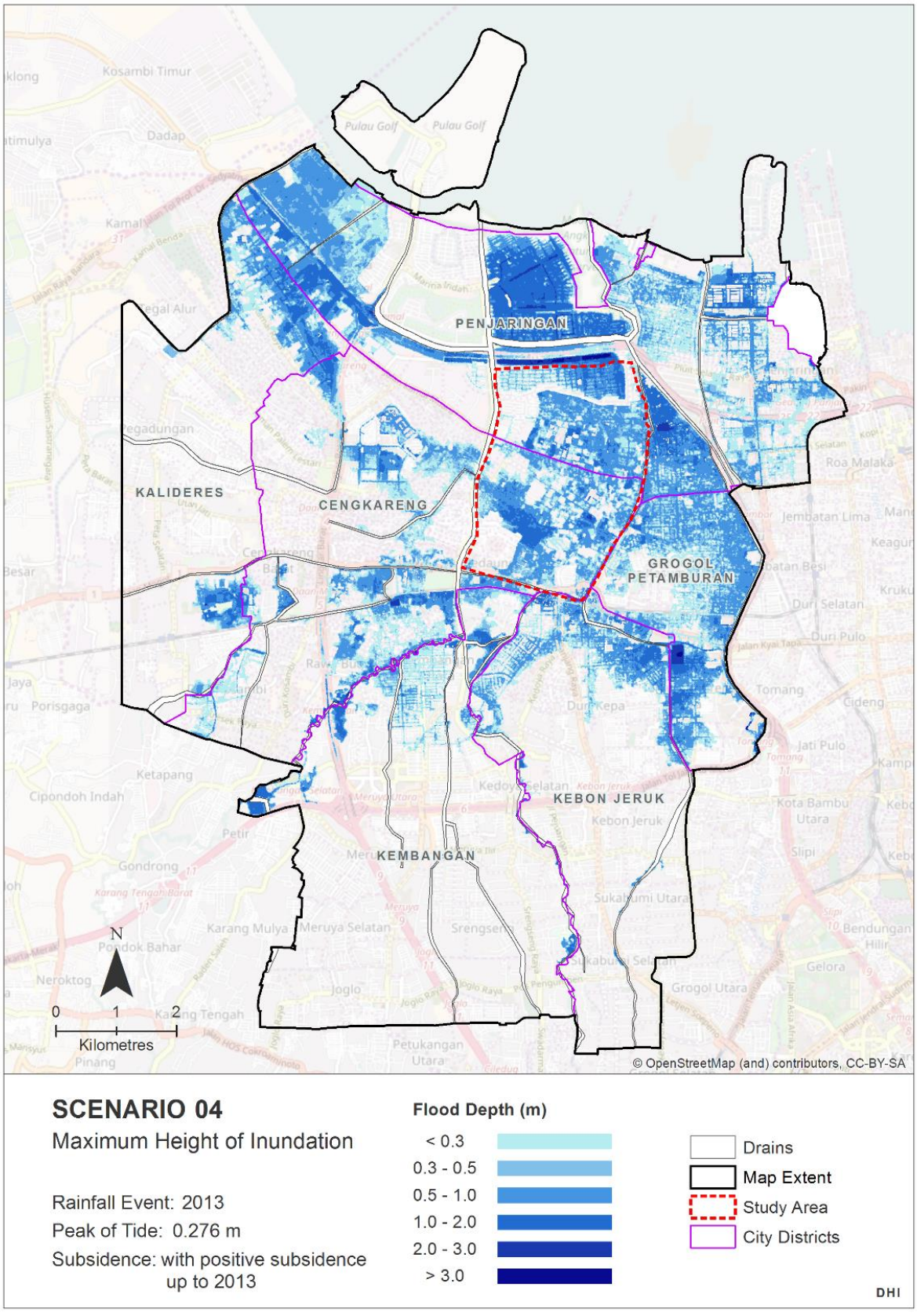
PENJARINGAN
KALIDERES
CENGKARENG
GROGOL PETAMBURAN
KEBON JERUK
KEMBANGAN
N
0 1 2
Kilometres
© OpenStreetMap (and) contributors, CC-BY-SA
SCENARIO 04
Maximum Height of Inundation
Rainfall Event: 2013
Peak of Tide: 0.276 m
Subsidence: with positive subsidence up to 2013
Flood Depth (m)
< 0.3
0.3 - 0.5
0.5 - 1.0
1.0 - 2.0
2.0 - 3.0
> 3.0
Drains
Map Extent
Study Area
City Districts
DHI

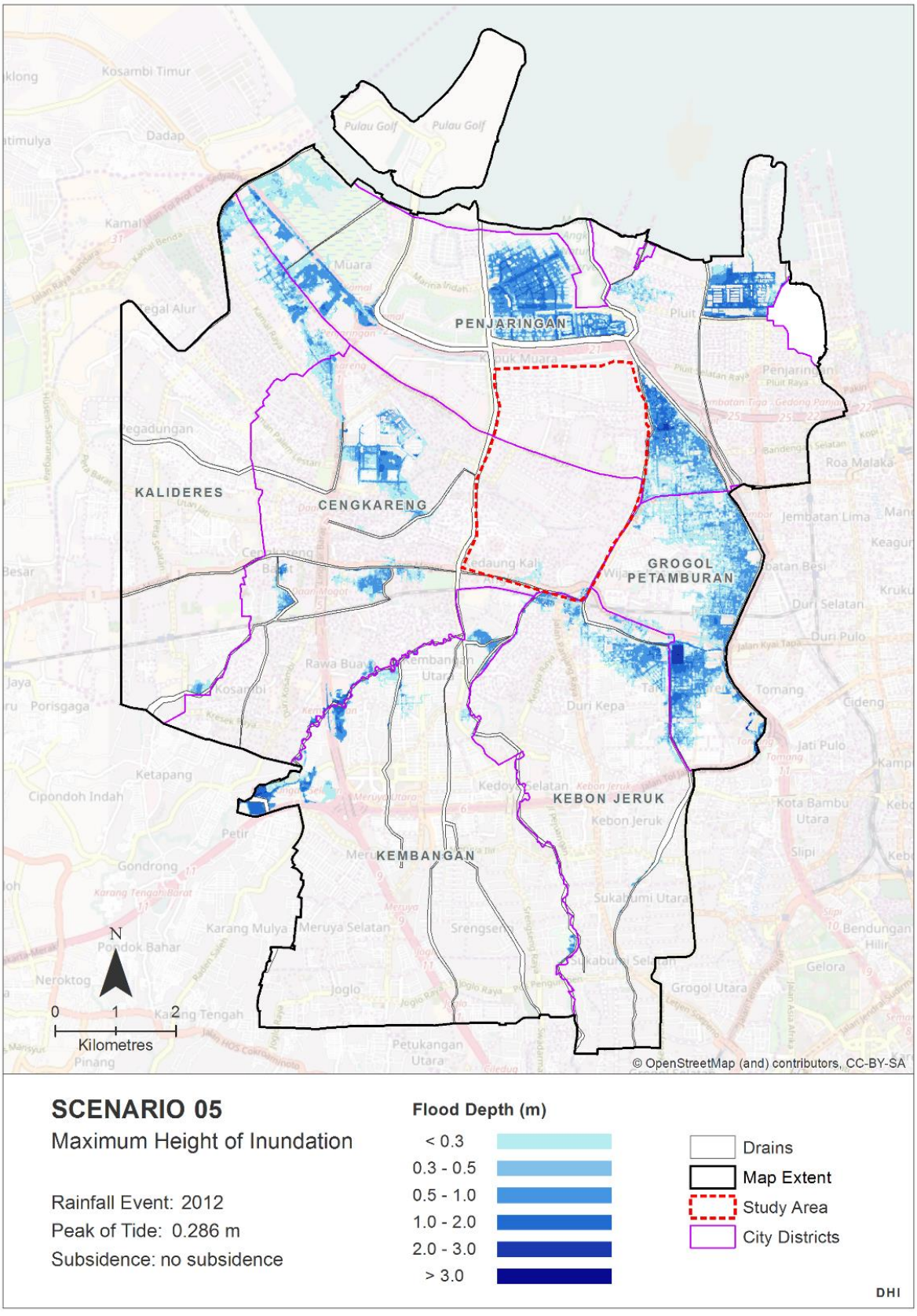
PENJARINGAN
KALIDERES
CENGKARENG
GROGOL PETAMBURAN
KEBON JERUK
KEMBANGAN
N
0 1 2
Kilometres
© OpenStreetMap (and) contributors, CC-BY-SA
SCENARIO 05
Maximum Height of Inundation
Rainfall Event: 2012
Peak of Tide: 0.286 m
Subsidence: no subsidence
Flood Depth (m)
< 0.3
0.3 - 0.5
0.5 - 1.0
1.0 - 2.0
2.0 - 3.0
> 3.0
Drains
Map Extent
Study Area
City Districts
DHI

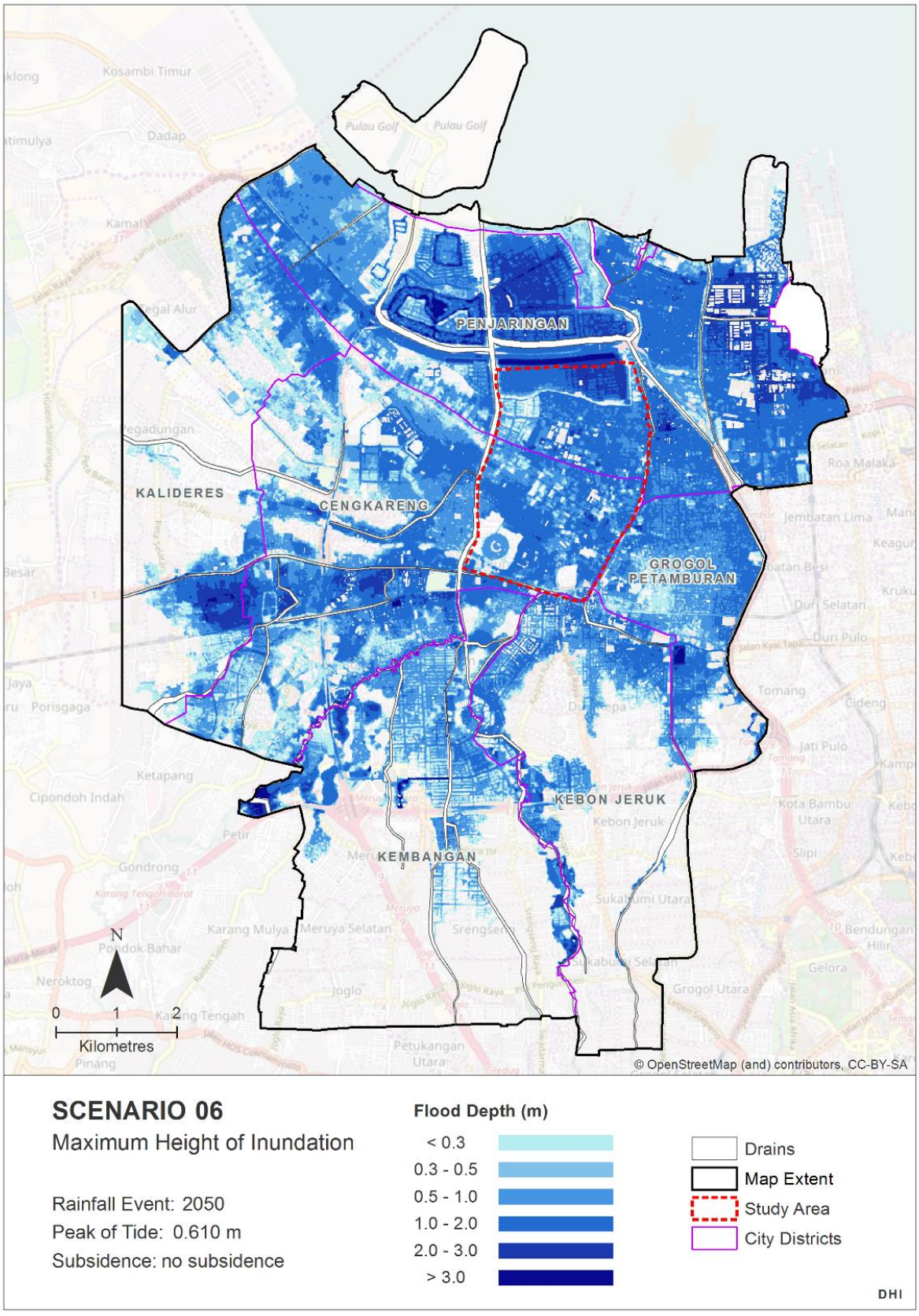
PENJARINGAN
KALIDERES
CENGKARENG
GROGOL PETAMBURAN
KEBON JERUK
KEMBANGAN
N
0
1
2
Kilometres
© OpenStreetMap (and) contributors, CC-BY-SA
SCENARIO 06
Maximum Height of Inundation
Rainfall Event: 2050
Peak of Tide: 0.610 m
Subsidence: no subsidence
Flood Depth (m)
< 0.3
0.3 - 0.5
0.5 - 1.0
1.0 - 2.0
2.0 - 3.0
> 3.0
Drains
Map Extent
Study Area
City Districts
DHI

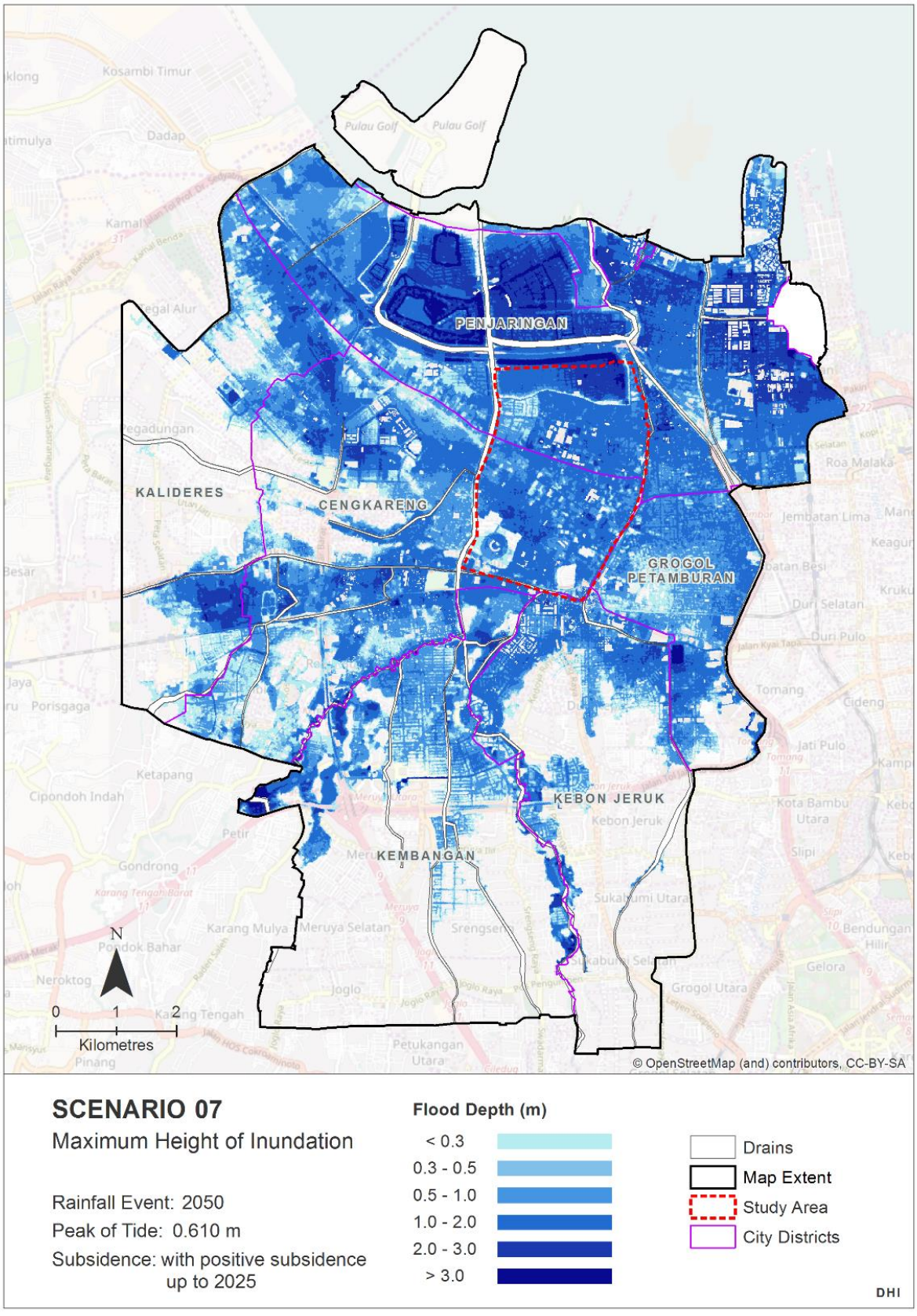
PENJARINGAN
KALIDERES
CENGKARENG
GROGOL PETAMBURAN
KEBON JERUK
KEMBANGAN
Pulau Golf
Kosambi Timur
Dadap
Kamal
Tegal Alur
Tegadungan
Roa Malaka
Jembatan Lima
Duri Selatan
Duri Pulo
Tomang
Cideng
Jati Pulo
Kota Bambu Utara
Slipi
Bendungan Hilir
Gelora
Grogol Utara
Kebon Jeruk
Sukabumi Utara
Meruya Selatan
Srengseng
Joglo
Petukangan Utara
Ketapang
Cipondoh Indah
Petir
Gondrong
Karang Mulya
Pondok Bahar
Neroktog
Porisgaga
Pinang
N
0
1
2
Kilometres
© OpenStreetMap (and) contributors, CC-BY-SA
SCENARIO 07
Maximum Height of Inundation
Rainfall Event: 2050
Peak of Tide: 0.610 m
Subsidence: with positive subsidence up to 2025
Flood Depth (m)
< 0.3
0.3 - 0.5
0.5 - 1.0
1.0 - 2.0
2.0 - 3.0
> 3.0
Drains
Map Extent
Study Area
City Districts
DHI

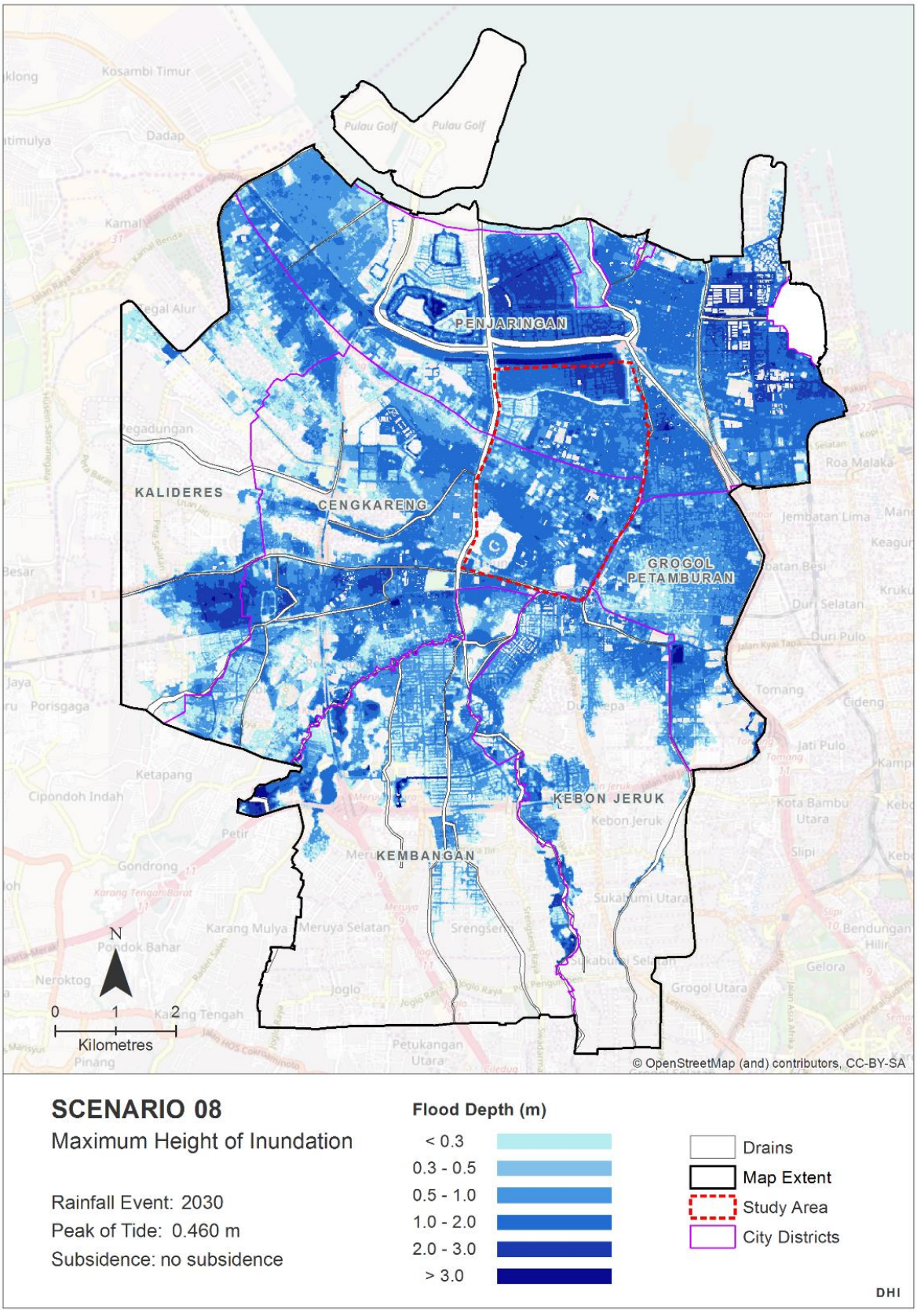
PENJARINGAN
KALIDERES
CENGKARENG
GROGOL PETAMBURAN
KEBON JERUK
KEMBANGAN
N
0
1
2
Kilometres
© OpenStreetMap (and) contributors, CC-BY-SA
SCENARIO 08
Maximum Height of Inundation
Rainfall Event: 2030
Peak of Tide: 0.460 m
Subsidence: no subsidence
Flood Depth (m)
< 0.3
0.3 - 0.5
0.5 - 1.0
1.0 - 2.0
2.0 - 3.0
> 3.0
Drains
Map Extent
Study Area
City Districts
DHI

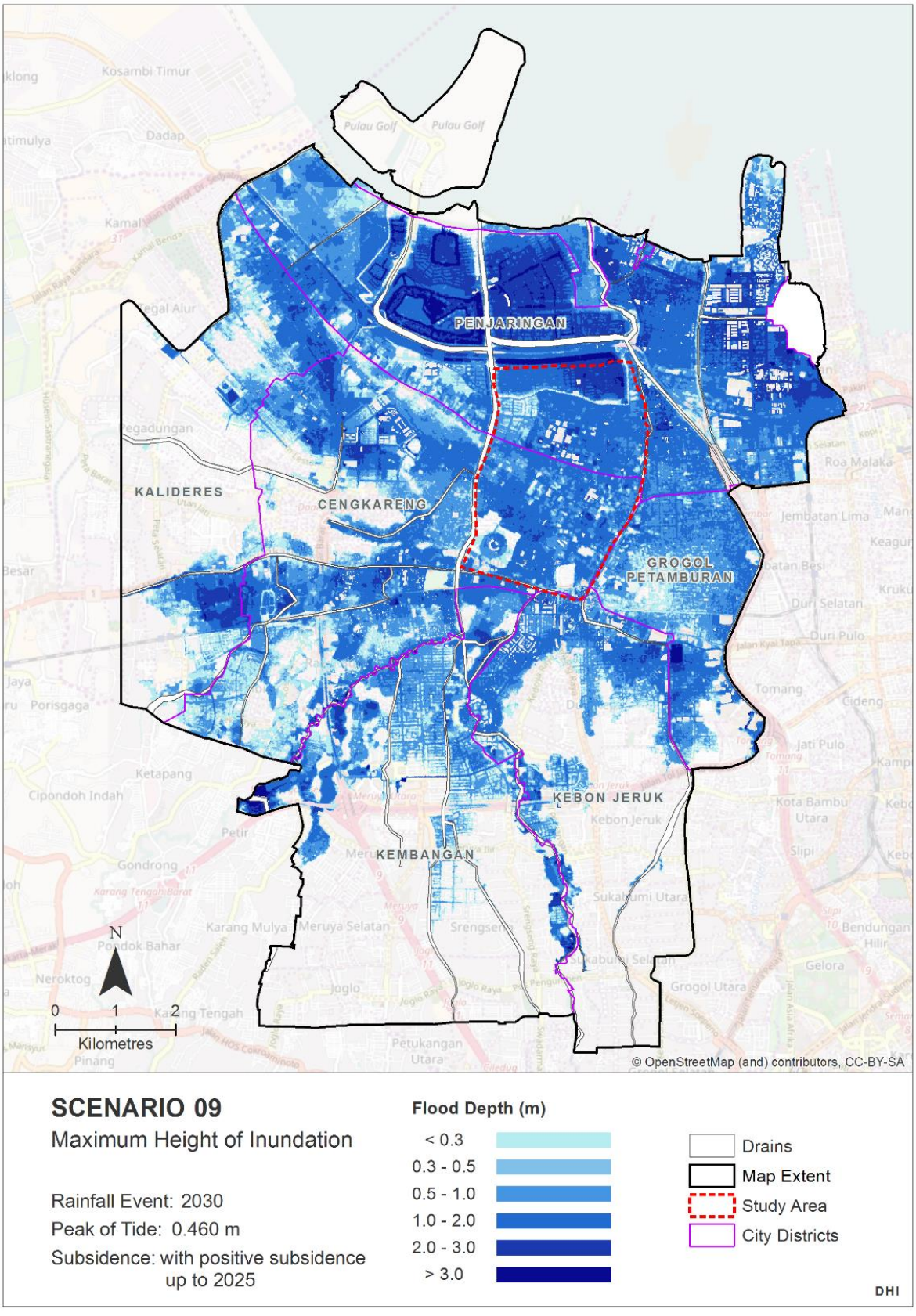
PENJARINGAN
KALIDERES
CENGKARENG
GROGOL PETAMBURAN
KEBON JERUK
KEMBANGAN
N
0
1
2
Kilometres
© OpenStreetMap (and) contributors, CC-BY-SA
SCENARIO 09
Maximum Height of Inundation
Rainfall Event: 2030
Peak of Tide: 0.460 m
Subsidence: with positive subsidence up to 2025
Flood Depth (m)
< 0.3
0.3 - 0.5
0.5 - 1.0
1.0 - 2.0
2.0 - 3.0
> 3.0
Drains
Map Extent
Study Area
City Districts
DHI

6 Discussion on Flooding in the Study Area

6.1 Analysis of Effects from Subsidence

To investigate the land subsidence effect toward flooding in the study area, flood maps from scenarios without land subsidence, i.e. using the base DEM, are compared with scenarios where land subsidence is applied. Figure 6.1 shows the difference of depths from 2012 to 2013 at the study area (refer to Section 2.2.2 for land subsidence details). The comparison is done by plotting the inundation depth differences between Scenarios 4 and 3 for 2013, and Scenarios 9 and 8 for 2030. These two years are selected since 2007 simulates negative land subsidence rates (i.e. ground levels increased), and both 2030 and 2050 apply land subsidence for the year 2025.

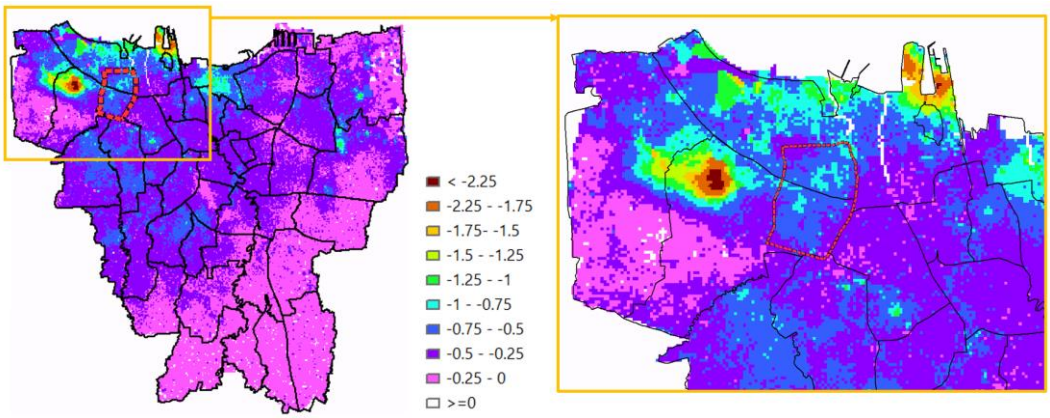

Figure 6.1 Subsidence depth from 2012-2025 in study area.

From comparison figures for 2013 and 2030 (Figure 6.2), we can see that the flood was worsened almost entirely in our study area (in Pantai Indah Kapuk poldel, Kapuk Muara polder, and Kapuk Poglar polder). Those impacted areas show lowered ground levels due the land subsidence (Figure 6.1). The accumulation subsidence depth for 13 years in study area range from 0.25 to 0.75 m. The comparison also show that the flood in other area is slightly reduced (represented by red colour), i.e. in Grogol Petamburan district. This is because the volume of the water from the inland flooding is the same, but the water tend to spread to the lowest topography.

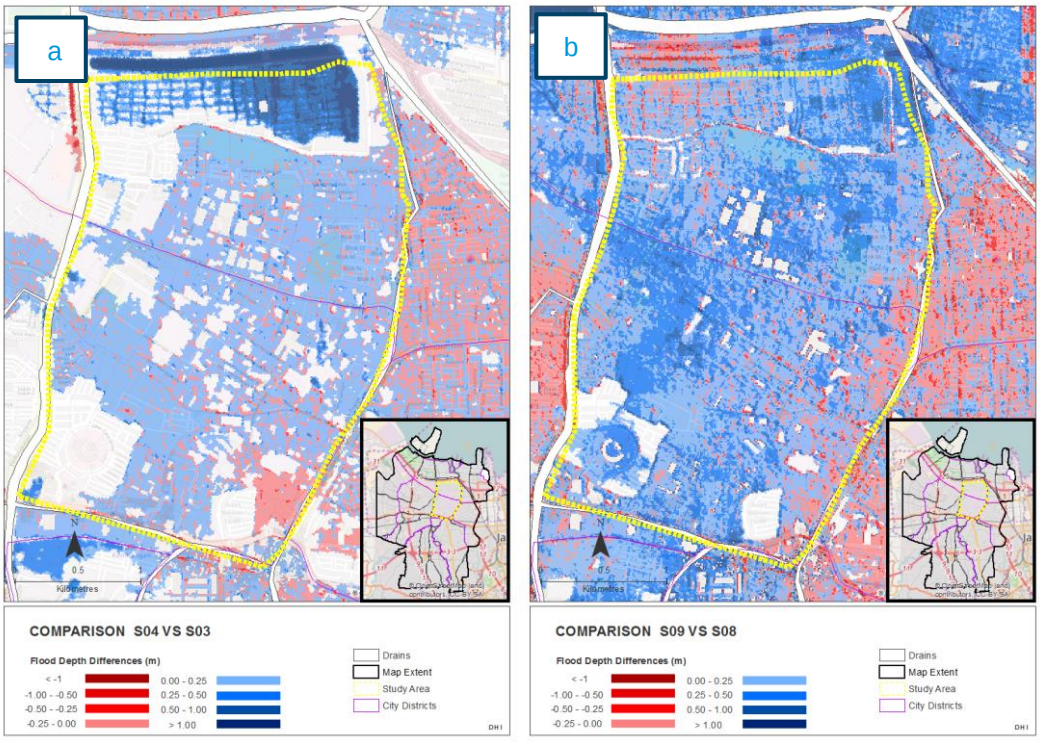

Figure 6.2 Flood depth differences in the study area between with-subsidence scenario and without-subsidence scenarios for year: (a) 2013, (b) 2030.

6.2 Analysis of Effects from Climate Change

As shown in Chapter 5, it is already evident that the increase of rainfall and tide consistently causes worse flooding. The effects of climate change conditions, where we simulated increased rainfall by a calculated factor (explained in Section2.3.2) and applied projected sea level rise (more in Section 2.4.1); it is expected to have higher inundation depth and wider coverage of flood areas. It is worth noting again that the median climate change factor for rainfall projects drought condition, i.e. decreased rainfall, in Jakarta region (Budiyono *et al.*, 2016). In Section 6.4, we see that the influence of tide in coastal flooding only happens when land subsidence is applied, and henceforth we focus our analysis in rainfall.

In order to evaluate the effects of climate change towards flooding in the study area, various maps of flood depth differences were generated. These comparison maps are produced by subtracting the inundation depths of 2030 and 2050 climate change years (Scenarios 8 and 6) and historical flood events in 2013 and 2007 (Scenarios 3 and 1). The scenarios chosen use uniform topographies from 2012 DEM, i.e. no land subsidence is applied.

Figure 6.3 shows the flood depths difference between 2030 and 2013 (Scenarios 8 and 3) and between 2050 and 2013 (Scenarios 6 and 3). The rainfall event in 2013 is calculated to have a frequency of 25-year return period (Budiyono *et al.*, 2016) while the design storms for 2030 and 2050 scenarios are derived from 50-year return period of rainfall plus their respective calculated climate change factors. Therefore, both frequency and factors increased the rainfall intensities, which also explains the increase of inundation depths as shown in Figure 6.3.

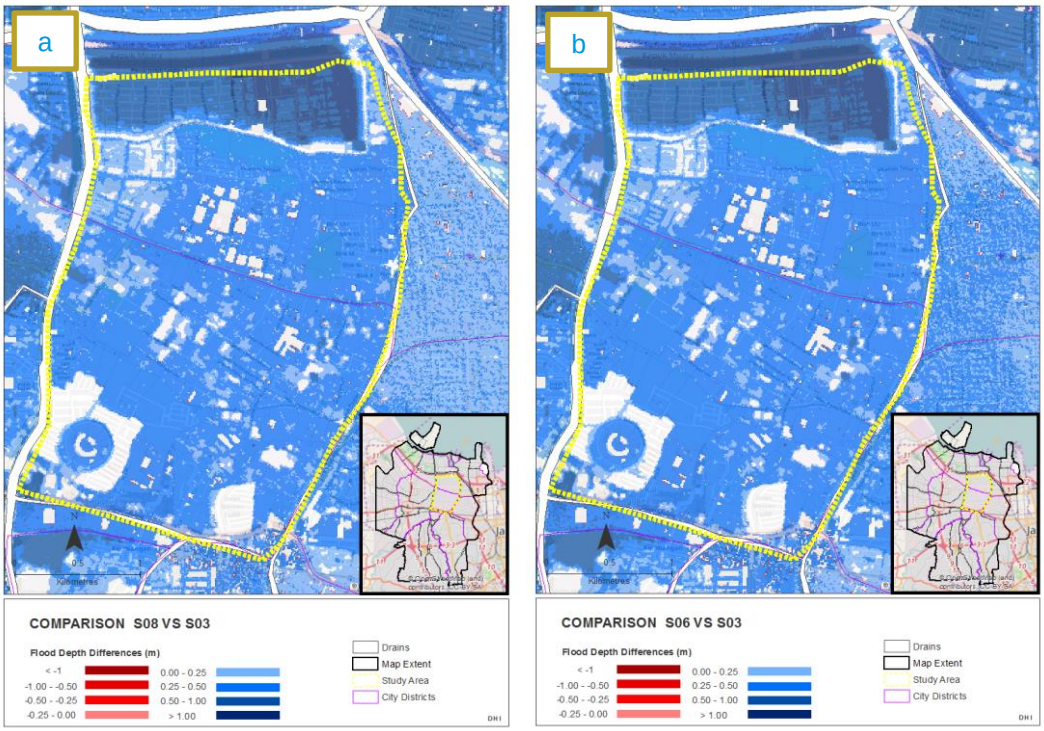

Figure 6.3 Flood depth differences in the study area between 2013 and climate change scenarios: (a) 2030 and (b) 2050

Similar comparison is made between 2030 and 2007 (Scenarios 8 and 1) and between 2050 and 2007 (Scenarios 6 and 1) as shown in Figure 6.4. The rainfall event in 2007 is calculated to have a frequency of 50-year return period (Budiyono *et al.*, 2016), which is the same frequency as in 2030 and 2050 scenarios with calculated climate change factors added: +1.33 and +1.44 respectively. Therefore, increased the rainfall intensities due to climate change alone is enough to increase the inundation depths at the study area as shown in Figure 6.3.

Among the three polders that are located in the study area, Pantai Indah Kapuk polder has the highest sensitivity from the effects of climate change. This is indicated by darker colour in that area observed in both Figure 6.3 and Figure 6.4. In that polder, the inundation depth differences can reach 2 m.

Besides the two comparisons, another map of flood depth differences between 2050 and 2030 has also been generated in Figure 6.5. In this case, we see the effects in flooding when rainfall is increased by +11%, given that the rainfall input for both scenarios are derived from the same design storms of 12 rainfall stations. Figure 6.5 shows that 2050 has higher inundation depths in almost the entire study area by 0.25 m.

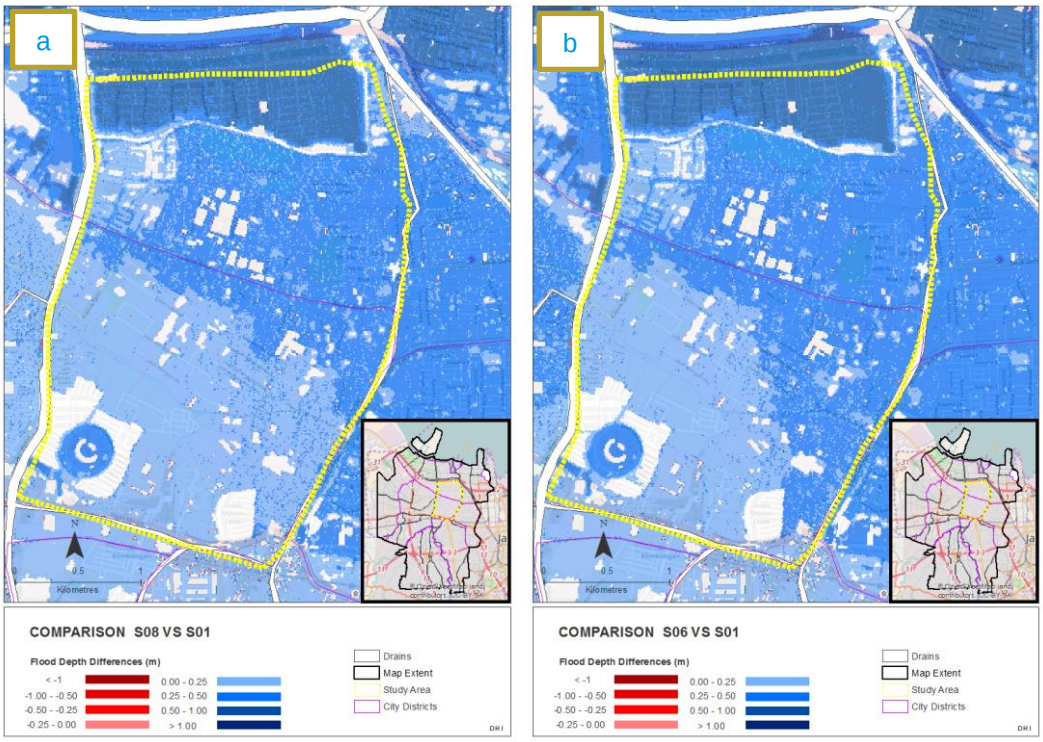

Figure 6.4 Flood depth differences in the study area between 2007 and climate change scenarios: (a) 2030 and (b) 2050

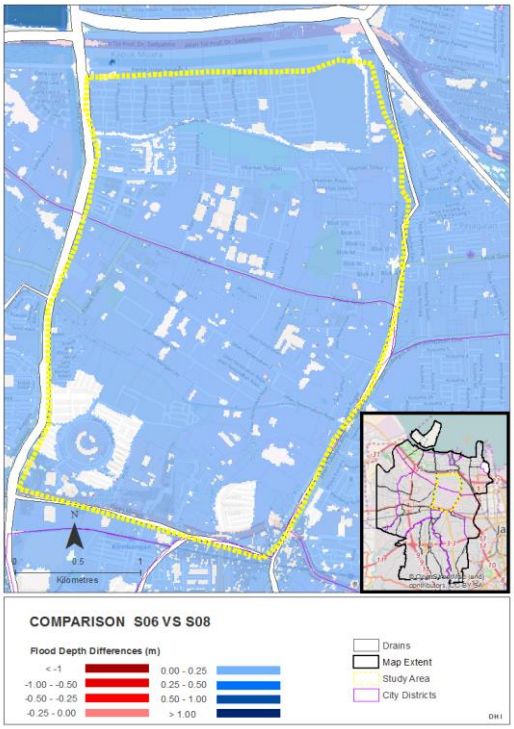

Figure 6.5 Flood depth differences in the study area between 2050 and 2030

6.3 Flood Trigger Locations

To identify the critical areas where flood mitigation should be prioritised, we use the dynamic flood maps that can show the progression of flooding within the 4-5 day simulation period. Figure 6.6 shows these areas where the flood start to occur: in the north part of Pantai Indah Kapuk polder (Penjaringan district), Pluit polder, west part of Penjaringan district, Teluk Gong polder (Grogol Petamburan district), and around Angke river.

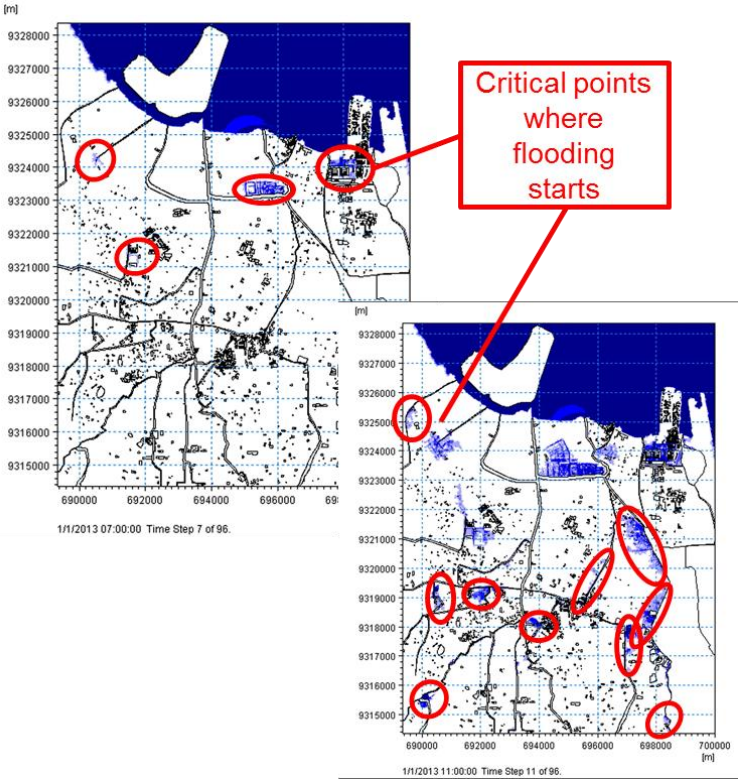

Figure 6.6 Inundation during the first few hours of 2013 flood event.

We can further zoom in to the drains where flooding occurs by plotting drain longitudinal profiles showing the water levels, bed slopes and cope levels. These profiles can be extracted from the 1D result as shown in Figure 6.7. Flooding occurs when the water level overtops the cope levels of the river bank, particularly at shallow parts of Mookevart river and Angke river.

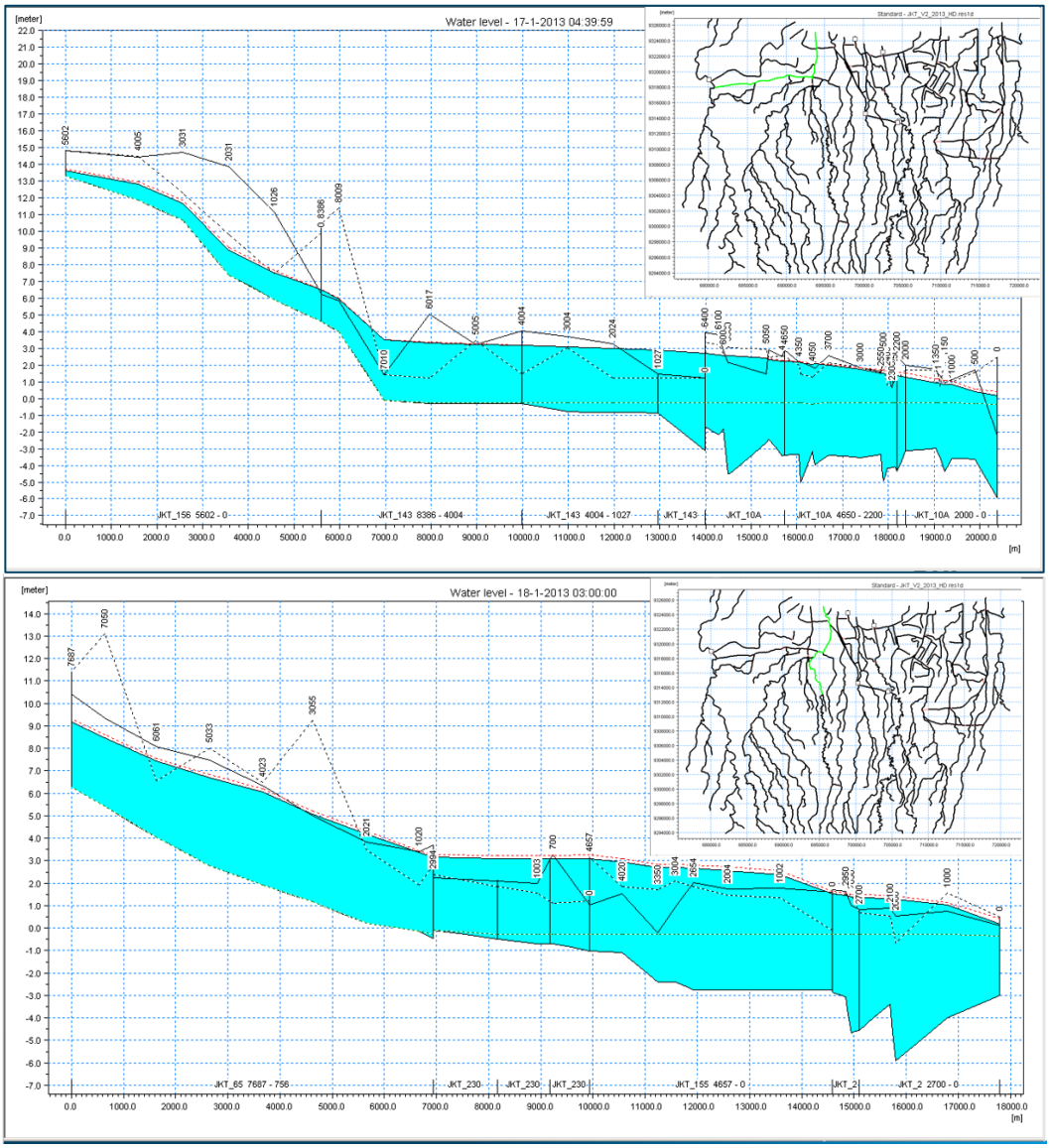

Figure 6.7 Vertical profile of the river water level during flood in 2013

Sets of dynamic flood maps show the flood areas increasing from Day 1 of the simulation period until Day 2 and 3 – when peak flood occurs; as well as the flood recession from the peak until Day 4 (or 5 for scenarios 1 and 2). From these plots, we can further assess areas that are vulnerable to slow-moving floods and pooling areas even after two days of receding rainfall, mostly due to low-lying topographies or depressed areas where access to drainage is not sufficient.

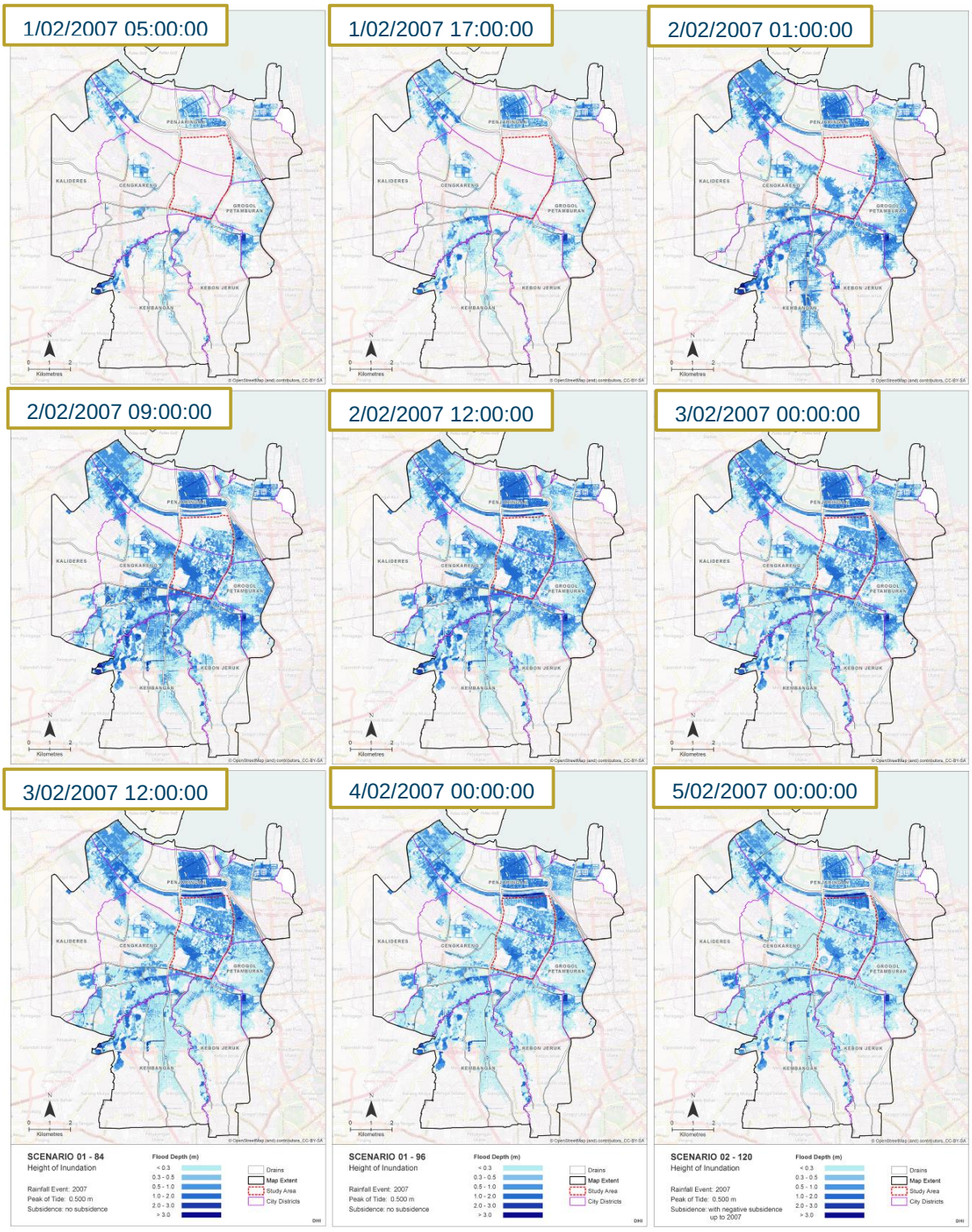

Figure 6.8 Dynamic flood maps from Scenario 1 model result

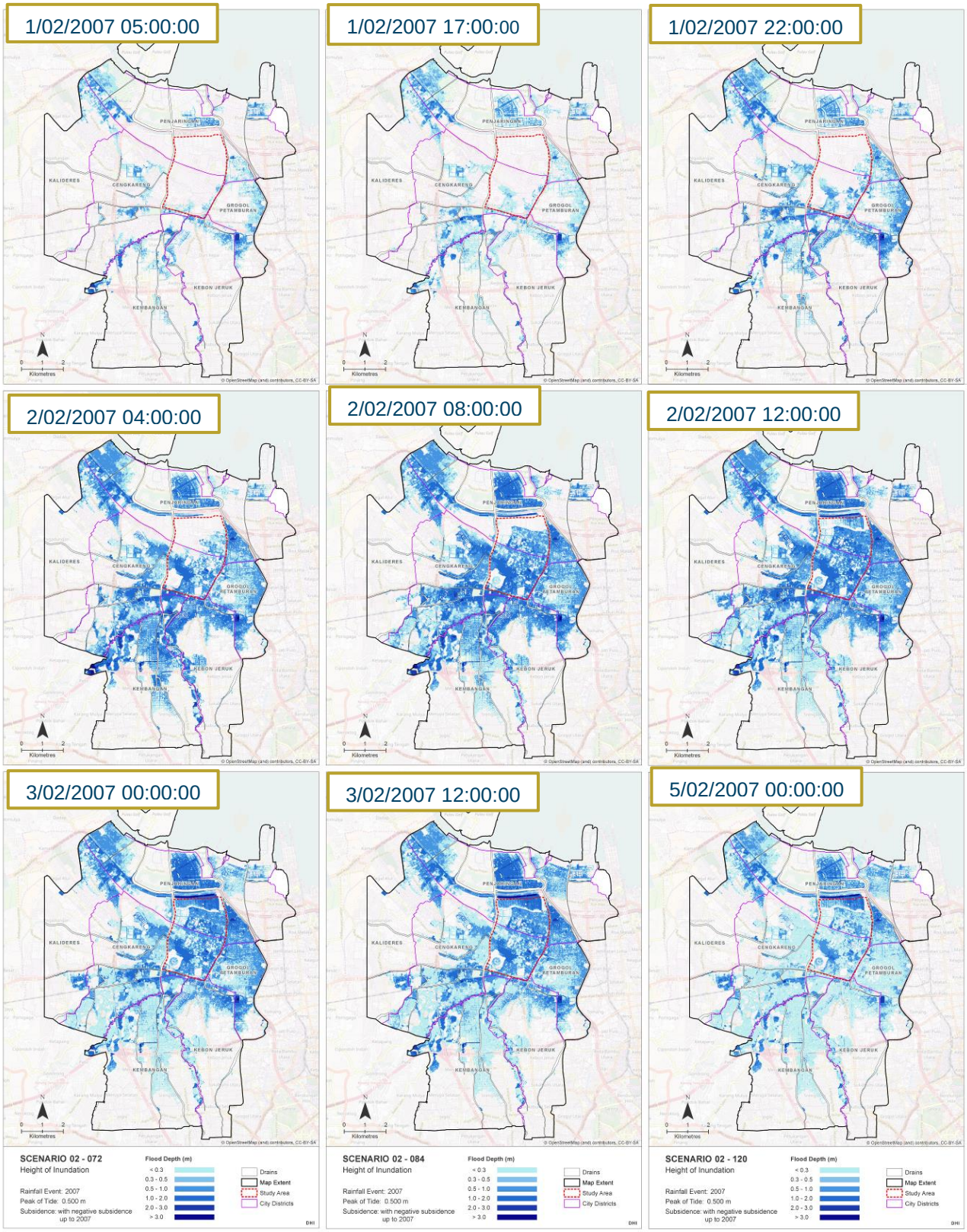

Figure 6.9 Dynamic flood maps from Scenario 2 model result

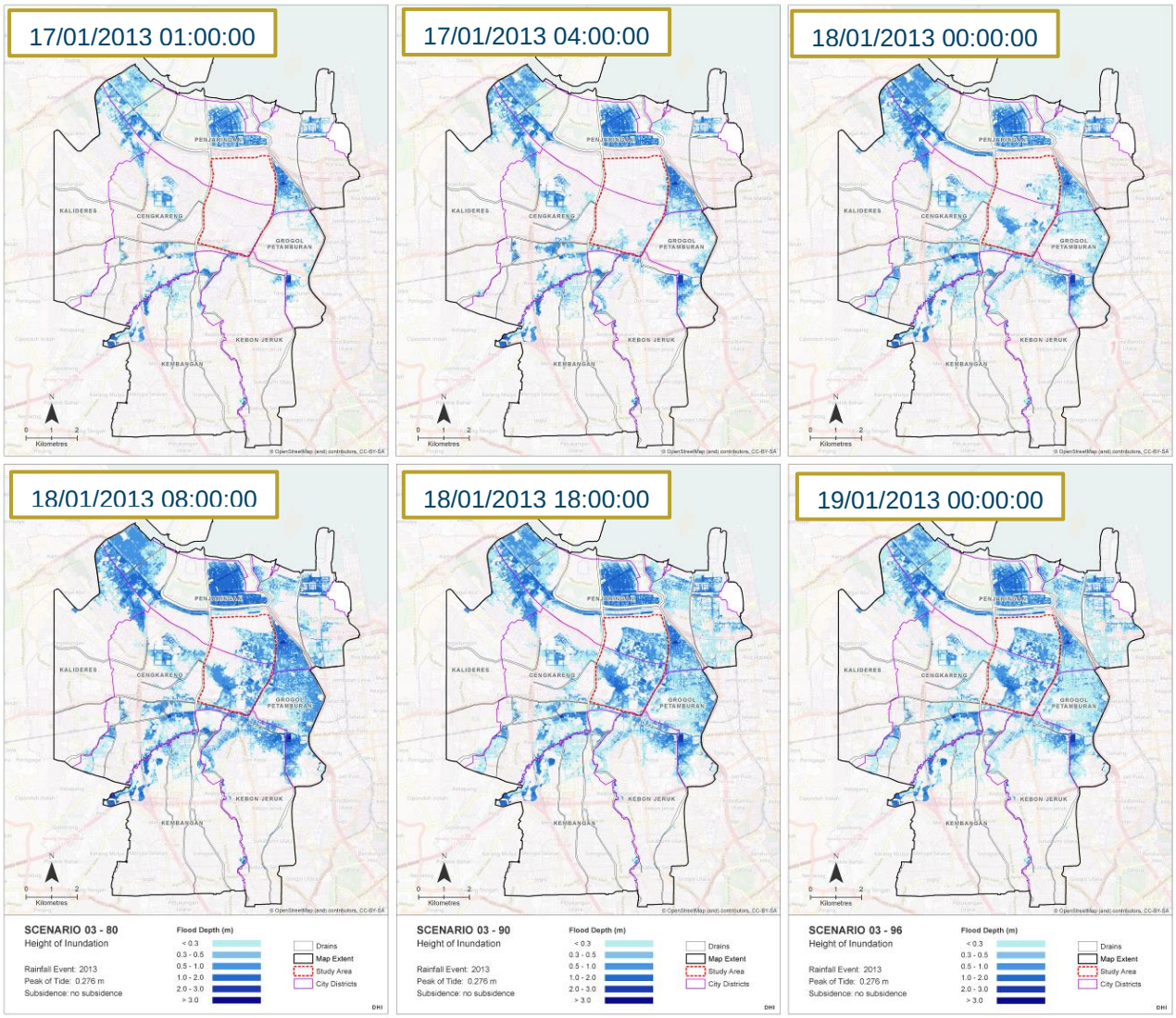

Figure 6.10 Dynamic flood maps from Scenario 3 model result

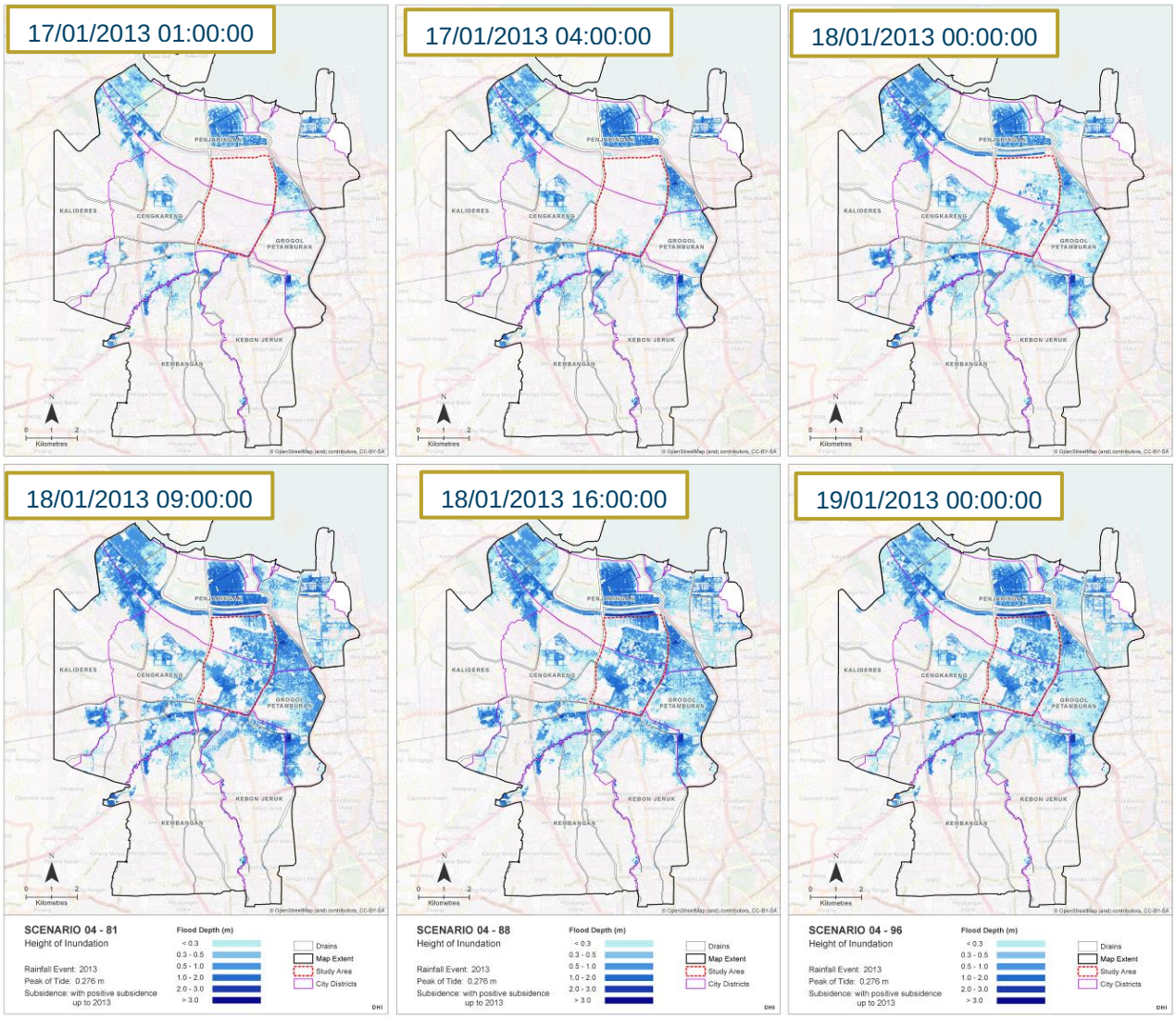

Figure 6.11 Dynamic flood maps from Scenario 4 model result

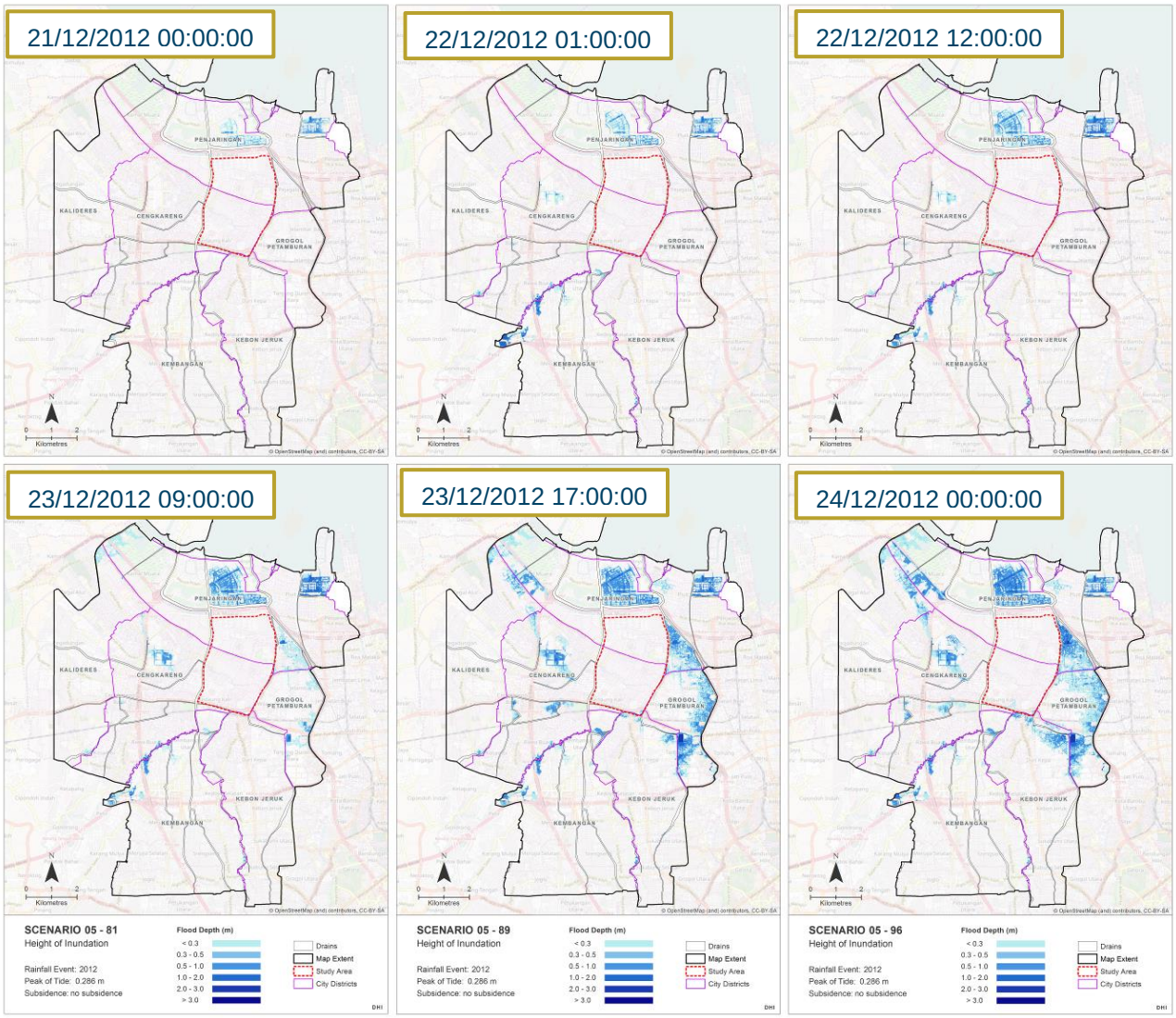

Figure 6.12 Dynamic flood maps from Scenario 5 model result

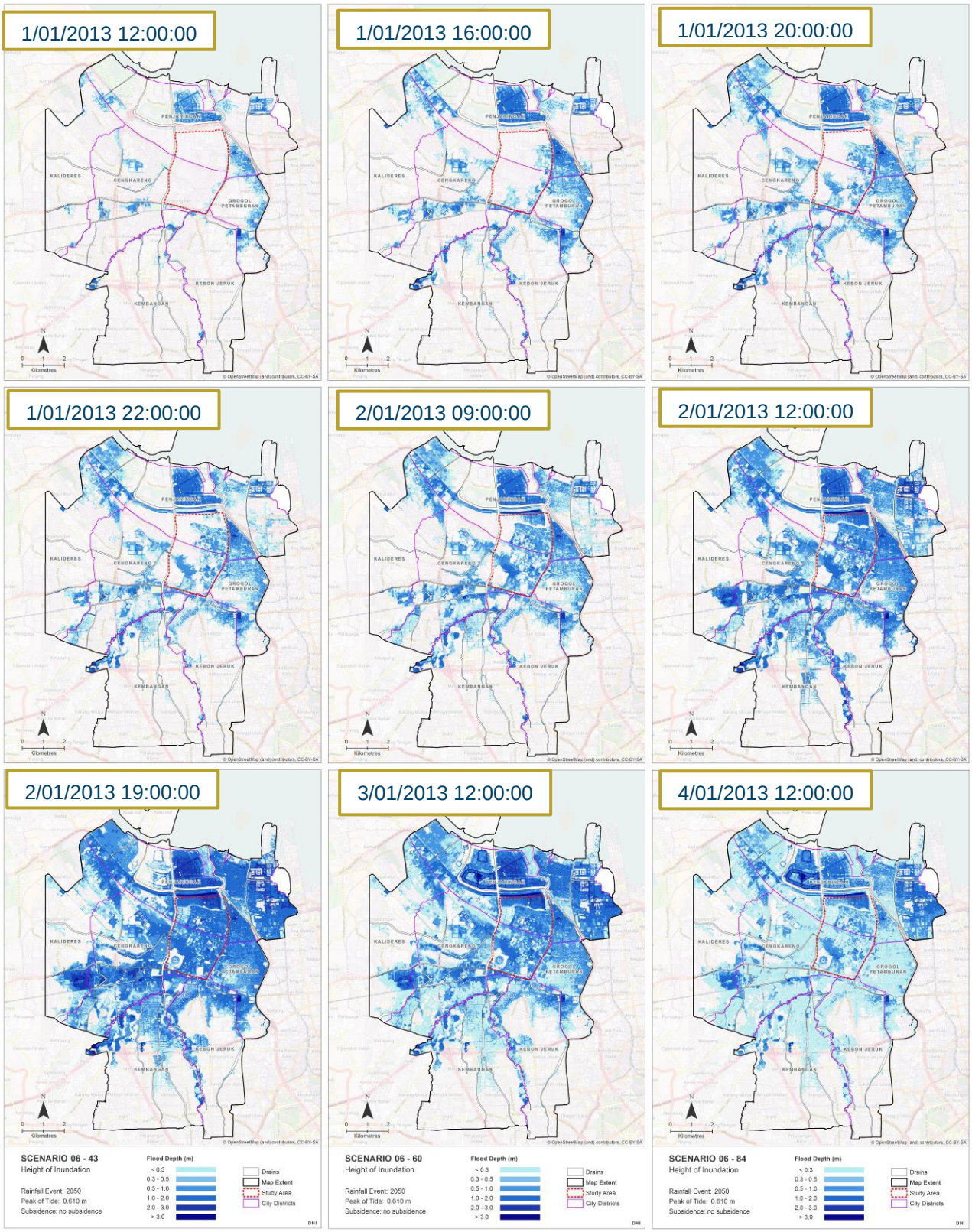

Figure 6.13 Dynamic flood maps from Scenario 6 model result. For 2050, the simulation period is not indicative of actual flood event, since rainfall/tide are derived from calculations

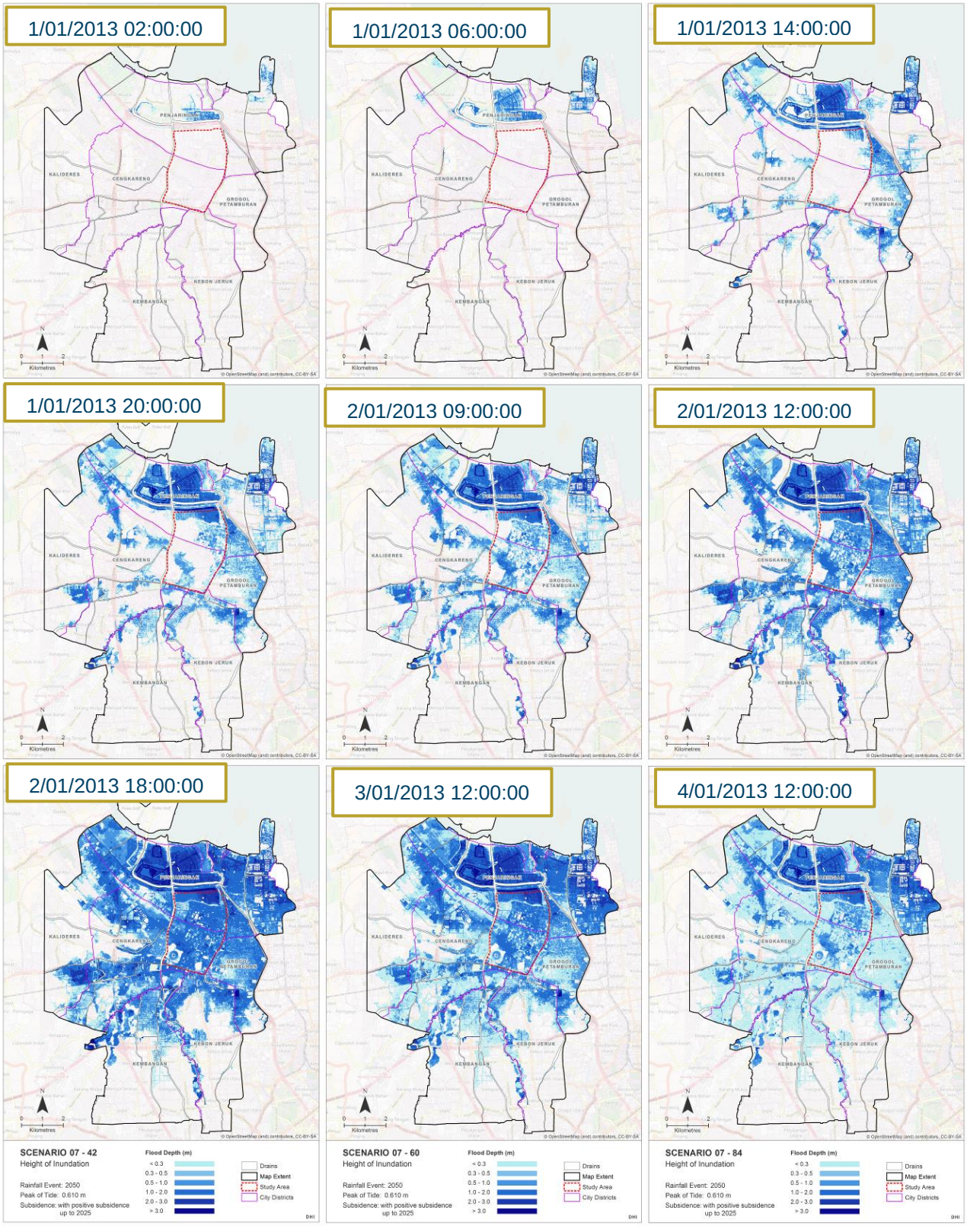

Figure 6.14 Dynamic flood maps from Scenario 7 model result. For 2050, the simulation period is not indicative of actual flood event, since rainfall/tide are derived from calculations

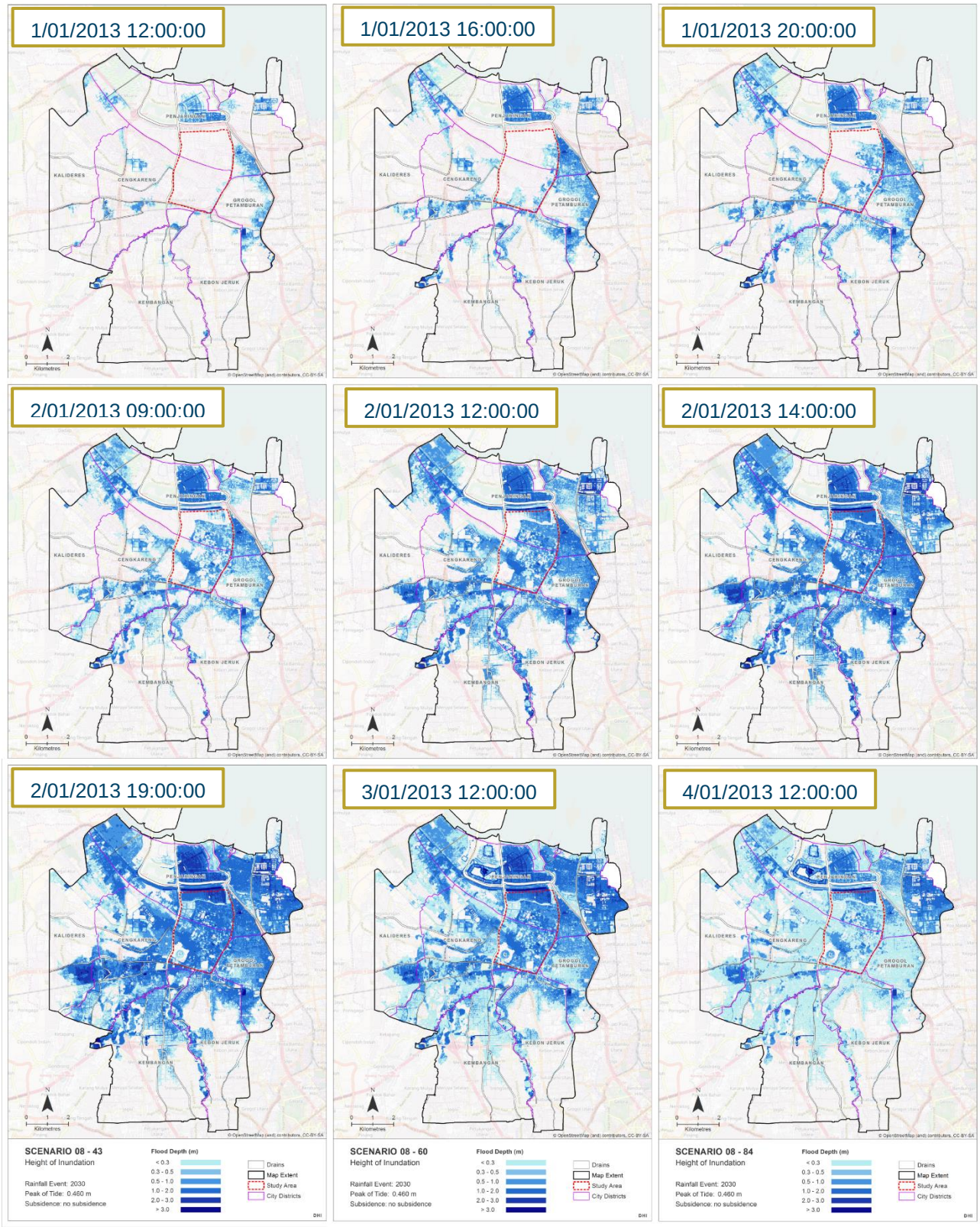

Figure 6.15 Dynamic flood maps from Scenario 8 model result. For 2030, the simulation period is not indicative of actual flood event, since rainfall/tide are derived from calculations

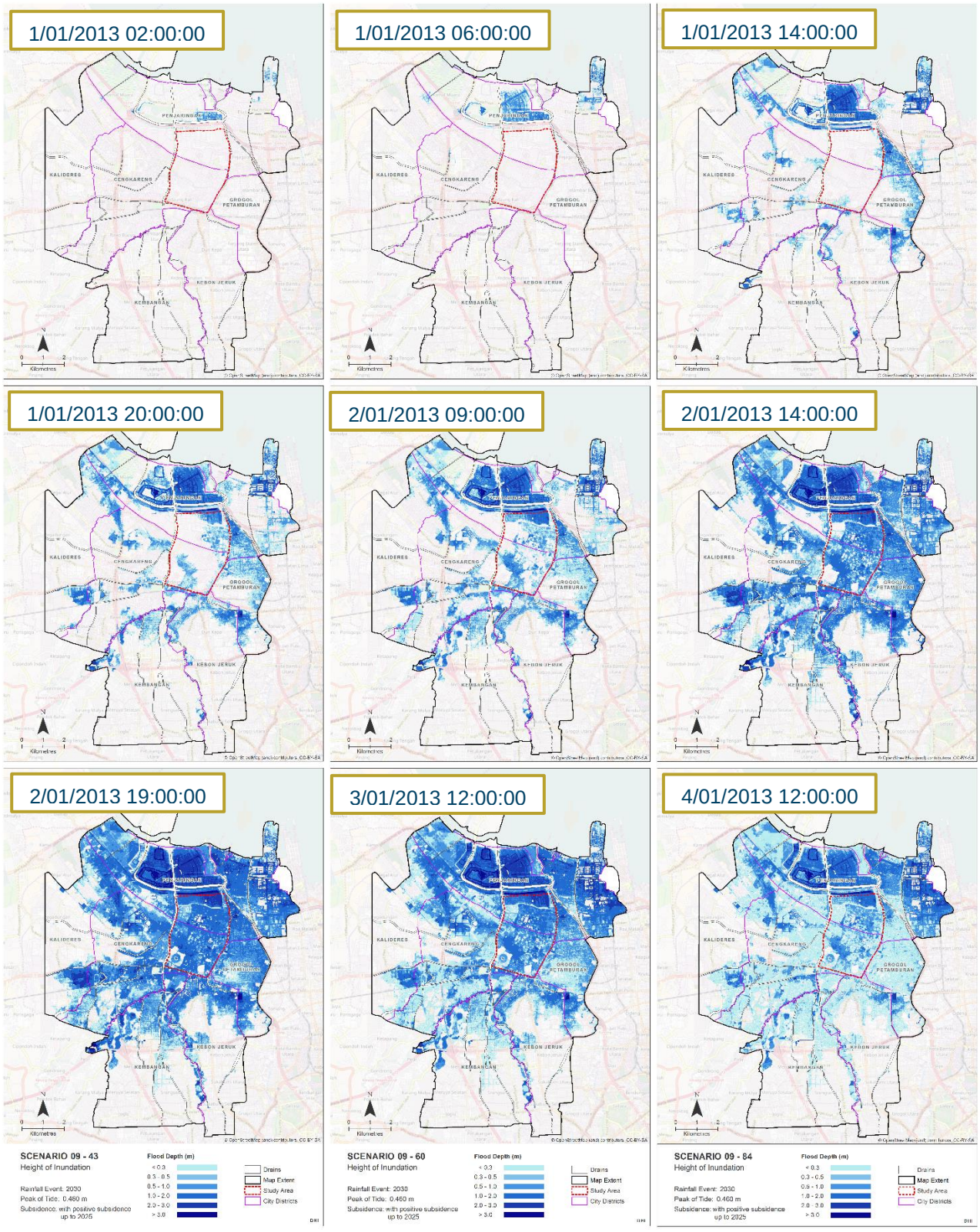

Figure 6.16 Dynamic flood maps from Scenario 9 model result. For 2030, the simulation period is not indicative of actual flood event, since rainfall/tide are derived from calculations

6.4 Analysis of Tidal Influence on Flooding

Test simulations have been done to further analyse the effects of tide in coastal flooding. We simulated two scenarios of 2030 tidal input without rainfall, i.e. no subsidence and with positive subsidence until 2025. Results in Figure 6.17 show that tide cause flooding in the projected subsidence in 2025, but not in 'no subsidence' scenario (i.e. 2012 ground levels). The flood caused by the tide has not reached the study area since the spreading of the flood only occurred in some part of Penjaringan district, especially in Pluit polder. It shows that tide will cause flooding but only when land subsidence is applied. Therefore, the flooding is mostly sensitive to the increase of rainfall.

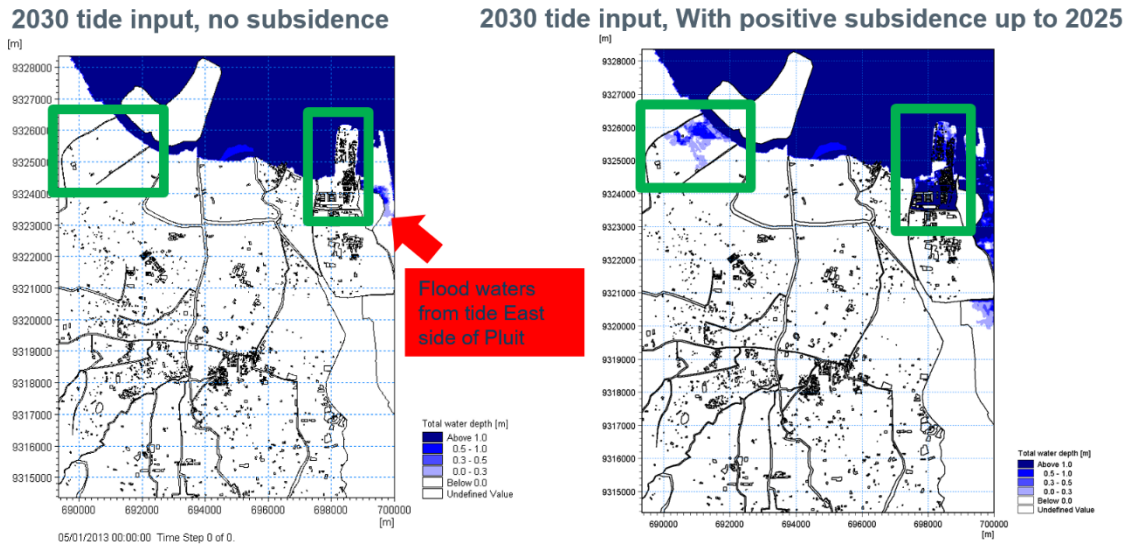

Figure 6.17 Model results with only 2030 tidal input. (Left) Without subsidence – 2012 DEM, and (right) with subsidence – until 2025.

6.5 Estimation of Retention Pond as Flood Mitigation Measure

The Blue Green Jakarta is the winning proposal in the Green Metropolis Jakarta 2050 competition. Figure 6.18 show the retention pond included in Blue Green Jakarta. The retention pond is planned to be located in Kapuk Polder system (study area), because this area is continuously flooded, notably in 2007 and 2013. The area is also affected by land subsidence. This retention pond is a proposed measure in reducing the flood by diverting the flood into the pond.

The retention pond is designed to help prevent the 50-year return period flood. The Jakarta flood event that have a return period of 50 year was the 2007 flood event. Therefore, to estimate the capacity of retention pond, model results from Scenario 2 (2007 flood event with subsidence) were used. Furthermore, model results from Scenario 9 (2030 with subsidence) were also used for the pond capacity estimation as a mitigation of future flooding from climate change and subsidence in 2030.

Figure 6.18 Retention lake plan in study area (Source: Sopaheluwakan, 2017)

Estimation of the retention pond capacity is done first by extracting the maximum flood depths (refer to Chapter 5) at the study area. The mean of these values is calculated as representative flood depth at the area of 8,923,969.67 m^2. Table 6.1 summarises the mean flood depth and the volume of the retention pond. Additionally, the height is calculated if the retention pond is designed to be placed in 200 ha area. This capacity estimation for 2030 (~11M m^3) is well within the estimation of Pond Capacity (10 – 15M m^3) described in the Blue Green Jakarta proposal.

Table 6.1 Estimation of the retention pond capacity

Year	Mean Flood Depth (m)	Pond Volume (m^3)	Depth in 200 ha Pond (m)
2007	0.84	7,463,854.30	3.73
2030	1.24	11,028,313.31	5.51

This page is intentionally left blank

7 Conclusions

From the results and analysis in the previous two chapters, we can conclude the following important points, i.e.:

1. The current flood model setup generates reasonable flood maps consistent with increasing rainfall, tide and subsidence.
2. Current flood maps are validated with other models and surveys on 2007 (~50-year return period) and 2013 (~25-year return period) flood events.
3. It is observed that flood is caused more by increased rainfall rather than tide and projected sea level rise.
4. It is also observed that land subsidence significantly worsens the flooding, similar to the findings of previous studies.
5. Further analysis of tidal influence show that coastal flooding from tides is observed only in future land subsidence scenarios (2025 projected ground levels).
6. If a worst-case climate change scenario is taken into account, i.e. increased rainfall, the study area is almost fully inundated compared to 2007 flood event.
7. The hydrodynamic model also provides the “weak points” where flood starts to overflow. This will help to mitigate the flood with different options

7.1 Recommendations for Future Studies

Recommendations made from this study are categorised into two parts: (1) Model performance and (2) Future modelling studies based from the conclusions above.

Model performance can be improved by: (a) discharge calibration using observed data, (b) cross-section measurements, (c) addition of more control structures and their operation rules. As described in Chapter 3 (Model Setup) and Chapter 4 (Model Calibration and Validation), the current Jakarta flood model is generated primarily from data extracted from the DEM. Model calibration was not performed due to the non-availability of data mentioned above. This recommendation will further improve the validation process and the confidence of the model use for scenario analysis to test for various mitigation options by the authorities.

From the conclusions drawn from this study, we recommend the following follow-up studies to be conducted for further analysis:

(a) Mitigation studies on preventing or impeding effects of land subsidence (Section 6.1 Analysis of Effects from Subsidence), such as impact assessment of the polder system with regards to groundwater recharge and thereby affecting the subsidence rate. We recommend using MIKE SHE, DHI’s advanced, flexible framework for hydrologic modelling that includes process models for evapotranspiration, overland flow, unsaturated flow, groundwater flow, and channel flow and their interactions, in conjunction with the current Jakarta MIKE flood model.

(b) Climate change impact on flooding using the mean values, i.e. less rainfall-drought conditions as stated in Section 6.2 (Analysis of Effects from Climate Change), in aid for policy-makers and stake-holders in assessing different climate change scenarios.

(c) Impact assessment of the GSW, since it is found in Section 6.4 (Analysis of Tidal Influence on Flooding) that tide influence on coastal flooding is observed during worst-case land subsidence conditions. Through this type of modelling, optimized design of GSW features with gate and pump operations is possible. The integrated

approach of GSW along with Polder system can be evaluated for optimal performance to reduce the maximum flood impacts.

(d) Polder system water management to mitigate the supply and demand issues in water supply in Jakarta City through the distributed approach instead of centralized approach. These polder system will also act as a local water supply for the community apart from flood mitigation, and increasing the groundwater level and thereby reducing the subsidence rate. The integrated catchment modelling such as MIKE SHE + MIKE Hydro River system will be the right modelling tools to test, evaluate and design such system for the community with such a holistic vision.

(e) Apart from flood mitigations, Jakarta will also needs a “flood early warning system (FEWS)” that very much dependent on Modelling (real time flood modelling), for efficient and effective way to manage the flooding in the city. DHI has an appropriate Decision Support System (DSS) such as MIKE Information, Planning and Operation (MIKE IPO) tools that leverage on modelling software (Example: MIKE Flood, MIKE Hydro River, etc).

(f) The current study concentrated only on a small study area that contain 3 polder system. However, interconnected polder system if any has to be simulated and accessed as one integrated system to access the real flood impact due to the interconnection or overflow from one system to the other.

(g) Effect of reclamation on back water and there by flood impacts in upstream and/or flood prone areas has to be simulated to understand the overall system with the proposed reclamation works.

(h) The study area model is schematized from the high resolution DEM whereas the rest of Jakarta upstream catchment schematization is derived from coarser DEM. The model schematization can be further improved with the same above approaches mentioned in this report if the high resolution DEM is available for other parts of the upstream catchments.

(i) Apart from GSW and polder systems, authorities can simulate and test the effectiveness of other mitigation measures such as drainage improvements, water sensitive urban drainage systems (WSUDs), rain water harvesting, etc.

8 References

BAPPENAS, (2010): *ICCSR – Scientific basis analysis and projection of sea level rise and extreme weather events*. Indonesia.

Bontemps, S., Defourny, P., Bogaert, E. Van, Kalogirou, V., & Perez, J. R., (2011): *GLOBCOVER 2009 Products Description and Validation Report*. ESA Bulletin, *136*, 53. https://doi.org/10013/epic.39884.d016. Data download: http://due.esrin.esa.int/page_globcover.php

Budiyono, Y., Aerts, J., Tollenaar, D., Ward, P., (2016): *River flood risk in Jakarta under scenarios of future change*, Nat Hazard Earth Syst. Sci., 16, 757-744, doi: 10.5194/nhess-16-757-2016

Chow, Ven Te, (1959): *Open-channel Hydraulics*. McGraw-Hill, New York. 680 pp.

Deltares, (2014): *Technical Review and Support Jakarta Flood Management System, Final Report - Phase 2*, The Government of Indonesia and World Bank, Indonesia.

DHI, (2016a): *Introduction to MIKE FLOOD: Integrated 1D-2D Flood Modelling for Urban, Riverine and Coastal Flooding*, presented in BPPT training, 11 October, South Tangerang, Indonesia.

DHI, (2016b): *MIKE FLOOD User Manual*, Hørsholm, Denmark.

FAO/IIASA/ISRIC/ISS-CAS/JRC, (2009): *Harmonized World Soil Database (version 1.1)*. FAO, Rome, Italy and IIASA, Laxenburg, Austria. Data download: http://www.fao.org/soils-portal/soil-survey/soil-maps-and-databases/harmonized-world-soil-database-v12/en/

Earth Observation Research Center (EORC) and Japan Aerospace Exploration Agency (JAXA), (2017): *ALOS Global Digital Surface Model (DSM) "ALOS World 3D-30m" (AW3D30) Dataset Product Format Description*. Retrieved from http://www.eorc.jaxa.jp/ALOS/en/aw3d30/aw3d30v11_format_e.pdf.

Farr, T.G. *et al*., (2007): *The Shuttle Radar Topography Mission*. Reviews of Geophysics, 45, p.33.

Lehner, B., Verdin, K., & Jarvis, A. (2006). *HydroSHEDS Technical Documentation*. Washington, DC: World Wildlife Fund US. Retrieved from http://hydrosheds.cr.usgs.gov

Maune, D. F., (2010): *Digital Elevation Model (DEM) Whitepaper NRCS High Resolution Elevation Data*. Fairfax, VA.

OpenStreetMap: http://www.openstreetmap.org

Metro Extracts: https://mapzen.com/data/metro-extracts/

Sopaheluwakan, J., (2017):. *Blue Green Jakarta 2030, Keynote Overview on Hydrodynamic Modeling and Social Economic Changes in Kapuk Polder System*, presented in Workshop: "Menuju Jakarta Berketahanan Iklim : Pemodelan Hidrodinamika untuk Penyusunan Tuntunan Pembangunan Infrastruktur Pengurangan Bencana Banjir dan Berketahanan Iklim di Jakarta", 21 April, Jakarta, Indonesia.

Thiessen, A.H., (1911): *Precipitation averages for large areas*, Mon. Wea. Rev., 39, 1082–1089, doi: 10.1175/1520-0493(1911)39<1082b:PAFLA>2.0.CO;2.

Van der Sleen, N and Lopez, J., (2013): *An analysis of the Pluit polder*, Jakarta, Bachelor thesis, Universitet Twente, Netherland.

Vosselman, G., (2000): *Slope based filtering of laser altimetry data*. International Archives of Photogrammetry and Remote Sensing, Vol. 33, Part B3/2, 33(Part B3/2), 678–684. https://doi.org/10.1016/S0924-2716(98)00009-4

APPENDIX A – COMPARISON OF SOBEK AND MIKE MODEL

This page is intentionally left blank

A Comparison between MIKE model and SOBEK model

Appendix A describes the comparison between the Jakarta flood model that is setup in this project (further called as MIKE model) and SOBEK model that is used in Budiyono, et al. (2015) and Budiyono et al. (2016). As described by the two referenced papers, the SOBEK model is produced by the Flood Hazard Mapping (FHM) framework by Deltares (2007) and Deltares (2009), as well as the Flood Management Information System (FMIS) projects by Deltares (2012) together with the Research and Development Center For Water Resources (Pusair) and the National Office for Climate (BMKG) for the province of DKI Jakarta (Special Capital Region of Jakarta) administration and the national government of Indonesia (Deltares et al. 2012 in Budiyono et al., 2016).

Table 1 summarises the differences between the two model setup, aside from the modelling software that is used from in the two studies.

Table 1 Comparison between MIKE and SOBEK model setup.

PARAMETER	MIKE	SOBEK
Upstream and downstream boundary condition	• Almost all boundary in upstream is coming from rainfall-runoff (Unit Hydrograph Model) • In downstream sea water level, computed based on astronomical tidal component were used	• All boundaries in upstream is coming from rainfall-runoff and in the upstream boundary discharge in Katulampa is include in the model • In downstream sea water level, computed based on astronomical tidal component were used [1]
Rainfall input	• 3-Hourly rainfall data from UPT station and hourly rainfall converted from daily data of *Pos hujan*	• Using return period rainfall for (1,5,10,25, 50) [1]
Structures included in the model	• Gates = 6 • Pump stations = 2	• Weir = 20 • Universal Weir = 2 • Pump station = 40 [2]
Status of East Banjir Canal in the model	• Included in the model	• EBC is not included in model 2007 (2007-2009) • EBC is included in model after FHM 1 and FHM 2 -- for Java flood insurance study (2011). [2]
Number of catchment	• 652 sub catchment	• +/- 450 sub catchment [2]

PARAMETER	MIKE	SOBEK
Grid type and resolution in 2D model	• Using flexible mesh (triangular grid) with 10m resolution in inland area, and	• Using rectangular grid 100x100m grid cells representing the entire flood-prone area and one nested grid with 50x50m cells representing part of the Ciliwung River upstream of Manggarai gate [2]

[1] Budiyono et al, (2016)

[2] Deltares, (2014)